Nuclear Energy Agency (NEA)
NEA/WKP(2026)1
June 2026
www.oecd-nea.org

NEA WORKING PAPER

SFCOMPO - Evaluation of Fukushima – Daini- 1 Samples - Assemblies 2F1ZN2 and 2F1ZN3 (Type 9×9-9)

Ugur MERTYUREK

OECD
BETTER POLICIES FOR BETTER LIVES

NEA
NUCLEAR ENERGY AGENCY

Nuclear Energy Agency

NEA/WKP(2026)1

Unclassified

English text only

16 June 2026

OECD Nuclear Energy Agency
STEERING COMMITTEE FOR NUCLEAR ENERGY

SFCOMPO - Evaluation of Fukushima – Daini- 1 Samples - Assemblies 2F1ZN2 and 2F1ZN3 (Type 9×9-9)

Evaluator:
Ugur Mertyurek, Oak Ridge National Laboratory (ORNL)

Internal Reviewers:
Ian Gauld (ORNL)
Germina Procop (ORNL)
Georgeta Radulescu (ORNL)

Independent Reviewers:
Jan Bostelman, P.E., PMP, Joseph Willett, P.E.
Bostelman Engineering LLC

JT03589437

This document, as well as any data and map included herein, are without prejudice to the status of or sovereignty over any territory, to the delimitation of international frontiers and boundaries and to the name of any territory, city or area.

OECD NEA Working Papers describe preliminary results or research in progress by the author(s) and are published to stimulate discussion on a broad range of issues on which the OECD Nuclear Energy Agency works.

Comments on Working Papers are welcomed and may be sent to the Nuclear Energy Agency.

All Nuclear Energy Agency Working Papers are available at www.oecd-nea.org/pub.This work is issued under the responsibility of the Secretary-General of the OECD and does not necessarily reflect the official views of OECD Member countries or its Nuclear Energy Agency. The opinions expressed and arguments employed are those of the author(s).

Please cite this working paper as:

NEA (2026), "SFCOMPO - Evaluation of Fukushima – Daini- 1 Samples - Assemblies 2F1ZN2 and 2F1ZN3 (Type 9×9-9)", OECD Publishing, Paris, https://doi.org/10.82155/tcs0-r539.

© OECD 2026

Attribution 4.0 International (CC BY 4.0).

This work is made available under the Creative Commons Attribution 4.0 International licence. By using this work, you accept to be bound by the terms of this licence (https://creativecommons.org/licenses/by/4.0).

Attribution – you must cite the work.

Translations – you must cite the original work, identify changes to the original and add the following text: *In the event of any discrepancy between the original work and the translation, only the text of original work should be considered valid.*

Adaptations – you must cite the original work and add the following text: *This is an adaptation of an original work by the OECD. The opinions expressed and arguments employed in this adaptation should not be reported as representing the official views of the OECD or of its Member countries.*

Third-party material – the licence does not apply to third-party material in the work. If using such material, you are responsible for obtaining permission from the third party and for any claims of infringement.

You must not use the OECD logo, visual identity or cover image without express permission or suggest the OECD endorses your use of the work.

Any dispute arising under this licence shall be settled by arbitration in accordance with the Permanent Court of Arbitration (PCA) Arbitration Rules 2012. The seat of arbitration shall be Paris (France). The number of arbitrators shall be one.

Foreword

This Working Paper contributes to the data evaluation work for the SFCOMPO database - the world's largest open database of destructive assay data for spent nuclear fuel. The database includes measurement data for over 750 fuel samples selected from fuel irradiated in 44 reactors of 8 types. The database provides descriptions of the measured fuel samples' characteristics and operation histories and includes datasets of measured nuclide concentrations for over 60 nuclides, key actinides and fission products, which span needs and interests of a variety of nuclear science and engineering applications, including criticality safety, reactor physics, nuclide inventory, nuclear data, decay heat, and radiation shielding.

The SFCOMPO database is maintained and developed by the Nuclear Energy Agency (NEA) and managed by the SFCOMPO Technical Review Group (TRG) by mandate from the NEA Nuclear Science Committee's Working Party of Nuclear Criticality Safety. One of the primary missions of the SFCOMPO TRG is to perform peer-review assessment of the datasets in the database and develop high-quality benchmarks and benchmark models based on these data. Destructive assay measurement data are widely recognised as one of the most reliable bases for validating the computational tools and associated nuclear data applied for predicting nuclide inventories in irradiated nuclear fuel.

Acknowledgements

The NEA acknowledges the contributions of the members of the Evaluated Spent Fuel Assay Database (SFCOMPO) Technical Review Group (TRG) for preparing this Working Paper.

Special thanks are also extended to U. Mertyurek (Oak Ridge National Laboratory [ORNL], United States), I. Gauld (ORNL, United States), G. Procop (ORNL, United States), G. Radulescu (ORNL, United States), J. Bostelman (Bostelman Engineering LLC, United States) and J. Willet (Bostelman Engineering LLC, United States) for their contributions to the paper.

Table of contents

List of abbreviations and acronyms **8**

Executive summary **9**

1. Description of experimental data **11**

1.1. Overview of the experiment 11
1.2. Design data 11
1.3. Reactor operating history data 13
1.4. Fuel sample data 24
1.5. Measurement data 25

2. Evaluation of experimental data **29**

2.1. Design data 29
2.2. Material compositions 30
2.3. Irradiation history 32
2.4. Reactor operating conditions 32
2.5. Measurements 33
2.6. Sample burn-up 34

3. Benchmark specifications **37**

3.1. Fuel design data 37
3.2. Material compositions and temperature(s) 38
3.3. Reactor operating conditions 39
3.4. Model simplifications 40

4. Uncertainty analysis **58**

4.1. Methods 58
4.2. Code and nuclear data library 58
4.3. Parameters and parameter uncertainty values 58
4.4. Individual parameter uncertainty results 58
4.5. Measurement uncertainties 80
4.6. Total uncertainty results 82

5. Results of sample calculations **83**

5.1. Codes and nuclear data libraries 83
5.2. Comparison of sample calculations and measurements 83

6. References **94**

Appendix A **96**

A.1. Polaris model for 2F1ZN3/C3/UB 96

List of figures

1. Enrichment profile of the Fukushima Daini-1 9×9-9 assemblies 13
2. Positions of assemblies 2F1ZN2 (left) and 2F1ZN3 (right) over cycles 12-16 14
3. Maximum and average linear power rate histories of assembly 2F1ZN3 [13] 22
4. Linear power rate around node 7 of assembly 2F2ZN2 [13] 23
5. Linear power rate around node 7 of assembly 2F2ZN3 [13] 23
6. Axial sample locations [1,4] 25
7. Fukushima Daini-1 9×9-9 lattice design 30
8. Enrichment profile of the Fukushima Daini-1 9×9-9 assemblies 38
9. Power histories for the 2F1ZN2/C2/GdB sample 60
10. Power histories for the 2F1ZN3/A9/UB sample 60
11. Power histories for the 2F1/ZN3/C3/UM sample 61
12. Change in C/M with sample power approach (pin power-based vs. node power-based) for the 2F1ZN2 assembly samples 62
13. Change in C/M with sample power approach (pin power-based vs. node power-based) for the 2F1ZN3 assembly samples 62
14. Change in C/M with 1% increase in fuel density for the 2F1ZN2 assembly samples 64
15. Change in C/M with 1% increase in fuel density for the 2F1ZN3 assembly samples 65
16. Change in C/M with 5% increase in void fractions for the 2F1ZN3 assembly samples 67
17. Change in C/M with 5% reduction in void fractions for the 2F1ZN3 assembly samples 68
18. Void fraction history of 2F1ZN3 assembly for top middle and bottom nodes 68
19. Change in C/M with 100 K increase in fuel temperature for the 2F1ZN3 assembly samples 70
20. Change in C/M with 100 K reduction in fuel temperature for the 2F1ZN3 assembly samples 70
21. Change in C/M with gap closure for the 2F1ZN3 assembly samples 72
22. Change in C/M with thermal expansion of fuel for the 2F1ZN3 assembly samples 73
23. Channel bow [30] 74
24. Modelled channel bow 74
25. Change in C/M with channel bow for the 2F1ZN3 assembly samples 76
26. Change in C/M with different channel radii 2F1ZN3 assembly samples 77
27. Change in C/M with 1% reduction in burn-up for the 2F1ZN3 assembly samples 78
28. Change in C/M with 1% increase in burn-up for the 2F1ZN3 assembly samples 78
29. C/M-1 for actinide and Nd nuclides for the 2F1ZN2 assembly samples 86
30. C/M-1 for actinide and Nd nuclides for the 2F1ZN3 assembly samples 86
31. C/M-1 for fission products for the 2F1ZN2 (C2GdT and C3UT) and 2F1ZN3 (A9UM, C2GdM, and C3UM) samples 87

List of tables

1. Fukushima Daini-1 reactor parameters 11
2. Fukushima Daini-1 9×9-9 assembly specifications 12
3. Reactor operating history [13,7] 14
4. Irradiation histories of nodes 5/6 in assembly 2F1ZN2 [7] 15
5. Irradiation histories of nodes 19/20 in 2F1ZN2 [7] 16
6. Irradiation histories of nodes 5/6 in 2F1ZN3 [7] 17
7. Irradiation histories of node 11 in 2F1ZN3 [7] 19
8. Irradiation history of node 19 in 2F1ZN3 [7] 21
9. Summary of Fukushima Daini-1 9×9-9 assembly fuel sample measurements 24
10. Measurement techniques and measured nuclides 26
11. Measured nuclides (atoms/total final U atoms) from the 1st measurement campaign [1] 26
12. Measured nuclides (atoms/total final U atoms) from the 2nd measurement campaign [4] 27
13. Measurement dates for the 1st measurement campaign [1] 28
14. Decay times in years for the 2nd measurement campaign [4] 28
15. Decay times in days for the first measurement campaign [1] 33
16. Decay times in days for the second measurement campaign [4] 33
17. Sample burn-ups 36
18. Fukushima Daini-1 9×9-9 assembly geometry parameters 37
19. Fukushima Daini-1 9×9-9 assembly material densities 38
20. Fukushima Daini-1 9×9-9 assembly material temperatures 39
21. Fukushima Daini-1 9×9-9 assembly fuel material initial isotopic composition [23] 39
22. Irradiation history of sample C2/GdT in assembly 2F1ZN2 [7] 40
23. Irradiation history of sample C2/GdB in assembly 2F1ZN2 [7] 41

24. Irradiation history of sample C3/UT in assembly 2F1ZN2 [7] 42
25. Irradiation history of sample C3/UB in assembly 2F1ZN2 [7] 43
26. Irradiation history of sample C2/GdT in assembly 2F1ZN3 [7] 44
27. Irradiation history of sample C2/GdM in assembly 2F1ZN3 [7] 45
28. Irradiation history of sample C2/GdB in assembly 2F1ZN3 [7] 46
29. Irradiation history of sample C3/UT in assembly 2F1ZN3 [7] 47
30. Irradiation history of sample C3/UM in assembly 2F1ZN3 [7] 48
31. Irradiation history of sample C3/UB in assembly 2F1ZN3 [7] 49
32. Irradiation history of sample A9/UT in assembly 2F1ZN3 [7] 50
33. Irradiation history of sample A9/UM in assembly 2F1ZN3 [7] 51
34. Irradiation history of sample A9/UB in assembly 2F1ZN3 [7] 52
35. Coolant density histories for cycle 12 [7] 53
36. Coolant density histories for cycle 13 [7] 54
37. Coolant density histories for cycle 14 [7] 55
38. Coolant density histories for cycle 15 [7] 56
39. Coolant density histories for cycle 16 [7] 57
40. Change in C/M with sample power history for the 2F1ZN3 assembly samples 63
41. Change in C/M with 1% increase in fuel density for the 2F1ZN3 assembly samples 66
42. Change in C/M with 5% change in void fraction for the 2F1ZN3 assembly samples 69
43. Change in C/M with 100 K change in fuel temperature for the 2F1ZN3 assembly samples 71
44. Change in fuel modelling parameters with thermal expansion 72
45. Change in C/M with thermal expansion of fuel for the 2F1ZN3 assembly samples 75
46. Assembly geometry manufacturing tolerances 77
47. Change in C/M for 1% change in burn-up in the 2F1ZN3 assembly samples 79
48. Change in C/M due to measurement uncertainties in 2F1ZN3 assembly samples 81
49. C/M-1 for the 2F1ZN2 assembly samples 84
50. C/M-1 for the 2F1ZN3 assembly samples 85
51. C/M-1 and uncertainties for the 2F1ZN3 assembly A9/UB sample 87
52. C/M-1 and uncertainties for the 2F1ZN3 assembly A9/UM sample 88
53. C/M-1 and uncertainties for the 2F1ZN3 assembly A9/UT sample 89
54. C/M-1 and uncertainties for the 2F1ZN3 assembly C2/GdB sample 89
55. C/M-1 and uncertainties for the 2F1ZN3 assembly C2/GdM sample 90
56. C/M-1 and uncertainties for the 2F1ZN3 assembly C2/GdT sample 91
57. C/M-1 and uncertainties for the 2F1ZN3 assembly C3/UB sample 92
58. C/M-1 and uncertainties for the 2F1ZN3 assembly C3/UM sample 92
59. C/M-1 and uncertainties for the 2F1ZN3 assembly C3/UT sample 93

List of abbreviations and acronyms

BWR	Boiling water reactor
C/M	Calculated-to-measured
ADSNF	Expert Group on Assay Data of the Spent Nuclear Fuel (NEA WPNCS)
EGADSNF	Expert Group on Assay Data of the Spent Nuclear Fuel (NEA WPNCS)
ENDF	Evaluated Nuclear Data File
FIMA	Fissions per initial metal atom
HR-ICP-MS	High-resolution inductively coupled plasma mass spectrometer
ID-MS	Isotopic dilution mass spectrometry
JAEA	Japan Atomic Energy Agency
JNES	Japan Nuclear Energy Safety Organization
NEA	Nuclear Energy Agency
NRA	Japan Regulation Authority
NSC	Nuclear Science Committee (NEA)
ORNL	Oak Ridge National Laboratory (United States)
PIE	Post-irradiation examination
PWR	Pressurised water reactor
RCA	Radiochemical assay
SFCOMPO	Evaluated Spent Fuel Assay Database
TD	Theoretical density
TIMS	Thermal ionisation mass spectrometry
TRG	Technical Review Group
WPNCS	Working Party on Nuclear Criticality Safety (NEA NSC)

Executive summary

The SFCOMPO database is the world's largest open database of destructive assay data for spent nuclear fuel. It serves as a basis for validation of predictive tools for nuclide transmutations and decay in nuclear fuel during and post-irradiation. It includes experimental data accompanied by comprehensive data evaluations addressing completeness, uncertainty, and reliability. It further offers computational benchmark models designed to validate computer simulations against the experimental data. Each data evaluation undergoes extensive reviews by the international expert community within the SFCOMPO Technical Review Group to ensure high quality datasets as required for the above-mentioned validation programmes.

This report provides a data evaluation for the SFCOMPO database for radiochemical assay (RCA) data for eight UO_2 and five UO_2-Gd_2O_3 spent nuclear fuel samples obtained from five fuel rods. These fuel rods were selected from two 9×9-9 lead test fuel assemblies (design like ATRIUM-9) that were irradiated in the Fukushima Daini Unit 1 boiling water reactor (BWR). The RCA data was collected as part of a validation study of burn-up calculations for BWR cores that was conducted by the Japan Regulation Authority (NRA). Both fuel assemblies have an identical fuel rod enrichment map, with the ^{235}U enrichments varying from 2.1% to 4.9%, and a same loading of 5 wt% in the gadolinia fuel rods.

The fuel assemblies were irradiated for three cycles and five cycles in the reactor. The reported burn-ups for the UO_2 fuel samples range from 38.9 to 68.4 GWd/MTU. The samples were cut from top, bottom, and mid-axial elevations of the fuel rods to capture the effect of axial power and void profile. Although power and void histories at the exact sample locations are not available, detailed nodal power and void fraction histories were provided, and they were used to derive sample-specific information.

The RCA measurements were performed by the Japan Atomic Energy Agency (JAEA) in two experimental campaigns. Only U, Pu, and Nd isotopes were measured in the first campaign. The second campaign included measurements for the isotopes of Eu, Sm, Gd, and Ru that are fission products important for burn-up credit. No confidence levels were provided for the reported measurement uncertainties, and it is not known if they represent one or two standard deviations.

This Working Paper provides fuel lattice design, nodal operating history, measurement data, benchmark specifications, and results of fuel sample calculations for the measured spent fuel samples. Calculation results are provided as the ratio of calculated-to-measured (C/M) nuclide concentrations in the fuel samples. A detailed uncertainty analysis on operating history and modelling parameters is presented. Nuclide inventories of the measured samples were predicted using the Polaris 6.3 code within SCALE 6.2.3 with the 56-group evaluated nuclear data file (ENDF)/B-VII.1 neutron cross-section library. The Working Paper was prepared in accordance with the format and data review procedures recommended in the Evaluation Guide for the Evaluated Spent Fuel Assay Database (SFCOMPO), which was published by the Expert Group on Assay Data of the Spent Nuclear Fuel (EGADSNF) of the Working Party on Nuclear Criticality Safety (WPNCS), under the guidance of the NEA Nuclear Science Committee (NSC).

A conservative uncertainty analysis for operating and modelling parameters was performed, considering uncorrelated expected uncertainties for similar core and fuel designs. Sample burn-up uncertainties are the largest contributors to the known sources of uncertainties in the analysed samples. The reported burn-up from core calculations and the

burn-ups calculated by matching the measured ^{148}Nd burn-up indicator fission product show a 0.5% to 4.2% relative discrepancy, from analyses performed with two other depletion codes (SRAC, MVP-BURN) and reported in the literature. The same relative variation is less than 2% for the Polaris depletion calculations. The discrepancy between the measured value for fissions per initial metal atom (FIMA) and the corresponding Polaris-calculated value is less than 1%.

In general, the relative difference between the calculated and the measured nuclide concentration for the major actinides ^{235}U and ^{239}Pu is less than 5%. The exceptions, in the case of ^{235}U, are observed for fuel samples selected from the UO_2 corner rod (up to 33.8%) and from fuel samples from gadolinia fuel rods (up to 15.5%). The largest C/M values for ^{235}U are observed for the fuel samples selected from bottom axial nodes of the fuel rod. Among the major actinides, ^{234}U shows the largest deviations of the calculated vs measurement values overall.

It is important to note that, except for the ^{235}U enrichment, the literature does not provide data on the initial uranium isotopic compositions. While ^{234}U concentrations are known to be sensitive to their initial values, several samples show a larger-than-expected difference of approximately 36% between measurements and predictions.

The large differences observed in isotopic comparisons for the samples from corner rod A9 align with predictions made by the SWAT/4 and MVP-BURN codes. These consistent discrepancies, particularly for corner rod samples, suggest significant unknown errors in the reported power and void fraction histories of the considered fuel samples. Nevertheless, the agreement across predictions from different transport codes, using various nuclear data libraries, supports the value of using these measurements for code validation purposes with the observed biases, rather than discarding them.

1. Description of experimental data

1.1. Overview of the experiment

As part of a validation study of burn-up calculations of boiling water reactor (BWR) cores conducted by the Japan Regulation Authority (NRA) (and initiated by the Japan Nuclear Energy Safety Organization [JNES]), physics and depletion analyses were performed with SRAC [1] and MVP-BURN [2] codes. The analyses were performed using post-irradiation examination (PIE) measurements of burn-up and relative nuclide inventories of eight samples taken from two 9×9-9 BWR lead test fuel assemblies irradiated in the Fukushima Daini Unit 1 reactor (2F1). These two assemblies are identified as 2F1ZN2 and 2F1ZN3.

Assembly 2F1ZN2 was discharged from the reactor on 9 May 2000, after three cycles of irradiation. Assembly 2F1ZN3 was irradiated for five cycles and discharged on 7 January 2003. The assembly design for both 2F1ZN2 and 2F1ZN3 is like the ATRIUM-9 design with a 9×9-9 lattice.

Measurements for isotopes of uranium, plutonium, and neodymium in eight samples selected from five different fuel rods of assemblies 2F1ZN2 and 2F1ZN3 were reported by Yamamoto et al. [3]. Measurements for additional five samples from the same fuel rods were later reported by Suzuki [4]; these included measurements of additional fission products. Supplementary design and operating information for the 9×9-9 assemblies were provided by Yamamoto [5] through an activity co-ordinated by the Nuclear Energy Agency (NEA) on spent fuel assay data. The supplementary data included the fuel rod enrichment layouts, time-dependent void fractions, and cumulative burn-ups for the assemblies at the axial locations (nodes) of all measured samples.

1.2. Design data

The Fukushima Daini Unit 1 nuclear power plant is a BWR-5 type reactor built by Toshiba with a rated electric power of 1 100 MW. Basic core parameters are provided in [3,6].

Table 1. Fukushima Daini-1 reactor parameters

Commissioning date [6]	April 1982
Reactor type [8]	BWR-5
Containment vessel [8]	Mark II
Rated power (MWe) [8]	1100
Thermal power (MWt) [8]	3293
Number of fuel assemblies [8]	764
Number of control rods [8]	185
Core flow (t/h) [3]	48.3×10^3
Steam temperature (C) [6]	282
Steam pressure (kg/cm^2 [gage]) [6]	66.8
Core pressure (kg/cm^2 [gage]) [3]	70.7
Coolant inlet temperature (C) [3]	286
Core effective height (m) [3]	3.71
Core equivalent diameter(m) [3]	4.75

The main design parameters for the analysed 9×9-9 fuel assemblies are provided in Table 2 [3,7]. All geometry units are converted to cm, and all diameters are converted to

radii for consistency. The radial location of the measured samples and the fuel rod enrichment map is illustrated in Figure 1 [7].

Table 2. Fukushima Daini-1 9×9-9 assembly specifications

Assembly data	
Assembly type (lattice)	9×9-9
Fuel assembly pitch (cm) [3]	15.2
Number of fuel rods [3]	72
Number of gadolinia rods [3]	12
Number of water rods [3]	1 (square channel)
Fuel rod pitch (cm) [3]	1.45
Channel thickness (cm) [7]	0.25
Channel bypass gap (cm) [7]	0.65
Channel material [3]	Zircaloy-2
Active fuel length (cm) [7]	371
Fuel rod data	
Pellet radius (cm) [3]	0.47*
Pin-cladding gap (cm) [3]	0.01*
Pellet material [3]	UO_2/Gd_2O_3-UO_2
Pellet U^{235} enrichment (%) [3]	2.1 to 4.9
Pellet Gd_2O_3 content (wt %) [3]	5.0*
Pellet density (%) [3]	97*
Clad outer radius (cm) [3]	0.55*
Clad thickness (cm) [3]	0.07 (Include Zr lining of 0.1* mm)
Clad material [3]	Zircaloy-2 (Zr lining)
Water box data	
Outer width (cm) [3]	3.85*
Water box material [3]	Zircaloy-2

* Rounded number

Figure 1. Enrichment profile of the Fukushima Daini-1 9×9-9 assemblies

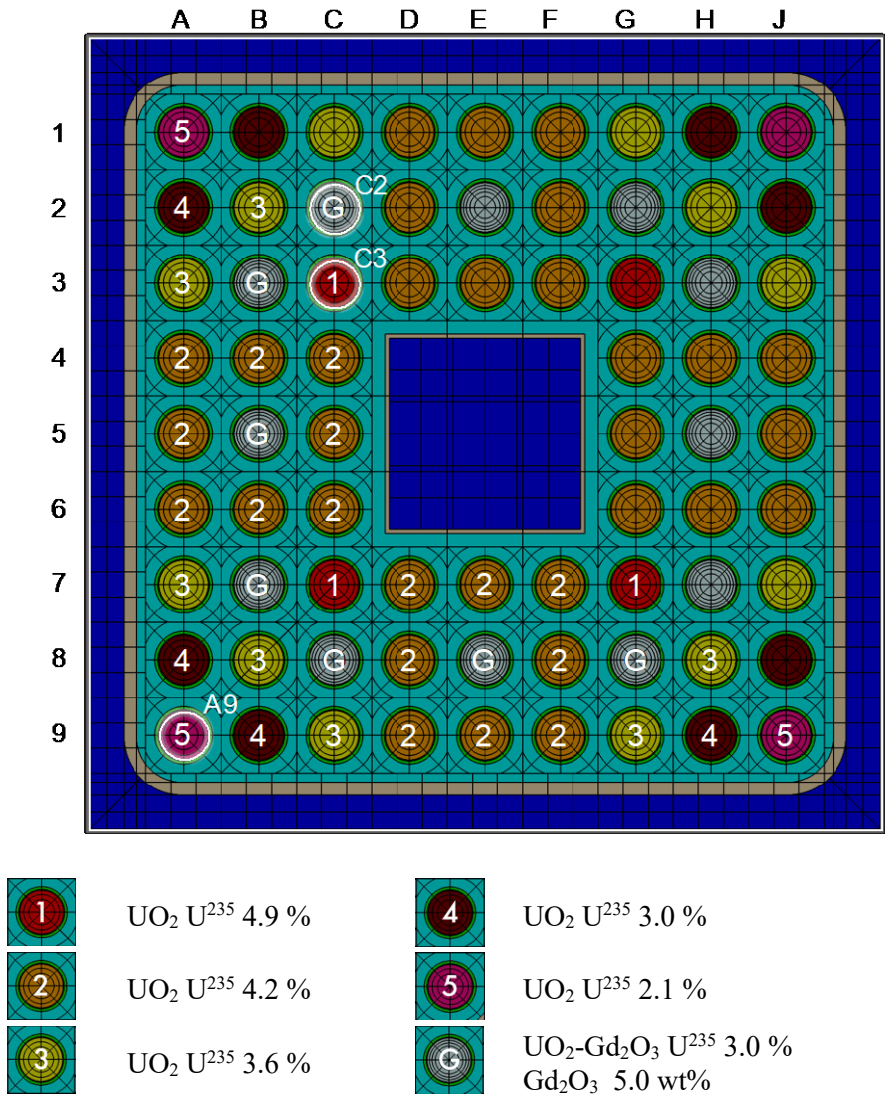

Source: ORNL, 2024.

1.3. Reactor operating history data

Operating history dates of the Fukushima Daini Unit 1 reactor for five cycles (Cycles 12–16) are provided in Table 3. Core positions of assemblies 2F1ZN2 and 2F1ZN3 during these five cycles are shown in Figure 2.

Table 3. Reactor operating history [13,7]

Cycle number	Date (month/day/year)	Operation
12	07/26/96	Startup
	07/28/96	Startup (power generation)
	04/12/97	Mid-shutdown
	04/18/97	Startup
	09/23/97	Shutdown
13	10/31/97	Startup
	11/02/97	Startup (power generation)
	12/06/97	Mid-shutdown
	02/15/98	Startup
	12/17/98	Shutdown
14	03/12/99	Startup
	03/13/99	Startup (power generation)
	05/09/00	Shutdown
15	06/15/00	Startup
	06/17/00	Startup (power generation)
	01/16/01	Mid-shutdown
	02/22/01	Startup
	08/13/01	Shutdown
16	11/09/01	Startup
	11/11/01	Startup (power generation)
	01/07/03	Shutdown

Figure 2. Positions of assemblies 2F1ZN2 (left) and 2F1ZN3 (right) over cycles 12-16

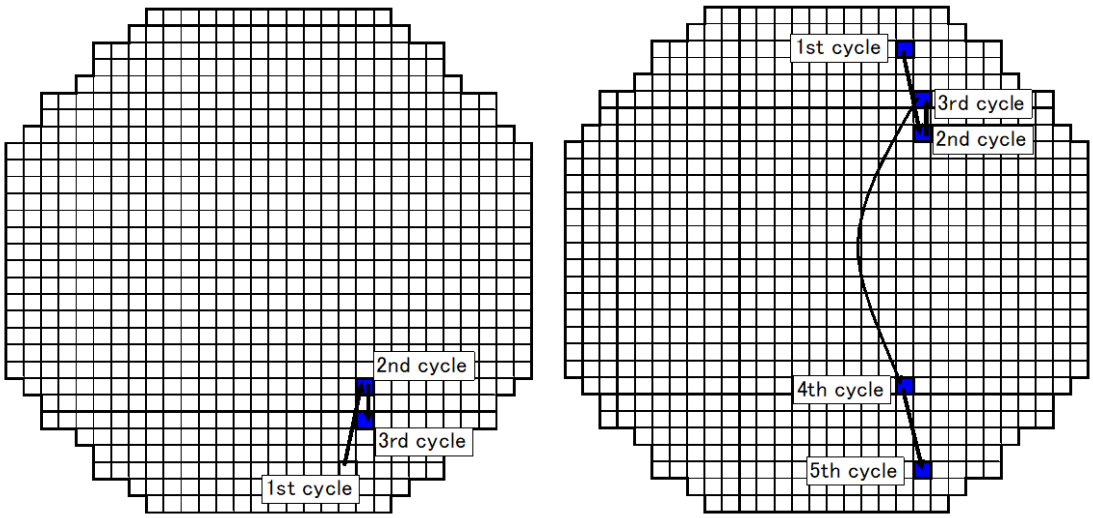

Source: ORNL, 2024.

1.3.1. Power and void history data

Limited axially averaged linear power histories are available for the fuel rods from which the samples were selected, as presented in Figure 3 through Figure 5. Rod numbers are consistent with Figure 1. Power histories for axial locations corresponding to the measured samples are not available. However, burn-up history is available for the axial nodes at the sample elevations [7]. The average nodal power corresponding to a specific irradiation time was derived by dividing the burn-up accumulated over that time and the duration (number of irradiation days). Table 4 through Table 8 list the available cumulative nodal burn-up, the calculated average nodal power, and the node average void fraction for nodes at sample locations.

Table 4. Irradiation histories of nodes 5/6 in assembly 2F1ZN2 [7]

Assembly:2F1ZN2 Node: 5/6

Cycle: 12			
Date[a]	Number of days	Node exposure (MWd/MTU)	Void fraction
07/28/96	Startup	Startup	Startup
08/1/96	4	127	0.139
09/02/96	32	1183	0.125
10/07/96	35	2326	0.134
11/18/96	42	3704	0.142
12/20/96	32	4801	0.153
01/20/97	31	5886	0.170
02/24/97	35	7162	0.199
03/31/97	35	8518	0.225
04/12/97	12	8983	0.225
04/18/97	Startup	Startup	Startup
04/25/97	7	9226	0.246
05/26/97	31	10465	0.245
06/27/97	32	11734	0.227
07/30/97	33	12982	0.191
09/05/97	37	14204	0.166
09/23/97	18	14798	0.166

Cycle: 13			
Date[a]	Number of days	Node exposure (MWd/MTU)	Void fraction
11/02/97	Startup	Startup	Startup
11/10/97	8	15031	0.257
12/06/97	26	15787	0.257
02/15/98	startup	Startup	Startup
02/20/98	5	16270	0.245
03/16/98	24	17245	0.236
04/17/98	32	18536	0.236
05/18/98	31	19780	0.236
06/19/98	32	21064	0.240
07/27/98	38	22616	0.255
08/28/98	32	23962	0.267
09/28/98	31	25279	0.265
10/26/98	28	26443	0.250
11/19/98	24	27397	0.228
12/17/98	28	28510	0.228

Cycle: 14			
Date[a]	Number of days	Node exposure (MWd/MTU)	Void fraction
03/13/99	Startup	Startup	Startup -
03/19/99	6	28592	0.193
04/19/99	31	29728	0.180
05/21/99	32	30861	0.179
06/07/99	17	31458	0.175
07/09/99	32	32592	0.171
08/09/99	31	33680	0.169
09/10/99	32	34803	0.169
10/15/99	35	36046	0.172
11/15/99	31	37140	0.166
12/27/99	42	38567	0.149
01/28/00	32	39558	0.111
02/25/00	28	40359	0.085
04/03/00	38	41321	0.064
04/28/00	25	41916	0.042
05/09/00	11	42178	0.042

a = Format month/day/year (MM/DD/YY)

Table 5. Irradiation histories of nodes 19/20 in 2F1ZN2 [7]

Assembly: 2F1ZN2 Node: 19/20

Cycle: 12			
Date[a]	Number of days	Node exposure (MWd/MTU)	Void fraction
07/28/96	Startup	Startup	Startup
08/01/96	4	127	0.676
09/02/96	32	1183	0.676
10/07/96	35	2326	0.691
11/18/96	42	3704	0.692
12/20/96	32	4801	0.702
01/20/97	31	5886	0.712
02/24/97	35	7162	0.725
03/31/97	35	8518	0.736
04/12/97	12	8834	0.736
04/18/97	Startup	Startup	Startup
04/25/97	7	9226	0.742
05/26/97	31	10465	0.743
06/27/97	32	11734	0.740
07/30/97	33	12982	0.744
09/05/97	37	14204	0.732
09/23/97	18	14789	0.732

Cycle: 13			
Date[a]	Number of days	Node exposure (MWd/MTU)	Void fraction
11/02/97	Startup	Startup	Startup
11/10/97	8	15031	0.770
12/06/97	26	15787	0.770
02/15/98	Startup	Startup	Startup
02/20/98	5	16270	0.765
03/16/98	24	17245	0.763
04/17/98	32	18536	0.764
05/18/98	31	19780	0.765
06/19/98	32	21064	0.766
07/27/98	38	22616	0.768
08/28/98	32	23962	0.769
09/28/98	31	25279	0.768
10/26/98	28	26443	0.763
11/19/98	24	27397	0.765
12/17/98	28	28510	0.765

Cycle: 14			
Date[a]	Number of days	Node exposure (MWd/MTU)	Void fraction
03/13/99	Startup	Startup	-
03/19/99	6	28592	0.729
04/19/99	31	29728	0.733
05/21/99	32	30861	0.743
06/07/99	17	31458	0.734
07/09/99	32	32592	0.737
08/09/99	31	33680	0.738
09/10/99	32	34803	0.736
10/15/99	35	36046	0.734
11/15/99	31	37140	0.729
12/27/99	42	38567	0.730
01/28/00	32	39558	0.712
02/25/00	28	40359	0.714
04/03/00	38	41321	0.708
04/28/00	25	41916	0.688
05/09/00	11	42178	0.688

a = Format month/day/year (MM/DD/YY)

Table 6. Irradiation histories of nodes 5/6 in 2F1ZN3 [7]

Assembly: 2F1ZN3 Node: 5/6

Cycle: 12			
Date[a]	Number of days	Node exposure (MWd/MTU)	Void fraction
07/28/96	Startup	Startup	Startup
08/01/96	4	127	0.139
09/02/96	32	1183	0.125
10/07/96	35	2326	0.134
11/18/96	42	3704	0.142
12/20/96	32	4801	0.153
01/20/97	31	5886	0.170
02/24/97	35	7162	0.199
03/31/97	35	8518	0.225
04/12/97[a]	12	8983	0.225
04/18/97	Startup	Startup	Startup
04/25/97	7	9226	0.246
05/26/97	31	10465	0.245
06/27/97	32	11734	0.227
07/30/97	33	12982	0.191
09/05/97	37	14204	0.166
09/23/97	18	14798	0.166

Cycle: 13			
Date[a]	Number of days	Node exposure (MWd/MTU)	Void fraction
11/02/97	Startup	Startup	Startup
11/10/97	8	15031	0.257
12/06/97	26	15787	0.257
02/15/98	Startup	Startup	Startup
02/20/98	5	16270	0.245
03/16/98	24	17245	0.237
04/17/98	32	18536	0.236
05/18/98	31	19780	0.236
06/19/98	32	21064	0.241
07/27/98	38	22616	0.256
08/28/98	32	23962	0.268
09/28/98	31	25279	0.265
10/26/98	28	26443	0.250
11/19/98	24	27397	0.228
12/17/98	28	28510	0.228

Cycle: 14			
Date[a]	Number of days	Node exposure (MWd/MTU)	Void fraction
03/13/99	Startup	Startup	Startup
03/19/99	6	28592	0.193
04/19/99	31	29728	0.18
05/21/99	32	30861	0.179
06/07/99	17	31458	0.175
07/09/99	32	32592	0.171
08/09/99	31	33680	0.169
09/10/99	32	34803	0.169
10/15/99	35	36046	0.172
11/15/99	31	37140	0.166
12/27/99	42	38567	0.149
01/28/00	32	39558	0.111
02/25/00	28	40359	0.085
04/03/00	38	41321	0.064
04/28/00	25	41916	0.042
05/09/00	11	42178	0.042

Cycle: 15			
Date[a]	Number of days	Node exposure (MWd/MTU)	Void fraction
06/17/00	Startup	Startup	Startup
06/22/00	5	42284	0.152
07/24/00	32	43261	0.135
08/28/00	35	44304	0.136
09/07/00	10	44601	0.133
10/10/00	33	45596	0.138
11/08/00	29	46474	0.135
12/11/00	33	47502	0.150
01/16/01	36	48623	0.150
02/22/01	Startup	Startup	Startup
02/26/01	4	48717	0.156
03/26/01	28	49623	0.161
04/27/01	32	50643	0.154
05/25/01	28	51482	0.132
06/22/01	28	52271	0.095
07/06/01	14	52642	0.087
08/06/01	31	53392	0.041
08/13/01	7	53561	0.041

a = Format month/day/year (MM/DD/YY)

Table 6. Irradiation histories of nodes 5/6 in 2F1ZN3 [7] (cont.)

Assembly: 2F1ZN3 Node: 5/6

Cycle: 16			
Date[a]	**Number of days**	**Node exposure (GWd/MTU)**	**Void fraction**
11/11/01	Startup	Startup	Startup
11/16/01	5	53605	0.000
12/21/01	35	54194	0.000
01/18/02	28	54656	0.000
02/22/02	35	55232	0.000
03/07/02	13	55448	0.000
04/05/02	29	55945	0.001
05/08/02	33	56518	0.001
06/14/02	37	57183	0.002
07/19/02	35	57848	0.004
08/23/02	35	58537	0.006
09/24/02	32	59169	0.004
10/21/02	27	59683	0.003
11/12/02	22	60082	0.003
12/04/02	22	60470	0.001
12/26/02	22	60823	0.000
01/07/03[a]	12	61016	0.000

a = Format month/day/year (MM/DD/YY)

Table 7. Irradiation histories of node 11 in 2F1ZN3 [7]

Assembly: 2F1ZN2 Node: 11

Cycle: 12			
Date[a]	Number of days	Node exposure (MWd/MTU)	Void fraction
07/28/96	Startup	Startup	Startup
08/01/96	4	114	0.466
09/02/96	32	1125	0.455
10/07/96	35	2249	0.471
11/18/96	42	3621	0.477
12/20/96	32	4695	0.491
01/20/97	31	5743	0.508
02/24/97	35	6927	0.534
03/31/97	35	8112	0.557
04/12/97	12	8518	0.557
04/18/97	Startup	Startup	Startup
04/25/97	7	8718	0.568
05/26/97	31	9792	0.567
06/27/97	32	10925	0.556
07/30/97	33	12142	0.535
09/05/97	37	13495	0.509
09/23/97	18	14153	0.509

Cycle: 13			
Date[a]	Number of days	Node exposure (MWd/MTU)	Void fraction
11/02/97	Startup	Startup	Startup
11/10/97	8	14403	0.589
12/06/97[a]	26	15214	0.589
02/15/98	Startup	Startup	Startup
02/20/98	5	15591	0.580
03/16/98	24	16529	0.574
04/17/98	32	17776	0.574
05/18/98	31	18985	0.576
06/19/98	32	20226	0.580
07/27/98	38	21690	0.589
08/28/98	32	22916	0.596
09/28/98	31	24096	0.594
10/26/98	28	25166	0.583
11/19/98	24	26079	0.571
12/17/98	28	28510	0.571

Cycle: 14			
Date[a]	Number of days	Node exposure (MWd/MTU)	Void fraction
03/13/99	Startup	Startup	Startup
03/19/99	6	27284	0.531
04/19/99	31	28416	0.526
05/21/99	32	29577	0.533
06/07/99	17	30196	0.526
07/09/99	32	31392	0.526
08/09/99	31	32558	0.525
09/10/99	32	33752	0.525
10/15/99	35	35043	0.524
11/15/99	31	36181	0.517
12/27/99	42	37706	0.505
01/28/00	32	38829	0.467
02/25/00	28	39805	0.444
04/03/00	38	41100	0.42
04/28/00	25	41957	0.384
05/09/00	11	42178	0.384

Cycle: 15			
Date[a]	Number of days	Node exposure (MWd/MTU)	Void fraction
06/17/00	Startup	Startup	Startup
06/22/00	5	42457	0.479
07/24/00	32	43521	0.465
08/28/00	35	44683	0.473
09/07/00	10	45014	0.461
10/10/00	33	46119	0.471
11/08/00	29	47077	0.463
12/11/00	33	48190	0.481
01/16/01	36	49404	0.481
02/22/01	Startup	Startup	Startup
02/26/01	4	49443	0.481
03/26/01	28	50356	0.486
04/27/01	32	51393	0.481
05/25/01	28	52292	0.459
06/22/01	28	53183	0.418
07/06/01	14	53628	0.419
08/06/01	31	54575	0.351
08/13/01	7	54789	0.000

a = Format month/day/year (MM/DD/YY)

Table 7. Irradiation histories of node 11 in 2F1ZN3 [7] (cont.)

Assembly: 2F1ZN3 Node: 11

Cycle: 16			
Date[a]	**Number of days**	**Node exposure (MWd/MTU)**	**Void fraction**
11/11/01	Startup	Startup	Startup
11/16/01	5	54854	0.161
12/21/01	35	55591	0.152
01/18/02	28	56183	0.159
02/22/02	35	56927	0.165
03/07/02	13	57207	0.164
04/05/02	29	57841	0.172
05/08/02	33	58564	0.185
06/14/02	37	59374	0.204
07/19/02	35	60141	0.222
08/23/02	35	60911	0.228
09/24/02	32	61616	0.213
10/21/02	27	62208	0.210
11/12/02	22	62684	0.207
12/04/02	22	63157	0.170
12/26/02	22	63610	0.139
01/07/03	12	63857	0.139

a = Format month/day/year (MM/DD/YY)

Table 8. Irradiation history of node 19 in 2F1ZN3 [7]

Assembly: 2F1ZN3 Node: 19

Cycle: 12			
Date[a]	Number of days	Node exposure (MWd/MTU)	Void fraction
07/28/96	Startup	Startup	Startup
08/01/96	4	93	0.669
09/02/96	32	925	0.669
10/07/96	35	1870	0.684
11/18/96	42	3039	0.685
12/20/96	32	3936	0.695
01/20/97	31	4812	0.705
02/24/97	35	5791	0.718
03/31/97	35	6756	0.73
04/12/97[a]	12	7087	0.73
04/18/97	Startup	Startup	Startup
04/25/97	7	7250	0.736
05/26/97	31	8118	0.737
06/27/97	32	9047	0.734
07/30/97	33	10077	0.737
09/05/97	37	11344	0.725
09/23/97	18	11960	0.725

Cycle: 13			
Date[a]	Number of days	Node exposure (MWd/MTU)	Void fraction
11/02/97	Startup	Startup	Startup
11/10/97	8	12144	0.763
12/6/97	26	12852	0.763
02/15/98	Startup	Startup	Startup
02/20/98	5	13168	0.758
03/16/98	24	13995	0.756
04/17/98	32	15105	0.757
05/18/98	31	16191	0.758
06/19/98	32	17298	0.759
07/27/98	38	18605	0.761
08/28/98	32	19690	0.762
09/28/98	31	20729	0.761
10/26/98	28	21682	0.756
11/19/98	24	22519	0.757
12/17/98	28	23495	0.571

Cycle: 14			
Date[a]	Number of days	Node exposure (MWd/MTU)	Void fraction
03/13/99	Startup	Startup	Startup
03/19/99	6	23690	0.723
04/19/99	31	24704	0.726
05/21/99	32	25770	0.736
06/07/99	17	26337	0.727
07/09/99	32	27392	0.731
08/09/99	31	28428	0.731
09/10/99	32	29509	0.729
10/15/99	35	30689	0.727
11/15/99	31	31725	0.722
12/27/99	42	33162	0.722
01/28/00	32	34259	0.703
02/25/00	28	35256	0.705
04/03/00	38	36694	0.698
04/28/00	25	37642	0.678
05/09/00	11	38059	0.678

Cycle: 15			
Date[a]	Number of days	Node exposure (MWd/MTU)	Void fraction
06/17/00	Startup	Startup	Startup
06/22/00	5	38159	0.694
07/24/00	32	39188	0.692
08/28/00	35	40334	0.702
09/07/00	10	40655	0.683
10/10/00	33	41675	0.693
11/08/00	29	42565	0.683
12/11/00	33	43576	0.695
01/16/01	36	44679	0.695
02/22/01	Startup	Startup	Startup
02/26/01	4	44753	0.688
03/26/01	28	45612	0.694
04/27/01	32	46598	0.694
05/25/01	28	47476	0.686
06/22/01	28	48384	0.666
07/06/01	14	48846	0.676
08/06/01	31	49887	0.637
08/13/01	7	50122	0.637

a = Format month/day/year (MM/DD/YY)

Table 8. Irradiation history of node 19 in 2F1ZN3 [7] (cont.)

Assembly: 2F1ZN3 Node: 19

Cycle: 16			
Date[a]	Number of days	Node exposure (MWd/MTU)	Void fraction
11/11/01	Startup	Startup	Startup
11/16/01	5	50167	0.435
12/21/01	35	50786	0.439
01/18/02	28	51298	0.451
02/22/02	35	51958	0.465
03/07/02	13	52203	0.449
04/05/02	29	52743	0.461
05/08/02	33	53369	0.474
06/14/02	37	54078	0.484
07/19/02	35	54748	0.498
08/23/02	35	55427	0.504
09/24/02	32	56083	0.497
10/21/02	27	56664	0.504
11/12/02	22	57149	0.508
12/04/02	22	57645	0.491
12/26/02	22	58156	0.467
01/07/03	12	58156	0.467

a = Format month/day/year (MM/DD/YY)

Figure 3. Maximum and average linear power rate histories of assembly 2F1ZN3 [13]

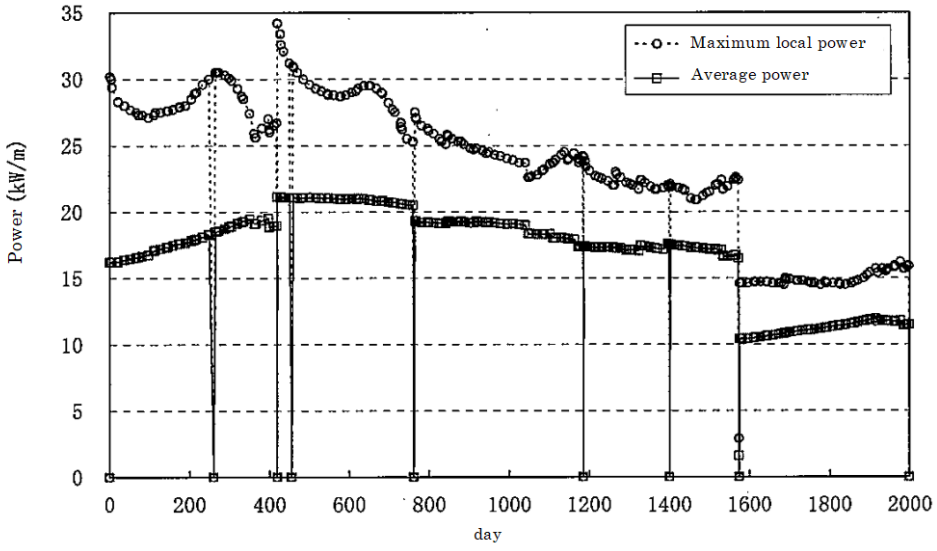

Source: ORNL, 2024.

Figure 4. Linear power rate around node 7 of assembly 2F2ZN2 [13]

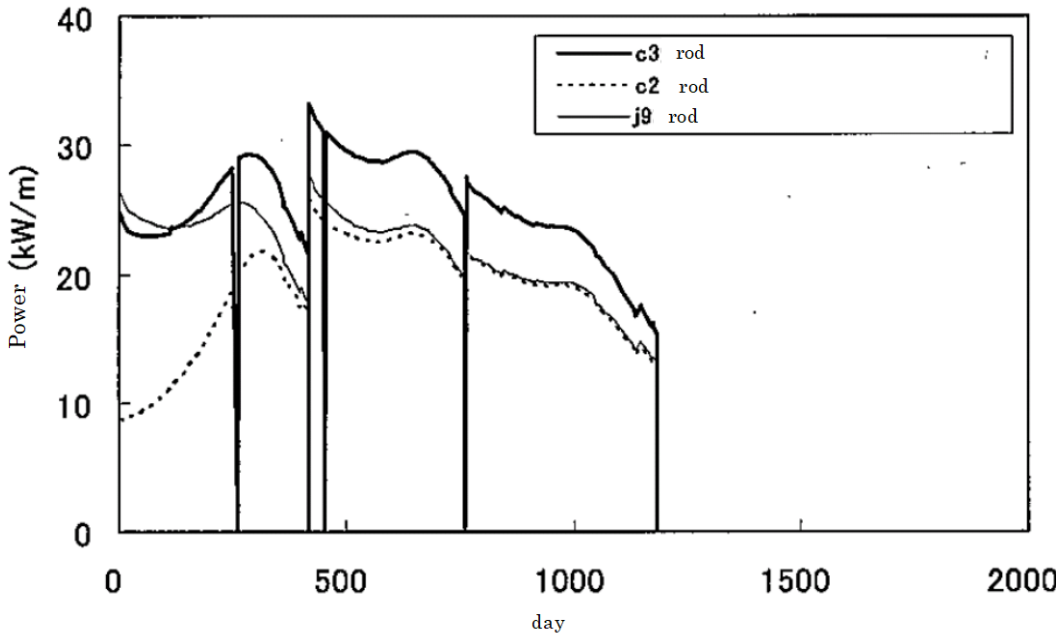

Source: ORNL, 2024.

Figure 5. Linear power rate around node 7 of assembly 2F2ZN3 [13]

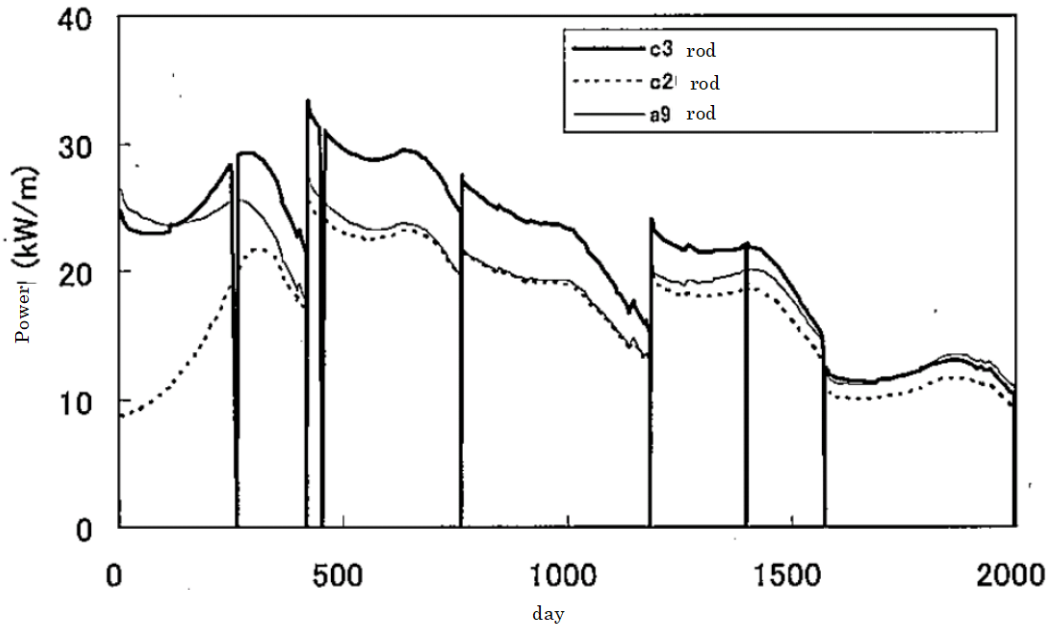

Source: ORNL, 2024.

1.4. Fuel sample data

Fuel samples were cut from bottom, middle and top elevations of UO_2 and UO_2-Gd_2O_3 fuel rods. The initial ^{235}U enrichments of the samples range from 2.1 to 4.9%. The fuel in the gadolinia fuel rods contained 5 wt% Gd_2O_3. Sample burn-ups ranged from 29 GWd/MTU (UO_2-Gd_2O_3 sample) to 68.4 GWd/MTU (UO_2 sample). The reported sample burn-ups [1,4] were estimated using the measured ^{148}Nd concentrations. A summary of the sample measurements and their characteristics are provided in Table 9. The sample locations are illustrated in Figure 6. This figure shows the sample locations relative to axial nodes, which were established by dividing the length of the active fuel into 24 equal segments. Top and bottom axial locations of samples from the first measured campaign are provided in [1] according to node location. However, for the second measured campaign of samples, only the axial locations of samples' midpoints were provided [7]. Sample axial locations relative to the bottom of the active fuel are calculated based on the nodal locations of the samples.

Table 9. Summary of Fukushima Daini-1 9×9-9 assembly fuel sample measurements

Assembly ID	Rod ID	Sample ID	Fuel type	Avg. void (%)	Enrichment (% ^{235}U)	Gd content (wt % Gd_2O_3)	Burn-up[b] (GWd/MTU)	Nodal location	Nodal history[a]	Axial location (cm)
2F1ZN2	C2	GdB	UO_2-Gd_2O_3	18	3.0	5.0	35.56	4.9-5.0	5/6	76.4-76.6
		GdT	UO_2-Gd_2O_3	74	3.0	5.0	29.0	18.9[c]	19/20	292.2[c]
	C3	UB	UO_2	18	4.9	0	47.49	5.1-5.4	5/6	79.3–79.5
		UT	UO_2	74	4.9	0	38.9	18.9[c]	19/20	292.1
2F1ZN3	A9	UB	UO_2	18	2.1	0	61.2	5.0-5.3	5/6	77.4-81.4
		UM	UO_2	38	2.1	0	68.0	10.7[c]	11	165.4[c]
		UT	UO_2	60	2.1	0	56.32	18.5-18.7	19	285.4-288.8
	C2	GdB	UO_2-Gd_2O_3	18	3.0	5.0	54.56	5.2[c]	5/6	78.6-82.6
		GdM	UO_2-Gd_2O_3	38	3.0	5.0	57.7	10.7[c]	11	165.4[c]
		GdT	UO_2-Gd_2O_3	60	3.0	5.0	46.32	18.5–18.7	19	285.4-289.4
	C3	UB	UO_2	11	4.9	0	68.25	5.1-5.4	5/6	78.6-82.6
		UM	UO_2	38	4.9	0	68.4	10.6[c]	11	163.9[c]
		UT	UO_2	60	4.9	0	59.05	18.5-18.7	19	285.4-289.4

[a] = average values of two adjacent nodes are used for the samples close to the node boundary.

[b] = reported measured burn-up that was estimated via Nd^{148} content and corrected with Nd^{147} and Nd^{148} absorption [1,2].

[c] = midpoint of axial node [4].

Figure 6. Axial sample locations [1,4]

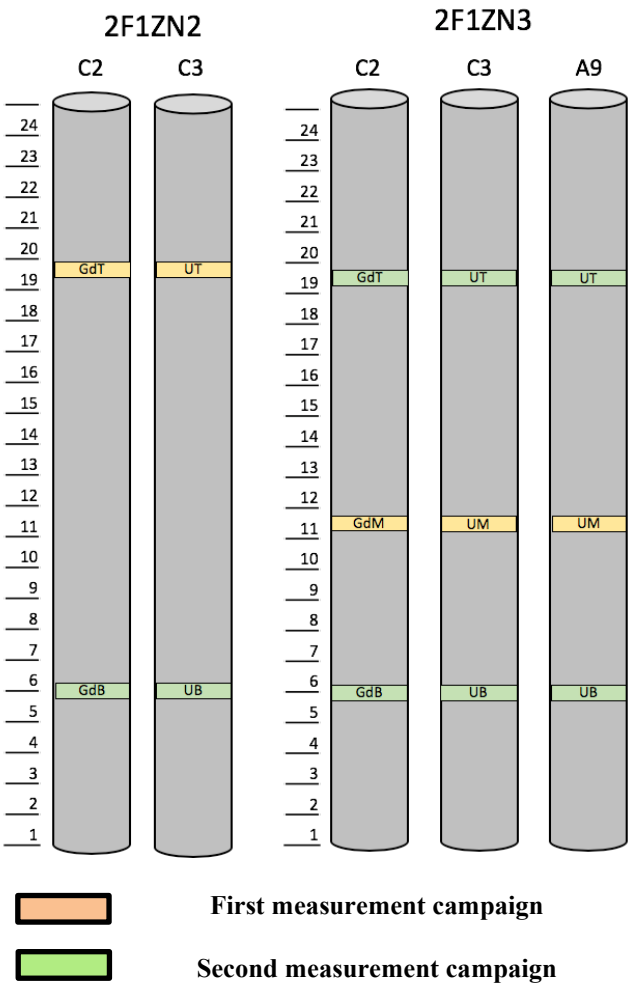

Source: ORNL, 2024.

1.5. Measurement data

The nuclide measurements were performed by the Japan Atomic Energy Agency (JAEA) in two campaigns. The first campaign of measurements only provided U, Pu and Nd isotopes. Isotopic dilution mass spectrometry (ID-MS) was applied to the Nd, U, and Pu isotopes with spikes in the forms of Nd^{150}, U^{233} and Pu^{242}, respectively. The reported measurement uncertainties are less than 0.1% for Nd isotopes, U^{235} and U^{238}; less than 1% for U^{234}; less than 2% for U^{236}; less than 0.3% for $Pu^{239, 240, 241, 242}$; and less than 0.5% for Pu^{238} [1]. No confidence levels are provided for the reported measurement uncertainties, and it is not known if they represent one or two standard deviations.

The second measurement campaign expanded measurements to include fission products. U, Pu and Nd isotopes were measured using ID-MS with thermal ionisation mass spectrometry (TIMS). Gamma spectroscopy was used for Cs^{134}, Cs^{137}, Eu^{154}, and Eu^{155} nuclides. Inventories of the other Eu isotopes as well as for Sm and Gd isotopes were measured using ID-MS with the high-resolution inductively coupled plasma mass spectrometer (HR-ICP-MS).

The measured isotopes and the measurement techniques used are listed in Table 10, and the measurement results are listed in Table 11 [1] and Table 12 [4]. Decay times for the measured sets are provided in Table 13 and Table 14.

Table 10. Measurement techniques and measured nuclides

Technique	Nuclides
ID-MS[a] + TIMS[b]	U^{234}, U^{235}, U^{236}, U^{238}, Pu^{238}, Pu^{239}, Pu^{240}, Pu^{241}, Pu^{242} Nd^{142}, Nd^{143}, Nd^{144}, Nd^{145}, Nd^{146}, Nd^{148}, Nd^{150}
ID-MS[a] + HR-ICP-MS[d]	Eu^{151}, Eu^{153}, Sm^{147}, Sm^{148}, Sm^{149}, Sm^{150}, Sm^{151}, Sm^{152}, Sm^{154} Gd^{152}, Gd^{154}, Gd^{155}, Gd^{156}, Gd^{157}, Gd^{158}, Gd^{160}
CCM[c] + HR-ICP-MS[d]	Mo^{95}, Tc^{99}, Ru^{101}, Rh^{103}, Ag^{109}, Cs^{133}
γ-ray spectroscopy	Cs^{134}, Cs^{137}, Eu^{154}, Eu^{155}
β -LSC[e]	Pm^{147}

[a]ID-MS = isotope dilution mass spectrometry.

[b]TIMS = thermal ionisation mass spectrometry.

[c]CCM = calibration curve method.

[d]HR-ICP-MS = high-resolution inductively coupled plasma mass spectrometry.

[e]β-LSC = β-ray liquid scintillation counting.

Table 11. Measured nuclides (atoms/total final U atoms) from the 1st measurement campaign [1]

Assembly	2F1ZN2		2F1ZN3						Reported relative measurement uncertainty (%)
Rod	C3	C2	C3	C2	A9	C3	C2	A9	
Sample	UB	GdB	UB	GdB	UB	UT	GdT	UT	
Fuel type	UO_2	UO_2-Gd_2O_3	UO_2	UO_2-Gd_2O_3	UO_2	UO_2	UO_2-Gd_2O_3	UO_2	
Axial node	5/6	5/6	5/6	5/6	5/6	19	19	19	
FIMA(%)[a]	4.943	3.685	7.071	5.624	6.266	6.116	4.773	5.766	
Burn-up (GWd/MTU)	47.49	35.56	68.25	54.56	61.2	59.05	46.32	56.32	
Nuclide	Atoms/total U atoms								
U^{234}	3.000E-04	2.000E-04	2.000E-04	1.000E-04	1.000E-04	2.000E-04	1.000E-04	1.000E-04	< 1.0
U^{235}	1.030E-02	6.200E-03	2.400E-03	1.400E-03	1.000E-04	7.300E-03	4.500E-03	7.000E-04	< 0.1
U^{236}	7.000E-03	4.300E-03	7.800E-03	4.700E-03	2.900E-03	7.700E-03	4.700E-03	3.100E-03	< 2.0
U^{238}	9.824E-01	9.893E-01	9.896E-01	9.938E-01	9.969E-01	9.848E-01	9.907E-01	9.961E-01	< 0.1
Pu^{238}	2.195E-04	1.637E-04	4.823E-04	3.559E-04	2.941E-04	5.232E-04	4.042E-04	4.081E-04	< 0.5
Pu^{239}	4.272E-03	4.175E-03	3.803E-03	3.663E-03	3.115E-03	5.586E-03	5.737E-03	4.342E-03	< 0.3
Pu^{240}	2.557E-03	2.560E-03	3.163E-03	3.023E-03	2.665E-03	3.493E-03	3.626E-03	3.128E-03	< 0.3
Pu^{241}	1.002E-03	9.873E-04	1.113E-03	1.068E-03	9.185E-04	1.456E-03	1.496E-03	1.310E-03	< 0.3
Pu^{242}	6.246E-04	6.394E-04	1.528E-03	1.484E-03	2.084E-03	1.025E-03	1.061E-03	1.754E-03	< 0.3
Total Pu	8.675E-03	8.526E-03	1.009E-02	9.593E-03	9.076E-03	1.208E-02	1.232E-02	1.094E-02	
Nd^{142}	5.670E-05	4.000E-05	1.625E-04	1.192E-04	2.008E-04	1.006E-04	7.098E-05	1.609E-04	< 0.1
Nd^{143}	1.846E-03	1.325E-03	1.683E-03	1.309E-03	9.224E-04	2.081E-03	1.582E-03	1.310E-03	< 0.1
Nd^{144}	3.506E-03	2.468E-03	5.926E-03	4.398E-03	5.157E-03	4.486E-03	3.298E-03	4.352E-03	< 0.1
Nd^{145}	1.688E-03	1.216E-03	2.184E-03	1.675E-03	1.662E-03	1.958E-03	1.485E-03	1.621E-03	< 0.1
Nd^{146}	1.734E-03	1.249E-03	2.750E-03	2.093E-03	2.453E-03	2.290E-03	1.722E-03	2.177E-03	< 0.1
Nd^{148}	8.921E-04	6.604E-04	1.307E-03	1.031E-03	1.162E-03	1.122E-03	8.698E-04	1.064E-03	< 0.1
Nd^{150}	4.040E-04	3.149E-04	6.235E-04	5.181E-04	6.109E-04	5.369E-04	4.363E-04	5.659E-04	< 0.1

a Fission per initial metal atom (FIMA).

Table 12. Measured nuclides (atoms/total final U atoms) from the 2nd measurement campaign [4]

Assembly	2F1ZN2				2F1ZN3					
Rod	C2		C3		C2		C3		A9	
Sample	GdT		UT		GdM		UM		UM	
Fuel type	UO_2-Gd_2O_3		UO_2		UO_2-Gd_2O_3		UO_2		UO_2	
Axial node[a]	18.9		18.9		10.7		10.6		10.7	
FIMA(%)[b]	2.889		3.969		5.606		7.079		6.565	
Burn-up (GWd/MTU)	27.89		38.15		54.45		68.42		64.18	
Nuclide	Atom/total U	Unc.(%)	Atom/total U	Unc.(%)	Atom/total U	Unc. (%)	Atom/total U	Unc. (%)	Atom/total U	Unc. (%)
U^{234}	1.699E-04	<1.4	3.293E-04	<1.4	1.407E-04	<1.4	2.336E-04	<1.4	6.870E-05	<1.4
U^{235}	1.123E-02	<0.3	1.743E-02	<0.3	2.320E-03	<0.3	3.687E-03	<0.3	2.300E-04	4
U^{236}	3.799E-03	<0.2	6.269E-03	<0.2	4.796E-03	<0.2	7.889E-03	<0.2	2.917E-03	<0.2
U^{238}	9.848E-01	<0.2	9.760E-01	<0.2	9.927E-01	<0.2	9.882E-01	<0.2	9.968E-01	<0.2
Pu^{238}	1.291E-04	<0.5	1.811E-04	<0.5	3.850E-04	<0.5	5.756E-04	<0.5	4.002E-04	<0.5
Pu^{239}	5.827E-03	<0.2	6.098E-03	<0.2	4.722E-03	<0.2	4.684E-03	<0.2	4.064E-03	<0.2
Pu^{240}	2.325E-03	<0.2	2.386E-03	<0.2	3.576E-03	<0.2	3.583E-03	<0.2	3.276E-03	<0.2
Pu^{241}	7.413E-04	<0.2	6.955E-04	<0.2	9.935E-04	<0.2	1.120E-03	<0.2	1.012E-03	<0.2
Pu^{242}	3.517E-04	<0.2	3.753E-04	<0.2	1.489E-03	<0.2	1.482E-03	<0.2	2.336E-03	<0.2
Nd^{142}	3.150E-05	<0.6	5.069E-05	<0.6	1.251E-04	<0.6	1.495E-04	<0.6	1.926E-04	<0.6
Nd^{143}	1.225E-03	<0.3	1.727E-03	<0.3	1.521E-03	<0.3	1.954E-03	<0.3	1.139E-03	<0.3
Nd^{144}	1.778E-03	<0.3	2.595E-03	<0.3	4.226E-03	<0.3	5.707E-03	<0.3	5.309E-03	<0.3
Nd^{145}	9.669E-04	<0.3	1.364E-03	<0.3	1.681E-03	<0.3	2.194E-03	<0.3	1.761E-03	<0.3
Nd^{146}	9.606E-04	0.3	1.367E-03	0.3	2.093E-03	0.3	2.758E-03	0.3	2.578E-03	0.3
Nd^{148}	5.154E-04	<0.3	7.107E-04	<0.3	1.032E-03	<0.3	1.316E-03	<0.3	1.227E-03	<0.3
Nd^{150}	2.503E-04	<0.7	3.265E-04	<0.7	5.246E-04	<0.7	6.366E-04	<0.7	6.495E-04	<0.7
Cs^{134}	6.450E-06	<4	1.010E-05	<4	4.170E-05	<4	5.350E-05	<4	5.450E-05	<4
Cs^{137}	1.540E-03	<4	2.180E-03	<4	3.470E-03	<4	4.320E-03	<4	3.900E-03	<4
Eu^{151}	2.308E-06	3.8	2.122E-06	1.4	2.037E-06	2.5	1.977E-06	1.3	1.530E-06	1.4
Eu^{153}	1.548E-04	2.6	1.852E-04	1.3	3.089E-04	2.1	3.533E-04	0.5	3.504E-04	0.7
Eu^{154}	1.560E-05	<4	2.000E-05	<4	3.770E-05	<4	4.360E-05	<4	3.830E-05	<4
Eu^{155}	2.690E-06	<6	3.420E-06	<6	9.630E-06	<6	1.130E-05	<6	1.120E-05	<6
Pm^{147}	1.750E-05	<5	2.400E-05	<5	3.650E-05	<5	4.470E-05	<5	3.140E-05	<5
Sm^{147}	4.006E-04	2.1	5.393E-04	1	5.434E-04	1.8	6.624E-04	1.2	4.591E-04	1.2
Sm^{148}	1.858E-04	2.4	2.592E-04	1.1	5.474E-04	1.8	6.923E-04	1.2	6.645E-04	1.2
Sm^{149}	5.097E-06	3.7	6.120E-06	1.9	3.450E-06	3.4	3.809E-06	1.5	3.515E-06	2.1
Sm^{150}	3.785E-04	2.2	5.062E-04	1	7.551E-04	1.8	9.152E-04	1.2	8.217E-04	1.3
Sm^{151}	1.788E-05	2.6	2.213E-05	1.9	1.755E-05	2.4	1.999E-05	1.5	1.613E-05	2.1
Sm^{152}	1.454E-04	1.9	1.789E-04	1	2.479E-04	1.6	2.871E-04	1.1	2.850E-04	1.1
Sm^{154}	6.609E-05	2.4	6.008E-05	1.2	1.302E-04	2	1.315E-04	1.2	1.612E-04	1.2
Gd^{152}	4.965E-05	4.3	9.162E-07	3.8	9.551E-06	5.9	7.599E-07	5.3	2.012E-06	5.8
Gd^{154}	1.397E-03	2	2.708E-05	1.4	1.075E-03	1.6	4.957E-05	1.3	4.477E-05	1.6
Gd^{155}	2.028E-05	8.2	1.025E-05	1.1	2.329E-05	8.5	1.935E-05	1.1	1.913E-05	1.3
Gd^{156}	2.677E-02	1.4	1.168E-04	0.8	2.677E-02	1.2	5.581E-04	0.8	8.463E-04	1
Gd^{157}	1.072E-05	6.2	3.505E-07	2	5.869E-06	10.1	5.287E-07	3.7	8.371E-07	3
Gd^{158}	3.241E-02	1.4	2.083E-05	1.1	3.357E-02	1.2	7.213E-05	0.9	1.176E-04	1.2
Gd^{160}	1.704E-02	1.6	1.653E-06	1.8	1.722E-02	1.4	4.505E-06	1.9	6.649E-06	2.1
Mo^{95}	1.770E-03	3.9	2.456E-03	4	3.154E-03	2.2	4.173E-03	4.5	3.316E-03	2.3
Tc^{99}	1.238E-03	3.1	1.664E-03	3.1	2.172E-03	2.4	2.816E-03	3.5	2.293E-03	2.4
Ru^{101}	1.648E-03	3	2.211E-03	3.1	3.215E-03	2	4.090E-03	3.8	3.844E-03	2.2
Rh^{103}	1.037E-03	2.6	1.259E-03	2.4	1.621E-03	2	1.879E-03	3.7	1.710E-03	1.9
Ag^{109}	1.022E-04	1.9	1.026E-04	2.1	2.296E-04	1.5	2.512E-04	1.5	3.812E-04	1.5
Cs^{133}	1.870E-03	3.9	2.451E-03	3.8	3.329E-03	3.1	4.065E-03	4.8	3.438E-03	3.5

a Relative height over 24 equally spaced nodes.

b Fission per initial metal atom (FIMA).

Table 13. Measurement dates for the 1st measurement campaign [1]

Assembly ID	Rod ID	Sample ID	Measurement Date [a]
2F1ZN2	C2	GdB	10/10/02
	C3	UB	10/10/02
2F1ZN3	A9	UB	10/04/05
		UT	10/04/05
	C2	GdB	08/26/05
		GdT	08/26/05
	C3	UB	08/26/05
		UT	08/26/05

a Format month/day/year MM/DD/YY.

Table 14. Decay times in years for the 2nd measurement campaign [4]

Assembly	2F1ZN2		2F1ZN3		
Rod	C2	C3	C2	C3	A9
Sample	GdT	UT	GdM	UM	UM
U^{234}	9.69	12.21	9.54	7.02	7.02
U^{235}	9.69	12.21	9.54	7.02	7.02
U^{236}	9.69	12.21	9.54	7.02	7.02
U^{238}	9.69	12.21	9.54	7.02	7.02
Pu^{238}	9.69	12.21	9.54	7.02	7.02
Pu^{239}	9.69	12.21	9.54	7.02	7.02
Pu^{240}	9.69	12.21	9.54	7.02	7.02
Pu^{241}	9.69	12.21	9.54	7.02	7.02
Pu^{242}	9.69	12.21	9.54	7.02	7.02
Nd^{142}	9.69	12.21	9.54	7.02	7.02
Nd^{143}	9.69	12.21	9.54	7.02	7.02
Nd^{144}	9.69	12.21	9.54	7.02	7.02
Nd^{145}	9.69	12.21	9.54	7.02	7.02
Nd^{146}	9.69	12.21	9.54	7.02	7.02
Nd^{148}	9.69	12.21	9.54	7.02	7.02
Nd^{150}	9.69	12.21	9.54	7.02	7.02
Cs^{134}	9.73	9.62	7.02	7.02	7.02
Cs^{137}	9.73	9.62	7.02	7.02	7.02
Eu^{151}	10.68	10.48	8.02	7.96	7.96
Eu^{153}	10.68	10.48	8.02	7.96	7.96
Eu^{154}	9.73	9.62	7.08	7.08	7.08
Eu^{155}	9.73	9.62	7.08	7.08	7.08
Pm^{147}	10.70	10.61	8.02	7.96	7.96
Sm^{147}	10.68	10.48	8.02	7.96	7.96
Sm^{148}	10.68	10.48	8.02	7.96	7.96
Sm^{149}	10.68	10.48	8.02	7.96	7.96
Sm^{150}	10.68	10.48	8.02	7.96	7.96
Sm^{151}	10.68	10.48	8.02	7.96	7.96
Sm^{152}	10.68	10.48	8.02	7.96	7.96
Sm^{154}	10.68	10.48	8.02	7.96	7.96
Gd^{152}	10.69	10.48	8.02	7.96	7.96
Gd^{154}	10.69	10.48	8.02	7.96	7.96
Gd^{155}	10.69	10.48	8.02	7.96	7.96
Gd^{156}	10.69	10.48	8.02	7.96	7.96
Gd^{157}	10.69	10.48	8.02	7.96	7.96
Gd^{158}	10.69	10.48	8.02	7.96	7.96
Gd^{160}	10.69	10.48	8.02	7.96	7.96
Mo^{95}	11.65	11.65	8.99	8.99	8.99
Tc^{99}	11.65	11.65	8.99	8.99	8.99
Ru^{101}	11.65	11.65	8.99	8.99	8.99
Rh^{103}	11.65	11.65	8.99	8.99	8.99
Ag^{109}	11.65	11.65	8.99	8.99	8.99
Cs^{133}	11.65	11.65	8.99	8.99	8.99

2. Evaluation of experimental data

2.1. Design data

The main design parameters for the analysed 9×9-9 fuel assemblies are provided in validation of SRAC95 Code [1] and the 2013 paper by Suzuki [4]. However, design parameters such as bypass gap widths, channel/central water channel thicknesses, and channel corner radii are not available. Moreover, only rounded dimensions were provided in these sources [1,2]. When publicly available, 9×9-9 assembly parameters with more significant digits were used herein instead of the dimensions provided [1,2]. Missing parameters were supplemented from data for similar assembly designs.

The Fukushima Daini-1 9×9-9 lattice design is illustrated in Figure 7. The Fukushima Daini-1 reactor is a BWR-5 reactor designed to be loaded with C-type lattices [9]. The C-type lattices have equal assembly gap distances and a 6-inch (15.24 cm) lattice pitch based on design data for La Salle and Limerick plants [10]. The outer radius and thickness of the clad is found in the literature [12] with more significant digits; these values are 0.559 cm for the outer radius and 0.0711 cm for the thickness. No public data are available for the central water channel clad thickness. However, the central water channel thickness of the Atrium-10 design is 0.0725 cm, as specified in literature [11]. All supplemental design information found in the literature confirms that the lattice design used in the "Burn-up Credit Criticality Safety Benchmark Phase III-C" [14] can be used to model Fukushima Daini-1 9×9-9 lattices. Therefore, except for fuel rod dimensions and channel corner radius, all assembly design parameters shown in Figure 7 are acquired from the "Burn-up Credit Criticality Safety Benchmark Phase III-C" [14] lattice specifications.

The channel corner radius of the 9×9-9 assembly is not publicly available, so it was assumed to be the same as the channel corner radius of an 8×8 assembly [15]. Note that the accuracy of the channel corner radius is not expected to change the accuracy of nuclide predictions unless the sample is located at the assembly corner. A sensitivity study was performed to show the effect of channel corner radius on nuclide densities for samples from the A9 rod in Section 4.4.4.4.

Figure 7. Fukushima Daini-1 9×9-9 lattice design

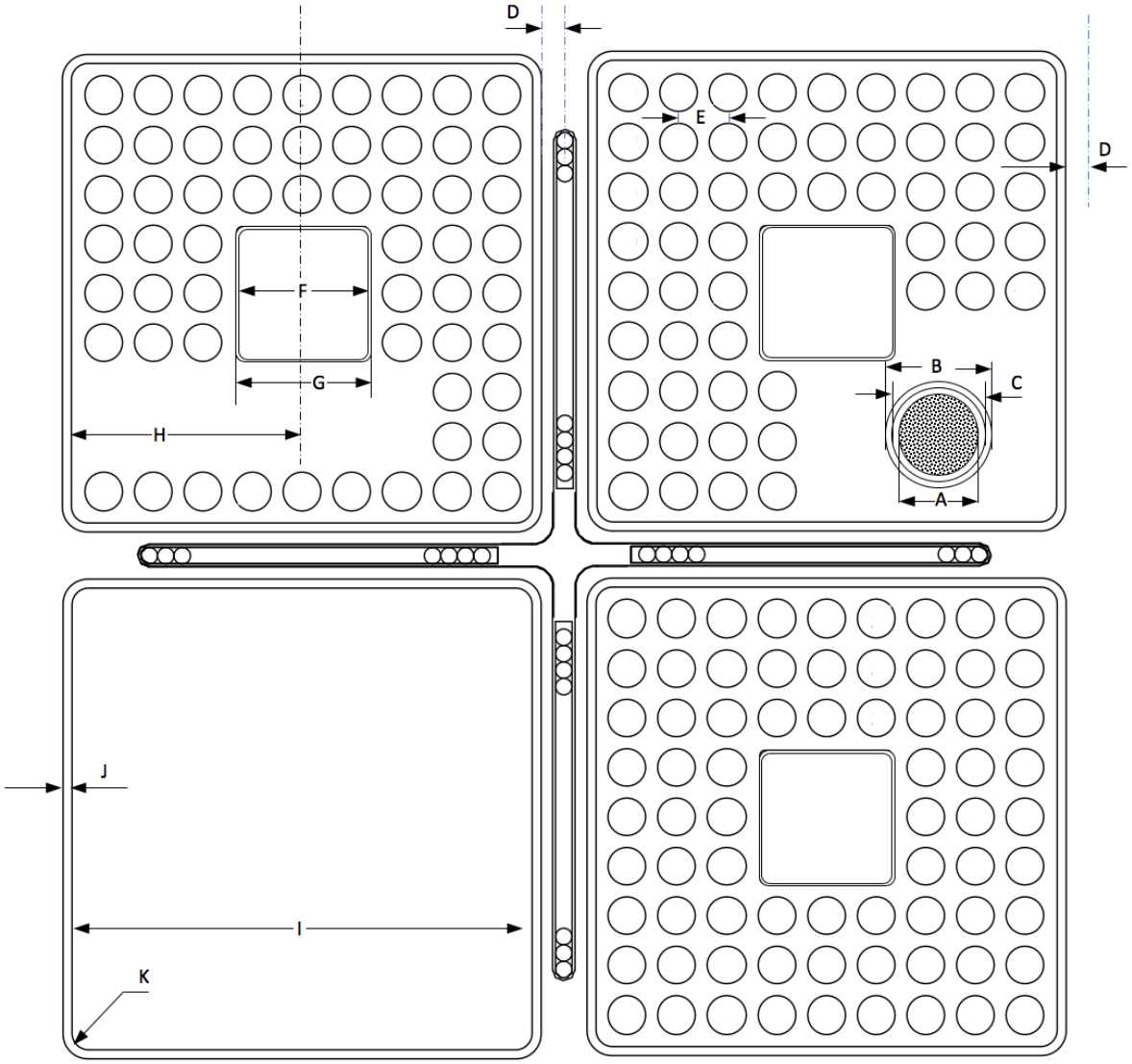

	Fuel Rod			Assembly		Water Box		
Dimension ID	A	B	C	D	E	F	G	H
Dimension (cm)	0.956	1.118	0.9758	0.67	1.45	3.70	3.85	6.70
Dimension ID	I	J	K					
Dimension (cm)	13.4	0.25	0.9652					

Source: ORNL, 2024.

2.2. Material compositions

2.2.1. Density data

2.2.1.1. Fuel density

The density of the UO_2 fuel is derived by multiplying the reference theoretical density (TD) with the provided TD % of the fuel (97%) [1]. The UO_2 reference density is assumed to be 10.96 ± 0.07 g/cm^3 at 273 K [22]. The reference density of Gd_2O_3-UO_2 pellets varies with the gadolinia weight percent in these pellets. Different proprietary correlations based on

different manufacturing processes are used in the industry [19,21]. The correlation expressed in Equation (1) and available in the literature is considered to have acceptable accuracy [32] and is used here:

$$\rho_{fuel}(TD) = \rho_{UO_2}(TD) - 0.031(Gd_2O_3 wt\%) \tag{1}$$

Chamfering and dishing information for the modelled pins is not provided. The dishing volume is assumed to be 1%. To reflect the change in pellet volume, the calculated fuel pellet densities are reduced by the dishing volume, as shown in Equation (2):

$$\rho_{fuel} = \rho_{fuel_{theoretical}} * (\frac{\text{TD }\%}{100}) * (1 - Chamfering\ or\ dishing\ volume\ \%/100) \tag{2}$$

2.2.1.2. Coolant/moderator density

The water density at saturation is a function of the void fraction. Water in the bypass region is assumed to be at saturation with no boiling. This is a valid assumption under normal operation. At saturation, coolant and moderator densities can be calculated from Equation (3) using saturated liquid (0.743 kg/cm^3) and vapour densities (0.0353 kg/cm^3) for the provided core pressure (70.7 kg/cm^2) [16]:

$$\rho_{Coolant} = \rho_l + \alpha(\rho_v - \rho_l), \tag{3}$$

where ρ_l and ρ_v are liquid and vapour water densities at saturation, and α is void fraction. Since void fractions at sample locations are not provided, assuming radially uniform void fraction distribution, node average void fractions for the axial nodes at sample locations (Table 4 through Table 8) are used to calculate coolant densities for each sample. However, intra-nodal void fraction distribution is not uniform and shows variations as a function of pin power and radial location (proximity to the water box and the channel box) [25]. Therefore, the coolant density around the samples can be significantly different than the node's average density.

2.2.1.3. Clad, gap and structural material density

Density of clad, water channel, and assembly channel are assumed to be the same as the Zircaloy-2 nominal density of 6.56 g/cm^3 [23]. The gap is assumed to consist of helium gas, with a density of 1.786E-4 g/cm^3 [23].

2.3. Irradiation history

Power histories for the measured samples are not provided. However, the power histories of the nodes at sample locations are available. If sample power histories are assumed to be proportional to corresponding nodal power histories, or if relative pin power distribution within the assembly does not change significantly with burn-up, then sample-specific powers can be derived by scaling nodal power histories to sample burn-up. This assumption is clearly not valid for gadolinia fuel rods, and the contribution of this assumption to calculated nuclide densities is discussed further in Section 4.4.1.

Since power is calculated through nodal burn-up, assumptions regarding power ramps at startups and shutdowns should be made. Since the first and the last dates at full power are not known, power is assumed to be constant at those depletion intervals.

2.4. Reactor operating conditions

2.4.1. Temperature data

Since temperature information is not available for fuel, clad, coolant or moderator (bypass) regions [1,7], several assumptions were made.

2.4.1.1. Fuel temperature

Fuel temperature varies radially and axially as a function of the axial power shape and coolant temperature. Fuel burn-up is also a determining factor in fuel temperature [17] since it impacts the physical dimensions and the thermal properties of the fuel pin. As shown in Equation (4), geometrically averaged fuel temperatures at different axial locations are available for a GE11 (9×9) fuel assembly [18]. However, Equation (4) does not represent effective fuel temperature for neutronic calculations; nor does it represent actual average fuel temperature based on a parabolic profile [19]. A fuel performance analysis for a GE11 fuel assembly [17] shows that the radially averaged fuel temperature is approximately 100 K lower than that predicted by Equation (4). Therefore, the burn-up independent axial temperature profile provided by Radulescu [18] is adapted with a -100 K bias for nodal temperatures:

$$T_{average}^{fuel} = {}^{1}/_{2}\, T_{surface}^{fuel} + {}^{1}/_{2}\, T_{center}^{fuel} \tag{4}$$

The effects of fuel temperature uncertainty on calculated relative nuclide concentrations are discussed in Section 4.4.3.

2.4.1.2. Coolant/moderator temperature

Since coolant and moderator (bypass) are at saturation at most parts of the fuel assembly, the coolant and moderator are assumed to be at saturated water temperature (559 K) [16] for the provided core pressure (70.7 kg/cm^2). However, it should be noted that during normal operation, moderator and coolant regions can have radial and axial pressure differentials, and subcooling/superheating can exist in water. However, the fuel samples considered herein are not near the top and bottom of the fuel rod where these effects are most likely.

2.4.1.3. Clad, gap and structural material temperature

The temperatures of the fuel gap, clad, and other structural material such as the channel wall and the water channel are at temperatures higher than the coolant. However, the gap and structural material temperatures have negligible effect on neutronics calculations and are assumed to be at the coolant temperature (558.15 K). During normal operation, clad temperature varies from 558-598 K between the outer and inner surfaces of the clad [17]. On the other hand, the gap temperature varies between fuel surface temperature (~750 K) and the clad's inner surface temperature (~598.15 K) until the gap is closed with fuel swelling after 30 GWd/MTU [17].

2.5. Measurements

Okumura et al. [1] and Suzuki et al. [4] list measured contents in atoms relative to total U atoms. Although it is not specified whether the normalisation was performed with final U atoms, the sum of all U atoms adds up to 1.00 and is therefore noted as the final U atoms in this evaluation. Decay times for the first measurement campaign were calculated from the measurement dates in Table 13 and presented in Table 15 in days. For consistency, decay times for the second measurement campaign were converted to days from Table 14 and presented in Table 16.

Table 15. Decay times in days for the first measurement campaign [1]

Assembly	2F1ZN2		2F1ZN3					
Rod	C2	C3	C2		C3		A9	
Sample	GdB	UB	GdB	GdT	UB	UT	UB	UT
U^{234}	884	884	962	962	962	962	1001	1001
U^{235}	884	884	962	962	962	962	1001	1001
U^{236}	884	884	962	962	962	962	1001	1001
U^{238}	884	884	962	962	962	962	1001	1001
Pu^{238}	884	884	962	962	962	962	1001	1001
Pu^{239}	884	884	962	962	962	962	1001	1001
Pu^{240}	884	884	962	962	962	962	1001	1001
Pu^{241}	884	884	962	962	962	962	1001	1001
Pu^{242}	884	884	962	962	962	962	1001	1001
Nd^{142}	884	884	962	962	962	962	1001	1001
Nd^{143}	884	884	962	962	962	962	1001	1001
Nd^{144}	884	884	962	962	962	962	1001	1001
Nd^{145}	884	884	962	962	962	962	1001	1001
Nd^{146}	884	884	962	962	962	962	1001	1001
Nd^{148}	884	884	962	962	962	962	1001	1001
Nd^{150}	884	884	962	962	962	962	1001	1001

Table 16. Decay times in days for the second measurement campaign [4]

Assembly	2F1ZN2		2F1ZN3		
Rod	C2	C3	C2	C3	A9
Sample	GdT	UT	GdM	UM	UM
U^{234}	3536.85	4456.65	3482.10	2562.30	2562.30
U^{235}	3536.85	4456.65	3482.10	2562.30	2562.30
U^{236}	3536.85	4456.65	3482.10	2562.30	2562.30
U^{238}	3536.85	4456.65	3482.10	2562.30	2562.30
Pu^{238}	3536.85	4456.65	3482.10	2562.30	2562.30
Pu^{239}	3536.85	4456.65	3482.10	2562.30	2562.30
Pu^{240}	3536.85	4456.65	3482.10	2562.30	2562.30
Pu^{241}	3536.85	4456.65	3482.10	2562.30	2562.30

Table 16. Decay times in days for the second measurement campaign [4] (continued)

Pu^{242}	3536.85	4456.65	3482.10	2562.30	2562.30
Nd^{142}	3536.85	4456.65	3482.10	2562.30	2562.30
Nd^{143}	3536.85	4456.65	3482.10	2562.30	2562.30
Nd^{144}	3536.85	4456.65	3482.10	2562.30	2562.30
Nd^{145}	3536.85	4456.65	3482.10	2562.30	2562.30
Nd^{146}	3536.85	4456.65	3482.10	2562.30	2562.30
Nd^{148}	3536.85	4456.65	3482.10	2562.30	2562.30
Nd^{150}	3536.85	4456.65	3482.10	2562.30	2562.30
Cs^{134}	3551.45	3511.30	2562.30	2562.30	2562.30
Cs^{137}	3551.45	3511.30	2562.30	2562.30	2562.30
Eu^{151}	3898.20	3825.20	2927.30	2905.40	2905.40
Eu^{153}	3898.20	3825.20	2927.30	2905.40	2905.40
Eu^{154}	3551.45	3511.30	2584.20	2584.20	2584.20
Eu^{155}	3551.45	3511.30	2584.20	2584.20	2584.20
Pm^{147}	3905.50	3872.65	2927.30	2905.40	2905.40
Sm^{147}	3898.20	3825.20	2927.30	2905.40	2905.40
Sm^{148}	3898.20	3825.20	2927.30	2905.40	2905.40
Sm^{149}	3898.20	3825.20	2927.30	2905.40	2905.40
Sm^{150}	3898.20	3825.20	2927.30	2905.40	2905.40
Sm^{151}	3898.20	3825.20	2927.30	2905.40	2905.40
Sm^{152}	3898.20	3825.20	2927.30	2905.40	2905.40
Sm^{154}	3898.20	3825.20	2927.30	2905.40	2905.40
Gd^{152}	3901.85	3825.20	2927.30	2905.40	2905.40
Gd^{154}	3901.85	3825.20	2927.30	2905.40	2905.40
Gd^{155}	3901.85	3825.20	2927.30	2905.40	2905.40
Gd^{156}	3901.85	3825.20	2927.30	2905.40	2905.40
Gd^{157}	3901.85	3825.20	2927.30	2905.40	2905.40
Gd^{158}	3901.85	3825.20	2927.30	2905.40	2905.40
Gd^{160}	3901.85	3825.20	2927.30	2905.40	2905.40
Mo^{95}	4252.25	4252.25	3281.35	3281.35	3281.35
Tc^{99}	4252.25	4252.25	3281.35	3281.35	3281.35
Ru^{101}	4252.25	4252.25	3281.35	3281.35	3281.35
Rh^{103}	4252.25	4252.25	3281.35	3281.35	3281.35
Ag^{109}	4252.25	4252.25	3281.35	3281.35	3281.35
Cs^{133}	4252.25	4252.25	3281.35	3281.35	3281.35

2.6. Sample burn-up

Detailed discussion of burn-up calculations based on measured data of burn-up indicator isotopes – Nd^{148}, Nd^{145}, Nd^{146}, and Cs^{137} – is available in the literature. A detailed summary is available in the SFCOMPO guidance [32]. Three separate burn-up estimates are provided in Suzuki et al. [4]. These estimates are based on analytical calculations using Nd^{148} measurements and core follow calculations using the SRAC and MVP-BURN codes. The average Nd^{148} yield and energy per fission used in these analytical calculations were obtained from MVP-BURN calculations. Additionally, the Nd^{148} concentrations were corrected for $Nd^{147}(n,\gamma)$ reactions. The percent fission per initial metal atom can be calculated as described in ASTM E321-96 [28]:

$$FIMA(\%) = \frac{N^{148}/Y^{148}}{U \ +Np \ +Pu \ +Cm \ +N^{148}/Y^{148}} \times 100, \tag{5}$$

where N_{148}/Y_{148} is the number of fissions based on measured Nd^{148} atom concentration (N_{148}) and effective fission yield of Nd^{148}(Y_{148}). The denominator in Equation (5) also includes the total measured atom concentrations for isotopes of U, Np, Pu, and Cm. Note

that measured Cm and Np concentrations are not available in the literature [14]. However, their contribution to the total sum of heavy metal atoms in the denominator is not significant.

In the present evaluation, the sample burn-ups were estimated based on code calculations (Polaris) by adjusting the nodal power until the calculated Nd^{148} concentrations match the measured Nd^{148} concentrations for each sample. These adjusted nodal powers also account for the difference in the derived node average power (Section 2.2.3) and the actual sample power (not available).

Different burn-up estimates for each sample are listed in Table 17. Reported FIMA values based on estimates with the MVP-BURN depletion code [4] are compared with FIMA values estimated in the current evaluation. The latter FIMA values were calculated using Equation (6) based on the total fission product concentrations predicted by Polaris. Initial uranium number densities are calculated using fuel density as shown in Equation (2), initial enrichments of the samples (see Figure 1) and distribution of the isotopes listed in Table 21:

$$FIMA(\%) = \frac{(Total\ Number\ of\ Fission\ Product\ Atoms\ )/2}{Number\ of\ Initial\ Uranium\ Atoms} \times\ 100 \tag{6}$$

The burn-up of each sample can be calculated from FIMA by multiplying with average energy per fission (C) in Equation (7):

$$Burnup = FIMA(\%)\ \times C, \tag{7}$$

where C(GWd) is energy/fission. Clearly, accurate calculation of FIMA depends on an accurate value of Y_{148}, and an accurate value of burn-up depends on an accurate value of average energy per fission, as well as FIMA. However, burn-up calculations for gadolinia-loaded samples should have additional contributions from the energy released in Gd^{157} and Gd^{155} (n,γ) reactions. The energy release per neutron capture ($\kappa_{n,\gamma}$) can vary based on the nuclear data set used in calculations; this introduces additional uncertainty/bias to burn-up calculations.

Table 17. Sample burn-ups

Assembly/rod/ sample	Burn-up (GWd/MTU)					FIMA (%)	
	Reported measured burn-up [1,2]	Based on SRAC [2]	Based on MVP-BURN [2]	Based on Polaris	Stdev/Mean[a] (%)	Reported measured value [2]	Calculated [Polaris]
2F1ZN2/C2/GDB	35.56	34.25	34.43	35.56	2.0	3.685	3.661
2F1ZN2/C2/GDT	27.89	28.44	28.7	28.17	1.2		2.884
2F1ZN2/C3/UB	47.49	46.51	46.1	46.54	1.3	4.943	4.930
2F1ZN2/C3/UT	38.15	39.05	38.77	37.39	1.9		3.959
2F1ZN3/A9/UB	61.2	56.18	57.24	60.59	4.2	6.266	6.208
2F1ZN3/A9/UM	64.18	60.28	61.29	63.54	3.0		6.504
2F1ZN3/A9/UT	56.32	57.16	57.64	55.73	1.5	5.766	5.725
2F1ZN3/C2/GDB	54.56	52.27	52.59	54.56	2.3	5.624	5.579
2F1ZN3/C2/GDM	54.45	53.82	54.35	55.00	0.9		5.615
2F1ZN3/C2/GDT	46.32	48.98	49.37	46.88	3.2	4.773	4.788
2F1ZN3/C3/UB	68.25	66.81	66.19	66.89	1.3	7.071	7.009
2F1ZN3/C3/UM	68.42	68.06	67.61	67.73	0.5		7.086
2F1ZN3/C3/UT	59.05	62.47	62.05	57.99	3.7	6.116	6.086

a. Stdev and mean are calculated for SRAC, MVP-BURN and Polaris burn-up estimates.

3. Benchmark specifications

3.1. Fuel design data

Based on the data provided in Section 1 and discussions in Chapter 2, data required for the fuel assembly geometry model is listed in Table 18 and illustrated in Figure 7. The radial locations of samples and the enrichment map are illustrated in Figure 8. Fuel, moderator, coolant, and structural material densities are provided in Table 19 and the material temperatures in Table 20. Distribution of isotopes for each material are presented in Table 21.

Table 18. Fukushima Daini-1 9×9-9 assembly geometry parameters

Assembly data	
Assembly type (lattice)	9×9-9
Fuel assembly pitch (cm) [14][a]	15.24
Number of fuel rods [1]	72
Number of gadolinia rods [1]	12
Number of water rods [1]	1 (square channel)
Fuel rod pitch (cm) [1][b]	1.45
Channel thickness (cm) [1] [b]	0.25
Channel bypass gap (cm) [14]	0.67
Channel corner radius [c] (cm) [15]	0.9652
Channel material [1]	Zircaloy-2
Active fuel length (cm) [7]	371
Fuel rod geometry	
Pin radius (cm) [1][g]	0.478
Pin material [1]	UO_2/Gd_2O_3-UO_2
Pin-cladding gap (cm) [1]	0.01
Clad outer radius (cm)[h] [12]	0.559
Clad thickness (cm)[j] [12]	0.0711
Clad material [1]	Zircaloy -2
Water box geometry	
Inner width [k] (cm) [14]	3.70
Outer width (cm) [1]	3.85
Water box material	Zircaloy -2

[a] Rounded number 15.2 cm [1].
[b] Rounded number.
[c] Assumed to be the same as an 8×8 assembly.
[g] Calculated rounded number 0.47 cm [1].
[h] Based on similar 9×9 GE11/GE13 dimensions. Rounded number 0.55 [1].
[j] Based on similar 9×9 GE11/GE13 dimensions. Rounded number 0.07 [1].
[k] Based on the thickness provided in BWR numerical benchmark [14]. This value is close to Atrium 10 water box thickness [11], which yields to an inner width of 3.685 cm.

Figure 8. Enrichment profile of the Fukushima Daini-1 9×9-9 assemblies

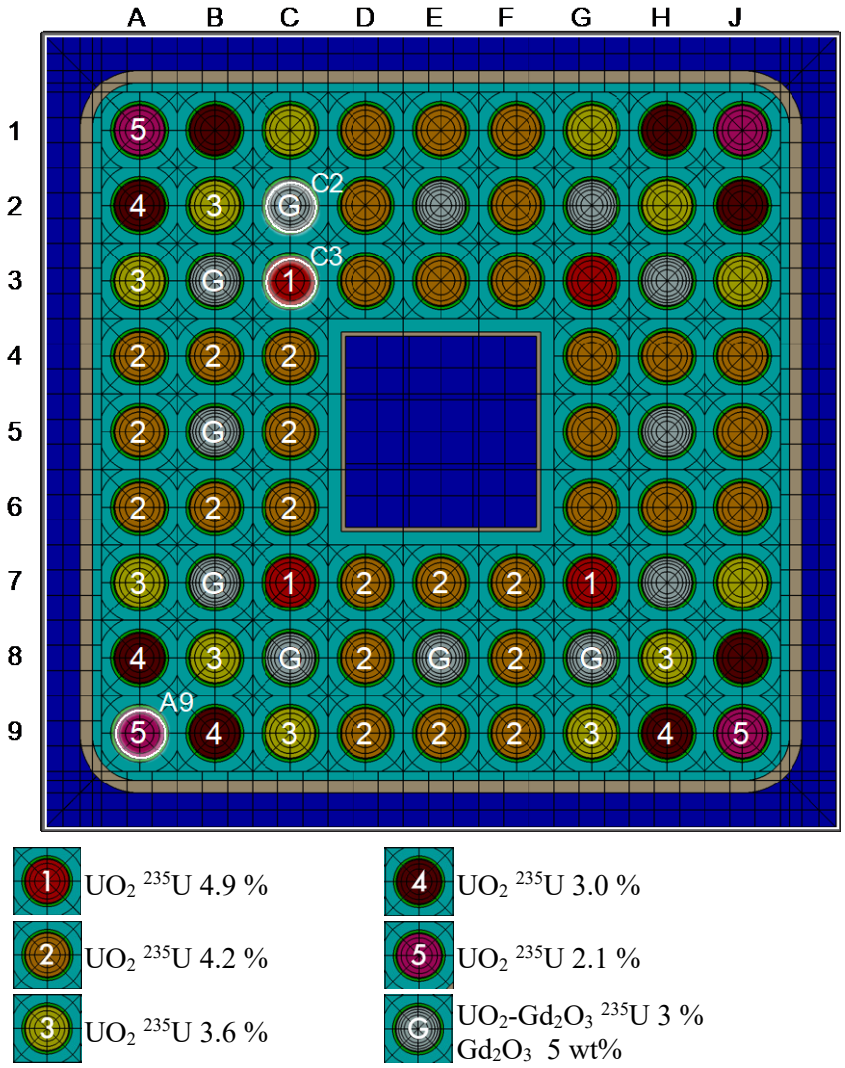

Source: ORNL, 2024.

3.2. Material compositions and temperature(s)

Material densities and temperatures used in modelling 2F1ZN2 and 2F1ZN3 assemblies are listed in Table 19 and Table 20, respectively. Fuel and structural material isotope distributions are calculated using the predefined isotopic distributions of the material as available in SCALE [22] and are presented in Table 21. The isotopic distributions for U are based on the provided U^{235} enrichments and the U isotopic correlations in [22].

Table 19. Fukushima Daini-1 9×9-9 assembly material densities

Fuel density	g/cm³
Gd_2O_3-UO_2	10.32
UO_2	10.52
Coolant/moderator density	
Saturated liquid	0.7430
Saturated vapour	0.0353
Clad/water box/channel wall material	6.56
Fuel gap density	1.786E-4

Table 20. Fukushima Daini-1 9×9-9 assembly material temperatures

Axial fuel temperature	K
2F1ZN2/C2/GdT, 2F1ZN2/C3/UT, 2F1ZN3/C2/GdT,2F1ZN3/C3/UT, 2F1ZN3/A9/UT	800.00
2F1ZN3/C2/GdM,2F1ZN3/C3/UM, 2F1ZN3/A9/UM	900.00
2F1ZN2/C2/GdB, 2F1ZN2/C3/UB, 2F1ZN3/C2/GdB,2F1ZN3/C3/UB, 2F1ZN3/A9/UB	800.00
Coolant/moderator temperature	559.00
Clad/water box/channel wall temperature	559.00

Table 21. Fukushima Daini-1 9×9-9 assembly fuel material initial isotopic composition [23]

Material	Isotope	Weight fraction (%)
Zircaloy-2	Zr^{*}	98.250
	Sn^{*}	1.450
	Fe^{*}	0.135
	Cr^{*}	0.100
	Ni^{*}	0.055
	Hf^{*}	0.010
Gadolinium*	Gd^{152}	0.193
	Gd^{154}	2.134
	Gd^{155}	14.581
	Gd^{156}	20.297
	Gd^{157}	15.617
	Gd^{158}	24.946
	Gd^{160}	22.232
Uranium (4.9 % ^{235}U)**	U^{234}	0.043
	U^{235}	4.900
	U^{236}	0.023
	U^{238}	95.034
Uranium (4.2 % ^{235}U)**	U^{234}	0.037
	U^{235}	4.200
	U^{236}	0.019
	U^{238}	95.744
Uranium (3.6 % ^{235}U)**	U^{234}	0.031
	U^{235}	3.600
	U^{236}	0.017
	U^{238}	96.352
Uranium (3.0 % ^{235}U)**	U^{234}	0.025
	U^{235}	3.000
	U^{236}	0.014
	U^{238}	96.961
Uranium (2.1 % ^{235}U)**	U^{234}	0.017
	U^{235}	2.100
	U^{236}	0.010
	U^{238}	97.873

*From natural abundance.
**Bowman and Suto [34].

3.3. Reactor operating conditions

The irradiation and void fraction histories for the analysed samples are listed in Table 23 through Table 34. For convenience, coolant densities corresponding to void fractions are calculated using steam tables as described in Section 2.2.1.2. and as presented in Table 35 through Table 39.

3.4. Model simplifications

There is no simplification or approximation in the benchmark model compared to the information provided in Chapter 1.

Table 22. Irradiation history of sample C2/GdT in assembly 2F1ZN2 [7]

CYCLE12		
Time (days)	Void fraction (%)	Power (MW/MTU)
4	67.6	17.02
16	67.6	18.91
16	67.6	18.91
17.5	69.1	19.58
17.5	69.1	19.58
21	69.2	20.29
21	69.2	20.29
16	70.2	20.41
16	70.2	20.41
15.5	71.2	20.58
15.5	71.2	20.58
17.5	72.5	20.43
17.5	72.5	20.43
17.5	73.6	20.17
17.5	73.6	20.17
12	73.6	20.17
6		0.00
7	74.2	16.89
15.5	74.3	20.43
15.5	74.3	20.43
16	74	21.21
16	74	21.21
16.5	74.4	22.75
16.5	74.4	22.75
18.5	73.2	24.88
18.5	73.2	24.88
18	73.2	24.88
40		0.00

CYCLE13		
Time (days)	Void fraction (%)	Power (MW/MTU)
8	77	17.00
26	77	17.00
71		0.00
5	76.5	61.25
12	76.3	25.28
12	76.3	25.28
16	76.4	25.58
16	76.4	25.58
15.5	76.5	25.89
15.5	76.5	25.89
16	76.6	25.70
16	76.6	25.70
19	76.8	25.52
19	76.8	25.52
16	76.9	25.25
16	76.9	25.25
31	76.8	25.07
28	76.3	25.38
24	76.5	26.08
28	76.5	26.08
86		0.00

CYCLE14		
Time (days)	Void fraction (%)	Power (MW/MTU)
6	72.9	24.95
31	73.3	24.40
32	74.3	24.82
17	73.4	24.89
32	73.7	24.57
31	73.8	24.98
32	73.6	25.15
35	73.4	25.07
31	72.9	25.12
21	73	25.64
21	73	25.64
32	71.2	25.73
28	71.4	26.83
19	70.8	28.41
19	70.8	28.41
25	68.8	28.40
11	68.8	28.40

Table 23. Irradiation history of sample C2/GdB in assembly 2F1ZN2 [7]

CYCLE12		
Time (days)	Void fraction (%)	Power (MW/MTU)
4	13.9	26.77
16	12.5	27.82
16	12.5	27.82
17.5	13.4	27.53
17.5	13.4	27.53
14	14.2	27.66
14	14.2	27.66
14	14.2	27.66
16	15.3	28.9
16	15.3	28.9
15.5	17	29.51
15.5	17	29.51
11.67	19.9	30.74
11.67	19.9	30.74
11.67	19.9	30.74
11.67	22.5	32.66
11.67	22.5	32.66
11.67	22.5	32.66
12	22.5	32.66
6		0
7	25	29.28
10.33	25	33.7
10.33	25	33.7
10.33	25	33.7
10.67	23	33.43
10.67	23	33.43
10.67	23	33.43
11	19	31.88
11	19	31.88
11	19	31.88
12.33	17	27.85
12.33	17	27.85
12.33	17	27.85
9	17	27.85
9	17	27.85
40		0

CYCLE13		
Time (days)	Void fraction (%)	Power (MW/MTU)
8	26	24.5
13	26	24.5
13	26	24.5
71		0
5	25	81.5
12	24	34.25
12	24	34.25
16	24	34.01
16	24	34.01
15.5	24	33.83
15.5	24	33.83
16	24	33.83
16	24	33.83
19	26	34.43
19	26	34.43
16	27	35.46
16	27	35.46
15.5	27	35.82
15.5	27	35.82
28	25	35.05
24	23	33.51
28	23	33.51
86		0

CYCLE14		
Time (days)	Void fraction (%)	Power (MW/MTU)
6	19.3	11.52
31	18	30.9
32	17.9	29.85
17	17.5	29.61
32	17.1	29.88
31	16.9	29.59
32	16.9	29.59
35	17.2	29.94
31	16.6	29.75
42	14.9	28.65
32	11.1	26.11
28	8.5	24.12
38	6.4	21.34
25	4.2	20.07
11	4.2	20.07

Table 24. Irradiation history of sample C3/UT in assembly 2F1ZN2 [7]

CYCLE12		
Time (days)	Void fraction (%)	Power (MW/MTU)
4	67.6	22.59
16	67.6	25.10
16	67.6	25.10
17.5	69.1	25.99
17.5	69.1	25.99
14	69.2	26.93
14	69.2	26.93
14	69.2	26.93
16	70.2	27.10
16	70.2	27.10
15.5	71.2	27.31
15.5	71.2	27.31
17.5	72.5	27.13
17.5	72.5	27.13
17.5	73.6	26.77
17.5	73.6	26.77
12	73.6	26.77
6		0.00
7	74.2	22.41
15.5	74.3	27.12
15.5	74.3	27.12
16	74	28.15
16	74	28.15
16.5	74.4	30.18
16.5	74.4	30.18
12.33	73.2	33.02
12.33	73.2	33.02
12.33	73.2	33.02
9	73.2	33.02
9	73.2	33.02
40		0.00
4	67.6	22.59
16	67.6	25.10
16	67.6	25.10
17.5	69.1	25.99
17.5	69.1	25.99
14	69.2	26.93
14	69.2	26.93
14	69.2	26.93
16	70.2	27.10

CYCLE13		
Time (days)	Void fraction (%)	Power (MW/MTU)
8	77	22.56
13	77	22.56
13	77	22.56
71		0.00
5	76.5	81.29
12	76.3	33.55
12	76.3	33.55
10.67	76.4	33.95
10.67	76.4	33.95
10.67	76.4	33.95
15.5	76.5	34.36
15.5	76.5	34.36
16	76.6	34.11
16	76.6	34.11
19	76.8	33.88
19	76.8	33.88
16	76.9	33.51
16	76.9	33.51
15.5	76.8	33.28
15.5	76.8	33.28
28	76.3	33.69
24	76.5	34.60
28	76.5	34.60
86		0.00

CYCLE14		
Time (days)	Void fraction (%)	Power (MW/MTU)
6	72.9	33.11
15.5	73.3	32.39
15.5	73.3	32.39
16	74.3	32.94
16	74.3	32.94
17	73.4	33.03
16	73.7	32.61
16	73.7	32.61
15.5	73.8	33.14
15.5	73.8	33.14
16	73.6	33.38
16	73.6	33.38
35	73.4	33.27
31	72.9	33.34
42	73	34.04
32	71.2	34.14
28	71.4	35.61
38	70.8	37.70
25	68.8	37.69
11	68.8	37.69

Table 25. Irradiation history of sample C3/UB in assembly 2F1ZN2 [7]

CYCLE12		
Time (days)	Void fraction (%)	Power (MW/MTU)
4	13.9	35.04
10.67	12.5	36.42
10.67	12.5	36.42
10.67	12.5	36.42
11.67	13.4	36.04
11.67	13.4	36.04
11.67	13.4	36.04
10.5	14.2	36.20
10.5	14.2	36.20
10.5	14.2	36.20
10.5	14.2	36.20
10.67	15.3	37.83
10.67	15.3	37.83
10.67	15.3	37.83
10.33	17	38.62
10.33	17	38.62
10.33	17	38.62
11.67	19.9	40.23
11.67	19.9	40.23
11.67	19.9	40.23
11.67	22.5	42.75
11.67	22.5	42.75
11.67	22.5	42.75
6	22.5	42.75
6	22.5	42.75
6		0.00
7	25	38.32
10.33	25	44.10
10.33	25	44.10
10.33	25	44.10
10.67	23	43.76
10.67	23	43.76
10.67	23	43.76
11	19	41.73
11	19	41.73
11	19	41.73
18.5	17	36.45
18.5	17	36.45
18	17	36.45
40		0.00

CYCLE13		
Time (days)	Void fraction (%)	Power (MW/MTU)
8	26	32.07
26	25.7	32.07
71		0.00
5	25	106.66
12	24	44.83
12	24	44.83
16	24	44.51
16	24	44.51
15.5	24	44.28
15.5	24	44.28
16	24	44.28
16	24	44.28
19	26	45.07
19	26	45.07
16	27	46.41
16	27	46.41
15.5	27	46.87
15.5	27	46.87
14	25	45.87
14	25	45.87
24	23	43.87
28	23	43.87
86		0.00

CYCLE14		
Time (days)	Void fraction (%)	Power (MW/MTU)
6	19.3	15.08
31	18	40.44
32	17.9	39.07
17	17.5	38.75
32	17.1	39.10
31	16.9	38.73
32	16.9	38.72
35	17.2	39.19
31	16.6	38.95
42	14.9	37.50
32	11.1	34.17
28	8.5	31.57
38	6.4	27.93
25	4.2	26.26
11	4.2	26.26

Table 26. Irradiation history of sample C2/GdT in assembly 2F1ZN3 [7]

CYCLE12		
Time (days)	Void fraction (%)	Power (MW/MTU)
4	66.9	18.61
16	66.9	20.82
16	66.9	20.82
17.5	68.4	21.61
17.5	68.4	21.61
21	68.5	22.28
21	68.5	22.28
16	69.5	22.44
16	69.5	22.44
15.5	70.5	22.62
15.5	70.5	22.62
17.5	71.8	22.39
17.5	71.8	22.39
17.5	73	22.08
17.5	73	22.08
12	73	22.08
6		0.00
7	73.6	18.66
15.5	73.7	22.42
15.5	73.7	22.42
16	73.4	23.24
16	73.4	23.24
16.5	73.7	24.99
16.5	73.7	24.99
12.33	72.5	27.41
12.33	72.5	27.41
12.33	72.5	27.41
18	72.5	27.41
40		0.00

CYCLE13		
Time (days)	Void fraction (%)	Power (MW/MTU)
8	76.3	21.81
13	76.3	21.80
13	76.3	21.80
71		0.00
5	75.8	50.59
12	75.6	27.58
12	75.6	27.58
16	75.7	27.78
16	75.7	27.78
15.5	75.8	28.05
15.5	75.8	28.05
16	75.9	27.69
16	75.9	27.69
12.67	76.1	27.53
12.67	76.1	27.53
12.67	76.1	27.53
32	76.2	27.15
31	76.1	26.84
28	75.6	27.25
24	75.7	27.92
28	57.1	30.45
86		0.00
CYCLE14		
6	72.3	25.96
31	72.6	26.19
32	73.6	26.67
17	72.7	26.70
32	73.1	26.39
31	73.1	26.76
32	72.9	27.05
35	72.7	26.99
31	72.2	26.76
21	72.2	27.39
21	72.2	27.39
32	70.3	27.44
28	70.5	28.51
19	69.8	30.30
19	69.8	30.30
25	67.8	30.36
11	67.8	30.36
39		0.00

CYCLE15		
Time (days)	Void fraction (%)	Power (MW/MTU)
5	69.4	15.96
32	69.2	25.76
35	70.2	26.26
10	68.3	25.65
33	69.3	24.75
29	68.3	24.54
33	69.5	24.54
36	69.5	24.54
37		0.00
4	68.8	14.83
28	69.4	24.56
32	69.4	24.66
28	68.6	25.11
28	66.6	25.97
14	67.6	26.42
31	63.7	26.89
7	63.7	26.89
90		0.00
CYCLE16		
5	43.5	7.19
35	43.9	14.16
28	45.1	14.64
35	46.5	15.10
13	44.9	15.09
29	46.1	14.91
33	47.4	15.19
37	48.4	15.34
35	49.8	15.32
35	50.4	15.53
32	49.7	16.41
27	50.4	17.23
22	50.8	17.65
22	49.1	18.05
22	46.7	18.59
12	46.7	18.59

Table 27. Irradiation history of sample C2/GdM in assembly 2F1ZN3 [7]

CYCLE 12		
Time (days)	Void fraction (%)	Power (MW/MTU)
4	46.6	24.54
16	45.5	27.21
16	45.5	27.21
17.5	47.1	27.65
17.5	47.1	27.65
14	47.7	28.13
14	47.7	28.13
14	47.7	28.13
16	49.1	28.91
16	49.1	28.91
15.5	50.8	29.12
15.5	50.8	29.12
11.67	53.4	29.14
11.67	53.4	29.14
11.67	53.4	29.14
11.67	55.7	29.16
11.67	55.7	29.16
11.67	55.7	29.16
12	55.7	29.16
6		0
7	56.8	24.57
15.5	56.7	29.84
15.5	56.7	29.84
16	55.6	30.49
16	55.6	30.49
11	53.5	31.76
11	53.5	31.76
11	53.5	31.76
12.33	50.9	31.49
12.33	50.9	31.49
12.33	50.9	31.49
9	50.9	31.49
9	50.9	31.49
40		0

CYCLE13		
Time (days)	Void fraction (%)	Power (MW/MTU)
8	6	26.89
13	19.4	26.89
13	19.4	26.89
71		0
5	58	64.80
12	57.4	33.66
12	57.4	33.66
16	57.4	33.56
16	57.4	33.56
15.5	57.6	33.58
15.5	57.6	33.58
16	58	33.40
16	58	33.40
19	58.9	33.18
19	58.9	33.18
16	59.6	33.00
16	59.6	33.00
15.5	59.4	32.79
15.5	59.4	32.79
28	58.3	32.91
24	57.1	32.76
28	57.1	32.76
86		0
CYCLE 14		
6	53.1	20.07
31	52.6	31.45
32	53.3	31.25
17	52.6	31.36
16	52.6	32.19
16	52.6	32.19
15.5	52.5	32.39
15.5	52.5	32.39
16	52.5	32.14
16	52.5	32.14
35	52.4	31.76
31	51.7	31.61
42	50.5	31.27
32	46.7	30.22
28	44.4	30.02
38	42	29.35
25	38.4	29.52
11	38.4	29.52
39		0

CYCLE15		
Time (days)	Void fraction (%)	Power (MW/MTU)
5	47.9	21.17
32	46.5	28.63
35	47.3	28.59
10	46.1	28.50
33	47.1	28.84
29	46.3	28.45
33	48.1	29.05
36	48.1	29.05
37		0
4	48.1	8.35
28	48.6	28.08
32	48.1	27.91
28	45.9	27.65
28	41.8	27.40
14	41.9	27.37
31	35.1	26.31
7	0	26.31
90		0
CYCLE16		
5	16.1	11.22
35	15.2	18.14
28	15.9	18.21
35	16.5	18.31
13	16.4	18.55
29	17.2	18.83
33	18.5	18.87
37	20.4	18.86
35	22.2	18.88
35	22.8	18.95
32	21.3	18.98
27	21	18.89
22	20.7	18.63
22	17	18.51
22	13.9	17.74
12	13.9	17.74

Table 28. Irradiation history of sample C2/GdB in assembly 2F1ZN3 [7]

CYCLE12		
Time (days)	Void fraction (%)	Power (MW/MTU)
4	13.9	28.39
16	12.5	29.51
16	12.5	29.51
11.67	13.4	29.20
11.67	13.4	29.20
11.67	13.4	29.20
14	14.2	29.34
14	14.2	29.34
14	14.2	29.34
16	15.3	30.65
16	15.3	30.65
15.5	17	31.30
15.5	17	31.30
11.67	19.9	32.60
11.67	19.9	32.60
11.67	19.9	32.60
11.67	22.5	34.64
11.67	22.5	34.64
11.67	22.5	34.64
12	22.5	34.64
6		0
7	24.60	31.05
10.33	24.50	35.77
10.33	24.50	35.77
10.33	24.50	35.77
10.67	22.70	35.4
10.67	22.70	35.4
10.67	22.70	35.4
11	19.10	33.84
11	19.10	33.84
11	19.10	33.84
12.33	16.60	29.51
12.33	16.60	29.51
12.33	16.60	29.51
9	16.60	29.51
9	16.60	29.51
40		0

CYCLE13		
Time (days)	Void fraction (%)	Power (MW/MTU)
8	25.7	26.16
13	25.7	26.16
13	25.7	26.16
71		0
5	24.50	85.57
24	23.60	36.33
16	23.60	36.08
16	23.60	36.08
15.5	23.60	35.85
15.5	23.60	35.85
16	24.00	35.88
16	24.00	35.88
19	25.50	36.52
19	25.50	36.52
16	26.70	37.64
16	26.70	37.64
15.5	26.50	37.96
15.5	26.50	37.96
14	25.00	37.17
14	25.00	37.17
24	22.80	35.54
28	22.80	35.54
86		0
CYCLE14		
6	19.3	12.22
15.5	18	32.8
15.5	18	32.8
16	17.9	31.63
16	17.9	31.63
17	17.5	31.4
16	17.1	31.72
16	17.1	31.72
31	16.9	31.38
32	16.9	31.38
35	17.2	31.76
31	16.6	31.53
42	14.9	30.38
32	11.1	27.72
28	8.5	25.55
38	6.4	22.64
25	4.2	21.25
11	4.2	21.25
39		0

CYCLE15		
Time (days)	Void fraction (%)	Power (MW/MTU)
5	15.2	19.43
32	13.5	27.3
35	13.6	26.65
10	13.3	26.56
33	13.8	26.96
29	13.5	27.07
33	15	27.86
36	15	27.86
37		0
4	15.6	20.91
28	16.1	28.93
32	15.4	28.5
28	13.2	26.79
28	9.5	25.2
14	8.7	23.7
31	4.1	21.63
7	4.1	21.63
90		0
CYCLE16		
5	0	7.81
35	0	15.05
28	0	14.75
35	0	14.72
13	0	14.86
29	0.1	15.32
33	0.1	15.53
37	0.2	16.07
35	0.4	16.99
35	0.6	17.6
32	0.4	17.66
27	0.3	17.02
22	0.3	16.22
22	0.1	15.77
22	0	14.35
12	0	14.35

Table 29. Irradiation history of sample C3/UT in assembly 2F1ZN3 [7]

CYCLE12		
Time (days)	Void fraction (%)	Power (MW/MTU)
4	66.9	23.02
16	66.9	25.75
16	66.9	25.75
17.5	68.4	26.73
17.5	68.4	26.73
14	68.5	27.57
14	68.5	27.57
14	68.5	27.57
16	69.5	27.76
16	69.5	27.76
15.5	70.5	27.99
15.5	70.5	27.99
17.5	71.8	27.71
17.5	71.8	27.71
17.5	73	27.30
17.5	73	27.30
12	73	27.30
6		0
7	73.6	23.08
15.5	73.7	27.72
15.5	73.7	27.72
16	73.4	28.75
16	73.4	28.75
11	73.7	30.91
11	73.7	30.91
11	73.7	30.91
12.33	72.5	33.91
12.33	72.5	33.91
12.33	72.5	33.91
9	72.5	33.91
9	72.5	33.91
40		0

CYCLE13		
Time (days)	Void fraction (%)	Power (MW/MTU)
8	76.3	26.97
13	76.3	26.97
13	76.3	26.97
71		0
5	75.8	62.57
12	75.6	34.12
12	75.6	34.12
10.67	75.7	34.35
10.67	75.7	34.35
10.67	75.7	34.35
15.5	75.8	34.69
15.5	75.8	34.69
16	75.9	34.26
16	75.9	34.26
19	76.1	34.07
19	76.1	34.07
16	76.2	33.58
16	76.2	33.58
31	76.1	33.19
28	75.6	33.19
24	75.7	33.70
14	57.1	34.54
14	57.1	37.67
86		37.67
CYCLE14		
6	72.3	32.11
31	72.6	32.39
16	73.6	32.39
16	73.6	32.99
17	72.7	32.99
32	73.1	33.03
31	73.1	32.65
16	72.9	32.65
16	72.9	33.10
17.5	72.7	33.10
17.5	72.7	33.46
31	72.2	33.46
42	72.2	33.39
32	70.3	33.10
28	70.5	33.88
38	69.8	33.95
25	67.8	35.26
11	67.8	37.48
39		37.55

CYCLE15		
Time (days)	Void fraction (%)	Power (MW/MTU)
5	69.4	19.80
32	69.2	31.85
35	70.2	32.44
10	68.3	31.75
33	69.3	30.58
29	68.3	30.38
33	69.5	30.38
36	69.5	30.38
37		0
4	68.8	18.35
28	69.4	30.38
32	69.4	30.52
28	68.6	31.06
28	66.6	32.12
14	67.6	32.68
31	63.7	33.25
7	63.7	33.25
90		0
CYCLE16		
5	43.5	8.90
35	43.9	17.51
28	45.1	18.11
35	46.5	18.68
13	44.9	18.66
29	46.1	18.44
33	47.4	18.79
37	48.4	18.97
35	49.8	18.95
35	50.4	19.21
32	49.7	20.31
27	50.4	21.32
22	50.8	21.83
22	49.1	22.32
22	46.7	23.00
12	46.7	23.00

Table 30. Irradiation history of sample C3/UM in assembly 2F1ZN3 [7]

CYCLE 12		
Time (days)	Void fraction (%)	Power (MW/MTU)
4	46.6	30.54
10.67	45.5	33.85
10.67	45.5	33.85
10.67	45.5	33.85
11.67	47.1	34.41
11.67	47.1	34.41
11.67	47.1	34.41
14	47.7	35
14	47.7	35
14	47.7	35
10.67	49.1	35.96
10.67	49.1	35.96
10.67	49.1	35.96
10.33	50.8	36.22
10.33	50.8	36.22
10.33	50.8	36.22
11.67	53.4	36.25
11.67	53.4	36.25
11.67	53.4	36.25
11.67	55.7	36.28
11.67	55.7	36.28
11.67	55.7	36.28
12	55.7	36.28
6		0
7	56.8	30.57
10.33	56.7	37.12
10.33	56.7	37.12
10.33	56.7	37.12
10.67	55.6	37.94
10.67	55.6	37.94
10.67	55.6	37.94
11	53.5	39.51
11	53.5	39.51
11	53.5	39.51
12.33	50.9	39.18
12.33	50.9	39.18
12.33	50.9	39.18
18	50.9	39.18
40	46.6	0

CYCLE13		
Time (days)	Void fraction (%)	Power (MW/MTU)
8	6	33.45
26	19.4	33.45
71		0
5	58	80.62
12	57.4	41.88
12	57.4	41.88
16	57.4	41.75
16	57.4	41.75
15.5	57.6	41.79
15.5	57.6	41.79
16	58	41.55
16	58	41.55
19	58.9	41.28
19	58.9	41.28
16	59.6	41.05
16	59.6	41.05
15.5	59.4	40.78
15.5	59.4	40.78
14	58.3	40.94
14	58.3	40.94
24	57.1	40.76
14	57.1	40.76
14	57.1	40.76
86		0
CYCLE 14		
6	53.1	24.97
31	52.6	39.13
32	53.3	38.87
17	52.6	39.01
32	52.6	40.05
31	52.5	40.3
32	52.5	39.98
35	52.4	39.52
31	51.7	39.33
42	50.5	38.9
32	46.7	37.6
28	44.4	37.35
38	42	36.51
25	38.4	36.73
11	38.4	36.73
39		0

CYCLE15		
Time (days)	Void fraction (%)	Power (MW/MTU)
5	47.9	26.34
32	46.5	35.63
35	47.3	35.57
10	46.1	35.47
33	47.1	35.88
29	46.3	35.39
33	48.1	36.14
36	48.1	36.14
37		0
4	48.1	10.4
28	48.6	34.94
32	48.1	34.72
28	45.9	34.4
28	41.8	34.1
14	41.9	34.06
31	35.1	32.73
7	0	32.73
90		0
CYCLE16		
5	16.1	13.96
35	15.2	22.56
28	15.9	22.65
35	16.5	22.78
13	16.4	23.08
29	17.2	23.42
33	18.5	23.47
37	20.4	23.46
35	22.2	23.48
35	22.8	23.57
32	21.3	23.61
27	21	23.49
22	20.7	23.18
22	17	23.04
22	13.9	22.06
12	13.9	22.06

Table 31. Irradiation history of sample C3/UB in assembly 2F1ZN3 [7]

CYCLE12		
Time (days)	Void fraction (%)	Power (MW/MTU)
4	13.9	34.80
10.67	12.5	36.17
10.67	12.5	36.17
10.67	12.5	36.17
11.67	13.4	35.80
11.67	13.4	35.80
11.67	13.4	35.80
10.5	14.2	35.97
10.5	14.2	35.97
10.5	14.2	35.97
10.5	14.2	35.97
10.67	15.3	37.58
10.67	15.3	37.58
10.67	15.3	37.58
10.33	17	38.37
10.33	17	38.37
10.33	17	38.37
11.67	19.9	39.96
11.67	19.9	39.96
11.67	19.9	39.96
11.67	22.5	42.47
11.67	22.5	42.47
11.67	22.5	42.47
6	22.5	42.47
6	22.5	42.47
6		0.00
7	24.6	38.06
10.33	24.5	43.85
10.33	24.5	43.85
10.33	24.5	43.85
10.67	22.7	43.40
10.67	22.7	43.40
10.67	22.7	43.40
11	19.1	41.49
11	19.1	41.49
11	19.1	41.49
18.5	16.6	36.17
18.5	16.6	36.17
18	16.6	36.17
40		0.00

CYCLE13		
Time (days)	Void fraction (%)	Power (MW/MTU)
8	25.7	32.07
26	25.7	32.06
71		0.00
5	24.5	104.91
12	23.6	44.53
12	23.6	44.53
16	23.6	44.23
16	23.6	44.23
15.5	23.6	43.95
15.5	23.6	43.95
16	24	43.98
16	24	43.98
19	25.5	44.77
19	25.5	44.77
16	26.7	46.14
16	26.7	46.14
15.5	26.5	46.53
15.5	26.5	46.53
14	25	45.57
14	25	45.57
24	22.8	43.57
28	22.8	43.57
86		0
CYCLE14		
6	19.3	14.98
31	18	40.21
32	17.9	38.78
17	17.5	38.49
32	17.1	38.88
31	16.9	38.48
32	16.9	38.47
35	17.2	38.94
31	16.6	38.65
42	14.9	37.24
32	11.1	33.99
28	8.5	31.32
38	6.4	27.75
25	4.2	26.05
11	4.2	26.05
39		0.00

CYCLE15		
Time (days)	Void fraction (%)	Power (MW/MTU)
5	15.20	23.81
32	13.50	33.47
35	13.60	32.66
10	13.30	32.56
33	13.80	33.06
29	13.50	33.19
33	15.00	34.15
36	15.00	34.15
37		0.00
4	15.60	25.64
28	16.10	35.47
32	15.40	34.94
28	13.20	32.85
28	9.50	30.89
14	8.70	29.05
31	4.10	26.52
7	4.10	26.52
90		0
CYCLE16		
5	0	9.57
35	0	18.44
28	0	18.09
35	0	18.04
13	0	18.22
29	0.1	18.79
33	0.1	19.03
37	0.2	19.70
35	0.4	20.83
35	0.6	21.58
32	0.4	21.65
27	0.3	20.86
22	0.3	19.88
22	0.1	19.34
22	0	17.59
12	0	17.59

Table 32. Irradiation history of sample A9/UT in assembly 2F1ZN3 [7]

CYCLE12		
Time (days)	Void fraction (%)	Power (MW/MTU)
4	66.9	22.79
16	66.9	25.48
16	66.9	25.48
17.5	68.4	26.46
17.5	68.4	26.46
14	68.5	27.27
14	68.5	27.27
14	68.5	27.27
16	69.5	27.47
16	69.5	27.47
15.5	70.5	27.70
15.5	70.5	27.70
17.5	71.8	27.41
17.5	71.8	27.41
17.5	73	27.02
17.5	73	27.02
12	73	27.02
6		0.00
7	73.6	22.84
15.5	73.7	27.44
15.5	73.7	27.44
16	73.4	28.45
16	73.4	28.45
11	73.7	30.59
11	73.7	30.59
11	73.7	30.59
12.33	72.5	33.56
12.33	72.5	33.56
12.33	72.5	33.56
9	72.5	33.56
9	72.5	33.56
40		0.00

CYCLE13		
Time (days)	Void fraction (%)	Power (MW/MTU)
8	76.3	25.73
13	76.3	25.72
13	76.3	25.72
71		0.00
5	75.8	59.68
12	75.6	32.55
12	75.6	32.55
10.67	75.7	32.76
10.67	75.7	32.76
10.67	75.7	32.76
15.5	75.8	33.09
15.5	75.8	33.09
16	75.9	32.67
16	75.9	32.67
19	76.1	32.49
19	76.1	32.49
16	76.2	32.03
16	76.2	32.03
31	76.1	31.65
28	75.6	32.14
24	75.7	32.94
14	57.1	35.93
14	57.1	35.93
86		0.00
CYCLE14		
6	72.3	30.62
31	72.6	30.90
16	73.6	31.47
16	73.6	31.47
17	72.7	31.51
32	73.1	31.14
31	73.1	31.57
16	72.9	31.91
16	72.9	31.91
17.5	72.7	31.84
17.5	72.7	31.84
31	72.2	31.57
42	72.2	32.32
32	70.3	32.38
28	70.5	33.63
38	69.8	35.74
25	67.8	35.82
11	67.8	35.82
39		0.00

CYCLE15		
Time (days)	Void fraction (%)	Power (MW/MTU)
5	69.4	18.91
32	69.2	30.38
35	70.2	30.97
10	68.3	30.28
33	69.3	29.20
29	68.3	29.01
33	69.5	28.91
36	69.5	28.91
37		0.00
4	68.8	17.49
28	69.4	28.98
32	69.4	29.11
28	68.6	29.62
28	66.6	30.63
14	67.6	31.17
31	63.7	31.72
7	63.7	31.72
90		0.00
CYCLE16		
5	43.5	8.49
35	43.9	16.71
28	45.1	17.27
35	46.5	17.81
13	44.9	17.80
29	46.1	17.59
33	47.4	17.91
37	48.4	18.10
35	49.8	18.08
35	50.4	18.33
32	49.7	19.37
27	50.4	20.33
22	50.8	20.83
22	49.1	21.30
22	46.7	21.94
12	46.7	21.94

Table 33. Irradiation history of sample A9/UM in assembly 2F1ZN3 [7]

CYCLE12		
Time (days)	Void fraction (%)	Power (MW/MTU)
4	46.6	28.35
10.67	45.5	31.43
10.67	45.5	31.43
10.67	45.5	31.43
11.67	47.1	31.96
11.67	47.1	31.96
11.67	47.1	31.96
14	47.7	32.50
14	47.7	32.50
14	47.7	32.50
10.67	49.1	33.39
10.67	49.1	33.39
10.67	49.1	33.39
10.33	50.8	33.64
10.33	50.8	33.64
10.33	50.8	33.64
11.67	53.4	33.66
11.67	53.4	33.66
11.67	53.4	33.66
11.67	55.7	33.69
11.67	55.7	33.69
11.67	55.7	33.69
12	55.7	33.69
6		0.00
7	56.8	28.38
10.33	56.7	34.47
10.33	56.7	34.47
10.33	56.7	34.47
10.67	55.6	35.23
10.67	55.6	35.23
10.67	55.6	35.23
11	53.5	36.70
11	53.5	36.70
11	53.5	36.70
12.33	50.9	36.38
12.33	50.9	36.38
12.33	50.9	36.38
9	50.9	36.38
9	50.9	36.38
40		0.00

CYCLE13		
Time (days)	Void fraction (%)	Power (MW/MTU)
8	6	31.07
26	19.4	31.07
71	0	0.00
5	58	74.86
24	57.4	38.89
16	57.4	38.78
16	57.4	38.78
15.5	57.6	38.81
15.5	57.6	38.81
16	58	38.59
16	58	38.59
19	58.9	38.33
19	58.9	38.33
16	59.6	38.13
16	59.6	38.13
15.5	59.4	37.88
15.5	59.4	37.88
14	58.3	38.03
14	58.3	38.03
24	57.1	37.85
14	57.1	37.85
14	57.1	37.85
86		0.00
CYCLE14		
6	53.1	23.19
15.5	52.6	36.33
15.5	52.6	36.33
16	53.3	36.10
16	53.3	36.10
17	52.6	36.23
32	52.6	37.18
31	52.5	37.42
32	52.5	37.13
35	52.4	36.70
31	51.7	36.53
42	50.5	36.13
32	46.7	34.92
28	44.4	34.68
38	42	33.91
25	38.4	34.11
11	38.4	34.11
39		0.00

CYCLE15		
Time (days)	Void fraction (%)	Power (MW/MTU)
5	47.9	24.46
32	46.5	33.09
35	47.3	33.04
10	46.1	32.94
33	47.1	33.31
29	46.3	32.87
33	48.1	33.56
36	48.1	33.56
37		0.00
4	48.1	9.65
28	48.6	32.44
32	48.1	32.24
28	45.9	31.95
28	41.8	31.66
14	41.9	31.63
31	35.1	30.39
7	0	30.39
90		0.00
CYCLE16		
5	16.1	12.97
35	15.2	20.95
28	15.9	21.04
35	16.5	21.15
13	16.4	21.43
29	17.2	21.75
33	18.5	21.80
37	20.4	21.78
35	22.2	21.81
35	22.8	21.89
32	21.3	21.92
27	21	21.82
22	20.7	21.53
22	17	21.39
22	13.9	20.49
12	13.9	20.49

Table 34. Irradiation history of sample A9/UB in assembly 2F1ZN3 [7]

CYCLE12		
Time (days)	Void fraction (%)	Power (MW/MTU)
4	13.9	31.85
10.67	12.5	33.1
10.67	12.5	33.1
10.67	12.5	33.1
11.67	13.4	32.76
11.67	13.4	32.76
11.67	13.4	32.76
14	14.2	32.91
14	14.2	32.91
14	14.2	32.91
10.67	15.3	34.38
10.67	15.3	34.38
10.67	15.3	34.38
10.33	17	35.11
10.33	17	35.11
10.33	17	35.11
11.67	19.9	36.57
11.67	19.9	36.57
11.67	19.9	36.57
11.67	22.5	38.86
11.67	22.5	38.86
11.67	22.5	38.86
12	22.5	38.86
6		0
7	24.6	34.83
10.33	24.5	40.12
10.33	24.5	40.12
10.33	24.5	40.12
10.67	22.7	39.71
10.67	22.7	39.71
10.67	22.7	39.71
11	19.1	37.96
11	19.1	37.96
11	19.1	37.96
12.33	16.6	33.1
12.33	16.6	33.1
12.33	16.6	33.1
9	16.6	33.1
9	16.6	33.1
40		0

CYCLE13		
Time (days)	Void fraction (%)	Power (MW/MTU)
8	25.7	29.34
26	25.7	29.338
71		0
5	24.5	95.99
24	23.6	40.75
16	23.6	40.47
16	23.6	40.47
15.5	23.6	40.22
15.5	23.6	40.22
16	24	40.25
16	24	40.25
19	25.5	40.97
19	25.5	40.97
16	26.7	42.22
16	26.7	42.22
15.5	26.5	42.58
15.5	26.5	42.58
14	25	41.7
14	25	41.7
24	22.8	39.87
14	22.8	39.87
14	22.8	39.87
86		0
CYCLE14		
6	19.3	13.71
15.5	18	36.79
15.5	18	36.79
32	17.9	35.48
17	17.5	35.22
32	17.1	35.58
31	16.9	35.2
32	16.9	35.2
35	17.2	35.62
31	16.6	35.36
42	14.9	34.08
32	11.1	31.09
28	8.5	28.66
38	6.4	25.39
25	4.2	23.83
11	4.2	23.83
39		0

CYCLE15		
Time (days)	Void fraction (%)	Power (MW/MTU)
5	15.2	21.79
32	13.5	30.62
35	13.6	29.89
10	13.3	29.79
33	13.8	30.24
29	13.5	30.37
33	15	31.25
36	15	31.25
37		0
4	15.6	23.46
28	16.1	32.45
32	15.4	31.97
28	13.2	30.05
28	9.5	28.26
14	8.7	26.58
31	4.1	24.27
7	4.1	24.27
90		0
CYCLE16		
5	0	8.76
35	0	16.88
28	0	16.55
35	0	16.51
13	0	16.67
29	0.1	17.19
33	0.1	17.42
37	0.2	18.03
35	0.4	19.06
35	0.6	19.75
32	0.4	19.81
27	0.3	19.09
22	0.3	18.19
22	0.1	17.69
22	0	16.09
12	0	16.09

Table 35. Coolant density histories for cycle 12 for different groups of samples [7]

Date[a]	Number of days	Void fraction (%)				Density (g/cm^3)			
		B*	M*	T1*	T2*	B	M	T1	T2
07/28/96	Startup	Startup	Startup	Startup	Startup	Startup	Startup	Startup	Startup
08/01/96	4	0.139	0.466	0.669	0.676	0.6446	0.4132	0.2695	0.2646
09/02/96	32	0.125	0.455	0.669	0.676	0.6545	0.4210	0.2695	0.2646
10/07/96	35	0.134	0.471	0.684	0.691	0.6482	0.4097	0.2589	0.2540
11/18/96	42	0.142	0.477	0.685	0.692	0.6425	0.4054	0.2582	0.2533
12/20/96	32	0.153	0.491	0.695	0.702	0.6347	0.3955	0.2511	0.2462
01/20/97	31	0.17	0.508	0.705	0.712	0.6227	0.3835	0.2441	0.2391
02/24/97	35	0.199	0.534	0.718	0.725	0.6022	0.3651	0.2349	0.2299
03/31/97	35	0.225	0.557	0.73	0.736	0.5838	0.3488	0.2264	0.2221
04/12/97	12	0.225	0.557	0.73	0.736	0.5838	0.3488	0.2264	0.2221
04/18/97	Startup	Startup	Startup	Startup	Startup	Startup	Startup	Startup	Startup
04/25/97	7	0.246	0.568	0.736	0.742	0.5689	0.3410	0.2221	0.2179
05/26/97	31	0.245	0.567	0.737	0.743	0.5696	0.3417	0.2214	0.2172
06/27/97	32	0.227	0.556	0.734	0.74	0.5824	0.3495	0.2235	0.2193
07/30/97	33	0.191	0.535	0.737	0.744	0.6078	0.3644	0.2214	0.2165
09/05/97	37	0.166	0.509	0.725	0.732	0.6255	0.3828	0.2299	0.2250
09/23/97	18	0.166	0.509	0.725	0.732	0.6255	0.3828	0.2299	0.2250

[a] MM/DD/YY format.

B: 2F1ZN2/C2/GdB, 2F1ZN2/C3/UB, 2F1ZN3/C2/GdB, 2F1ZN3/C3/UB, 2F1ZN3/C3/UB.

M: 2F1ZN3/C2/GdM, 2F1ZN3/C3/UM, 2F1ZN3/C3/UM.

T1: 2F1ZN3/C2/GdT, 2F1ZN3/C3/UT, 2F1ZN3/A9/UT.

T2: 2F1ZN2/C2/GdT, 2F1ZN2/C3/UT.

Table 36. Coolant density histories for cycle 13 for different groups of samples [7]

Date[a]	Number of days	Void fraction (%)				Density (g/cm³)			
		B*	M*	T1*	T2*	B	M	T1	T2
11/02/97	Startup	Startup	Startup	Startup	Startup	Startup	Startup	Startup	Startup
11/10/97	8	0.257	0.589	0.763	0.77	0.5611	0.3262	0.2030	0.1981
12/06/97	26	0.257	0.589	0.763	0.77	0.5611	0.3262	0.2030	0.1981
02/15/98	Startup	Startup	Startup	Startup	Startup	Startup	Startup	Startup	Startup
02/20/98	5	0.245	0.58	0.758	0.765	0.5696	0.3325	0.2066	0.2016
03/16/98	24	0.236	0.574	0.756	0.763	0.5760	0.3368	0.2080	0.2030
04/17/98	32	0.236	0.574	0.757	0.764	0.5760	0.3368	0.2073	0.2023
05/18/98	31	0.236	0.576	0.758	0.765	0.5760	0.3354	0.2066	0.2016
06/19/98	32	0.240	0.580	0.759	0.766	0.5732	0.3325	0.2059	0.2009
07/27/98	38	0.255	0.589	0.761	0.768	0.5625	0.3262	0.2044	0.1995
08/28/98	32	0.267	0.596	0.762	0.769	0.5540	0.3212	0.2037	0.1988
09/28/98	31	0.265	0.594	0.761	0.768	0.5555	0.3226	0.2044	0.1995
10/26/98	28	0.250	0.583	0.756	0.763	0.5661	0.3304	0.2080	0.2030
11/19/98	24	0.228	0.571	0.757	0.765	0.5816	0.3389	0.2073	0.2016
12/17/98	28	0.228	0.571	0.571	0.765	0.5816	0.3389	0.3389	0.2016

[a] MM/DD/YY format.

*B: 2F1ZN2/C2/GdB, 2F1ZN2/C3/UB, 2F1ZN3/C2/GdB, 2F1ZN3/C3/UB, 2F1ZN3/C3/UB.

M: 2F1ZN3/C2/GdM, 2F1ZN3/C3/UM, 2F1ZN3/C3/UM.

T1: 2F1ZN3/C2/GdT, 2F1ZN3/C3/UT, 2F1ZN3/A9/UT.

T2: 2F1ZN2/C2/GdT, 2F1ZN2/C3/UT.

Table 37. Coolant density histories for cycle 14 for different groups of samples [7]

Date[a]	Number of days	Void fraction (%)				Density (g/cm^3)			
		B*	M*	T1*	T2*	B	M	T1	T2
03/13/99	Startup	Startup	Startup	Startup	Startup	Startup	Startup	Startup	Startup
03/19/99	6	0.193	0.531	0.723	0.729	0.6064	0.3672	0.2313	0.2271
04/19/99	31	0.18	0.526	0.726	0.733	0.6156	0.3707	0.2292	0.2243
05/21/99	32	0.179	0.533	0.736	0.743	0.6163	0.3658	0.2221	0.2172
06/07/99	17	0.175	0.526	0.727	0.734	0.6192	0.3707	0.2285	0.2235
07/09/99	32	0.171	0.526	0.731	0.737	0.6220	0.3707	0.2257	0.2214
08/09/99	31	0.169	0.525	0.731	0.738	0.6234	0.3715	0.2257	0.2207
09/10/99	32	0.169	0.525	0.729	0.736	0.6234	0.3715	0.2271	0.2221
10/15/99	35	0.172	0.524	0.727	0.734	0.6213	0.3722	0.2285	0.2235
11/15/99	31	0.166	0.517	0.722	0.729	0.6255	0.3771	0.2320	0.2271
12/27/99	42	0.149	0.505	0.722	0.73	0.6376	0.3856	0.2320	0.2264
01/28/00	32	0.111	0.467	0.703	0.712	0.6644	0.4125	0.2455	0.2391
02/25/00	28	0.085	0.444	0.705	0.714	0.6828	0.4288	0.2441	0.2377
04/03/00	38	0.064	0.42	0.698	0.708	0.6977	0.4458	0.2490	0.2419
04/28/00	25	0.042	0.384	0.678	0.688	0.7133	0.4712	0.2632	0.2561
05/09/00	11	0.042	0.384	0.678	0.688	0.7133	0.4712	0.2632	0.2561

[a] MM/DD/YY format.

*B: 2F1ZN2/C2/GdB, 2F1ZN2/C3/UB, 2F1ZN3/C2/GdB, 2F1ZN3/C3/UB, 2F1ZN3/C3/UB.

M: 2F1ZN3/C2/GdM, 2F1ZN3/C3/UM, 2F1ZN3/C3/UM.

T1: 2F1ZN3/C2/GdT, 2F1ZN3/C3/UT, 2F1ZN3/A9/UT.

T2: 2F1ZN2/C2/GdT, 2F1ZN2/C3/UT.

Table 38. Coolant density histories for cycle 15 for different groups of samples [7]

Date[a]	Number of days	Void fraction (%)			Density (g/cm^3)		
		B*	M*	T1*	B	M	T1
06/17/00	Startup	Startup	Startup	Startup	Startup	Startup	Startup
06/22/00	5	0.152	0.479	0.694	0.6354	0.4040	0.2519
07/24/00	32	0.135	0.465	0.692	0.6475	0.4139	0.2533
08/28/00	35	0.136	0.473	0.702	0.6468	0.4083	0.2462
09/07/00	10	0.133	0.461	0.683	0.6489	0.4168	0.2596
10/10/00	33	0.138	0.471	0.693	0.6453	0.4097	0.2526
11/08/00	29	0.135	0.463	0.683	0.6475	0.4153	0.2596
12/11/00	33	0.150	0.481	0.695	0.6368	0.4026	0.2511
01/16/01	36	0.150	0.481	0.695	0.6368	0.4026	0.2511
02/22/01	Startup	Startup	Startup	Startup	Startup -	Startup	Startup
02/26/01	4	0.156	0.481	0.688	0.6326	0.4026	0.2561
03/26/01	28	0.161	0.486	0.694	0.6291	0.3991	0.2519
04/27/01	32	0.154	0.481	0.694	0.6340	0.4026	0.2519
05/25/01	28	0.132	0.459	0.686	0.6496	0.4182	0.2575
06/22/01	28	0.095	0.418	0.666	0.6758	0.4472	0.2717
07/06/01	14	0.087	0.419	0.676	0.6814	0.4465	0.2646
08/06/01	31	0.041	0.351	0.637	0.7140	0.4946	0.2922
08/13/01	7	0.041	0	0.637	0.7140	0.7430	0.2922

[a] MM/DD/YY format.

*B: 2F1ZN3/C2/GdB, 2F1ZN3/C3/UB, 2F1ZN3/C3/UB.

M: 2F1ZN3/C2/GdM, 2F1ZN3/C3/UM, 2F1ZN3/C3/UM.

T1: 2F1ZN3/C2/GdT, 2F1ZN3/C3/UT, 2F1ZN3/A9/UT.

Table 39. Coolant density histories for cycle 16 for different groups of samples [7]

Date[a]	Number of days	Void fraction (%)			Density (g/cm^3)		
		B*	M*	T1*	B	M	T1
11/11/01	Startup	Startup	Startup	Startup	Startup	Startup	Startup
11/16/01	5	0	0.161	0.435	0.7430	0.6291	0.4352
12/21/01	35	0	0.152	0.439	0.7430	0.6354	0.4323
01/18/02	28	0	0.159	0.451	0.7430	0.6305	0.4238
02/22/02	35	0	0.165	0.465	0.7430	0.6262	0.4139
03/07/02	13	0	0.164	0.449	0.7430	0.6269	0.4252
04/05/02	29	0.001	0.172	0.461	0.7423	0.6213	0.4168
05/08/02	33	0.001	0.185	0.474	0.7423	0.6121	0.4076
06/14/02	37	0.002	0.204	0.484	0.7416	0.5986	0.4005
07/19/02	35	0.004	0.222	0.498	0.7402	0.5859	0.3906
08/23/02	35	0.006	0.228	0.504	0.7388	0.5816	0.3863
09/24/02	32	0.004	0.213	0.497	0.7402	0.5923	0.3913
10/21/02	27	0.003	0.21	0.504	0.7409	0.5944	0.3863
11/12/02	22	0.003	0.207	0.508	0.7409	0.5965	0.3835
12/04/02	22	0.001	0.17	0.491	0.7423	0.6227	0.3955
12/26/02	22	0	0.139	0.467	0.7430	0.6446	0.4125
01/07/03	12	0	0.139	0.467	0.7430	0.6446	0.4125

[a] MM/DD/YY format.

*B: 2F1ZN3/C2/GdB, 2F1ZN3/C3/UB, 2F1ZN3/C3/UB.

M: 2F1ZN3/C2/GdM, 2F1ZN3/C3/UM, 2F1ZN3/C3/UM.

T1: 2F1ZN3/C2/GdT, 2F1ZN3/C3/UT, 2F1ZN3/A9/UT.

4. Uncertainty analysis

Due to the lack of detailed data for assembly design, fuel content and operating condition, the benchmark includes several assumptions. The uncertainties caused by these assumptions can be classified as follows:

- assembly geometry: manufacturing tolerances in specified pin dimensions, channel wall, water box, clad thickness, pin pitch, assembly pitch;
- material composition: manufacturing tolerances in declared enrichments or lack of detailed initial uranium isotopic composition;
- operating history:
  - axial and radial intra-nodal void fraction and pressure distribution;
  - temperature of fuel, coolant, and structural material;
  - fuel and structural material density;
  - sample power history and/or burn-up;
  - geometry changes due to operating history (i.e. gap closure, clad collapse, channel/rod bow).

As a representative set, uncertainties are mainly calculated for samples from the 2F1ZN3 assembly. However, to demonstrate that the other samples follow similar uncertainty trends, results for samples from the 2F1ZN2 assembly are also included in the analysis of major sources of uncertainties.

4.1. Methods

The effect of operating uncertainties was assessed via direct perturbations. While stochastic sampling can be used to estimate the effect of manufacturing tolerances, their contribution to the total uncertainty is expected to be small.

4.2. Code and nuclear data library

Nuclide inventories of the measured samples were predicted using the Polaris 6.3 code within SCALE 6.2.3 with the 56-group ENDF/B-VII.1 neutron cross-section library. Gadolinium-loaded fuel pins were modelled with seven equal volume rings. Details of Polaris models are available in the sample input file provided in the Appendix. Figure 8 illustrates the spatial meshing used in the calculations.

4.3. Parameters and parameter uncertainty values

The uncertainty of each parameter is discussed in detail in the next section.

4.4. Individual parameter uncertainty results

4.4.1. Power history

To accurately model the samples irradiation history, the power or burn-up of each sample should be known as a function of the irradiation time. Nodal power, which is radially averaged across the assembly at the sample elevation, is available from the core simulator.

However, due to heterogeneities in the assembly and the intra-nodal flux gradient, the power generated by the sample can differ from the node's average power. Moreover, the reported nodal power includes uncertainties due to inherent uncertainties in the core simulations.

The benchmark specifications provided in Chapter 3 assume that the power variations at sample locations are proportional to power variations in the nodal power during irradiation. The sample power specified in Chapter 3 was further adjusted herein to ensure that the predicted Nd^{148} concentration in the sample matched the corresponding measured concentration. While this approach for conserving the number of fissions based on Nd^{148} measurements is likely adequate for UO_2 fuel pins, it is not the same for the Gd fuel pins, which are expected to have a sample power history much different than the nodal power history. In this approach, 16 assembly depletion simulations are involved. First, eight simulations are run that use the node average power scaled with the reported sample burn-up corresponding to each of the eight samples. The results from these simulations are used to rescale the sample power based on the ratio of the calculated Nd^{148} content and its corresponding measured value for a total of eight simulations.

A second approach, which is considered more accurate, was used here to derive the sample power. While this approach is code-dependent, it provides a way to estimate the uncertainty in predicted isotope concentrations due to uncertainties in sample power data compared to the powers based on node average data. In this approach, a depletion simulation of the assembly uses the node average power as assembly power; the results provided by the code (Polaris) include a detailed pin power history for each pin in the assembly. After scaling to the reported pin burn-up, this detailed pin power history is then used in eight assembly calculations to determine the nuclides in each measured sample. Figure 9 through Figure 11 show the impact of the power history assumption for three selected samples: 2F1ZN2/C2/GdB, 2F1ZN3/A9/UB, 2F1ZN3/C3/UM. The powers shown in these figures are (1) the sample power obtained by scaling the node average power with the sample burn-up, and (2) the sample power obtained by scaling the pin power history with the sample burn-up. Both adjustments use the derived sample burn-up that ensures the predicted Nd^{148} concentration matches the measured value for this nuclide.

Figure 9. Power histories for the 2F1ZN2/C2/GdB sample

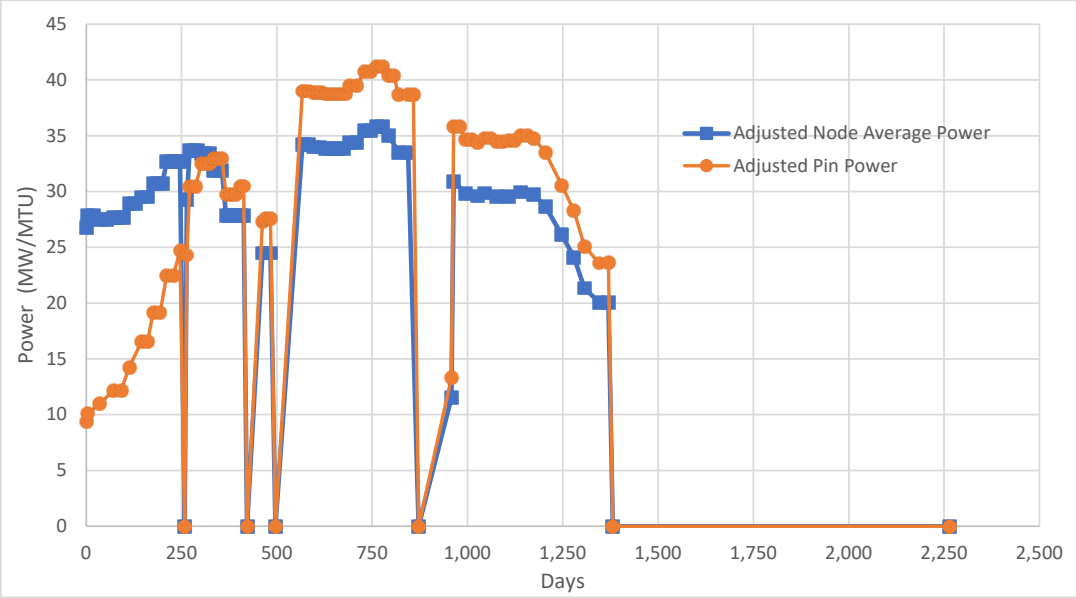

Source: ORNL, 2024.

Figure 10. Power histories for the 2F1ZN3/A9/UB sample

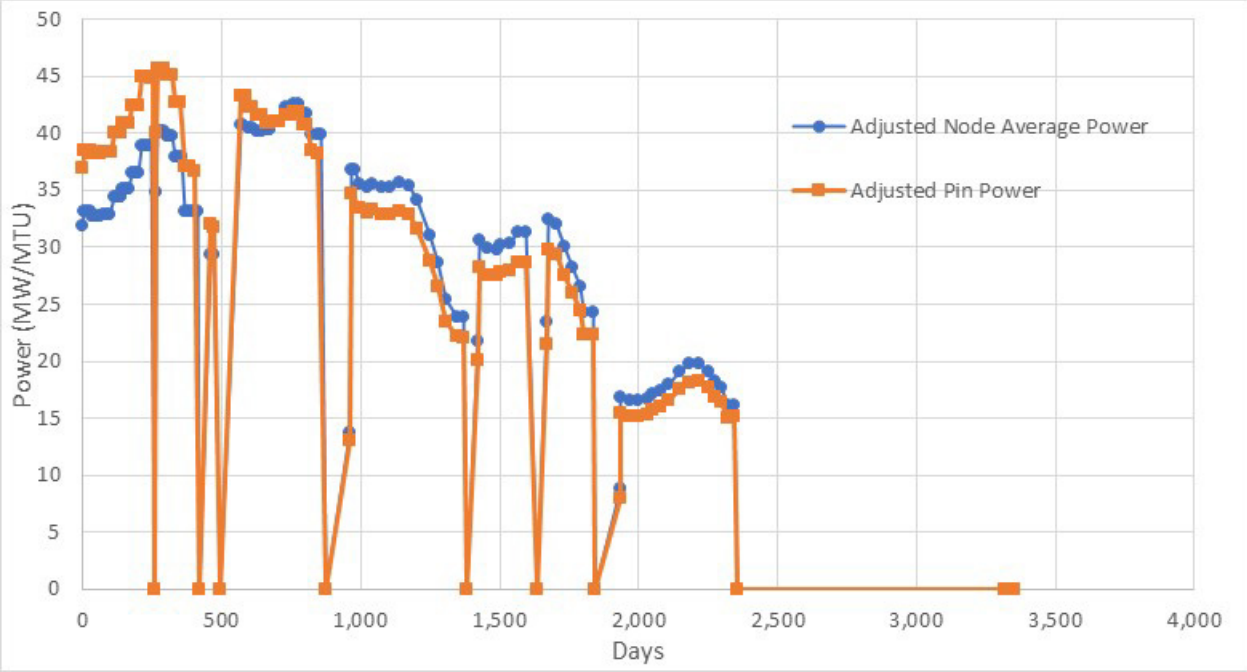

Source: ORNL, 2024.

Figure 11. Power histories for the 2F1/ZN3/C3/UM sample

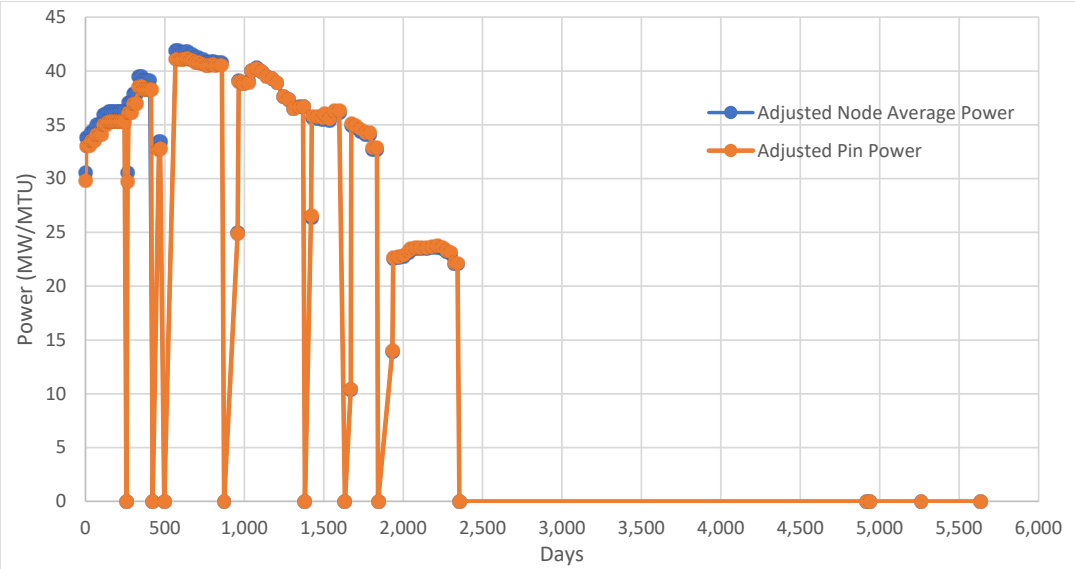

Source: ORNL, 2024.

The difference caused in C/M ratios shown in Equation (8) results from the use of two different sample power estimates, as described above and as shown in Figure 12 and Figure 13 for samples from the 2F1ZN2 and 2F1ZN3 assemblies:

$$\Delta_{C/M} = \frac{C}{M}\Big|_P - \frac{C}{M}\Big|_N , \quad (8)$$

where P is the adjusted pin power, and N is the adjusted node average power.

While the change in U^{235} C/M is less than 1% for most samples, the relative difference for samples in the bottom (2F1Z3/A9/UB) and middle axial location (2F1Z3/A9/UM) increases to 1-2%. The Pu^{238} shows the largest change at >4%. However, special attention should be given to corner rods. The data used in Figure 13 are provided in Table 40.

Figure 12. Change in C/M with sample power approach (pin power-based vs. node power-based) for the 2F1ZN2 assembly samples

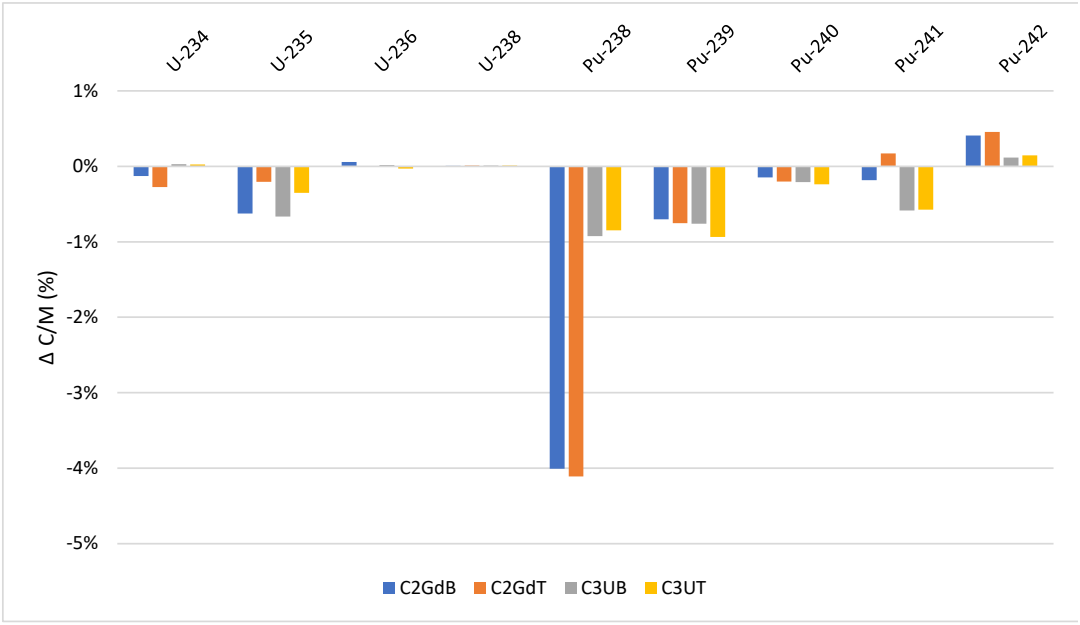

Source: ORNL, 2024.

Figure 13. Change in C/M with sample power approach (pin power-based vs. node power-based) for the 2F1ZN3 assembly samples

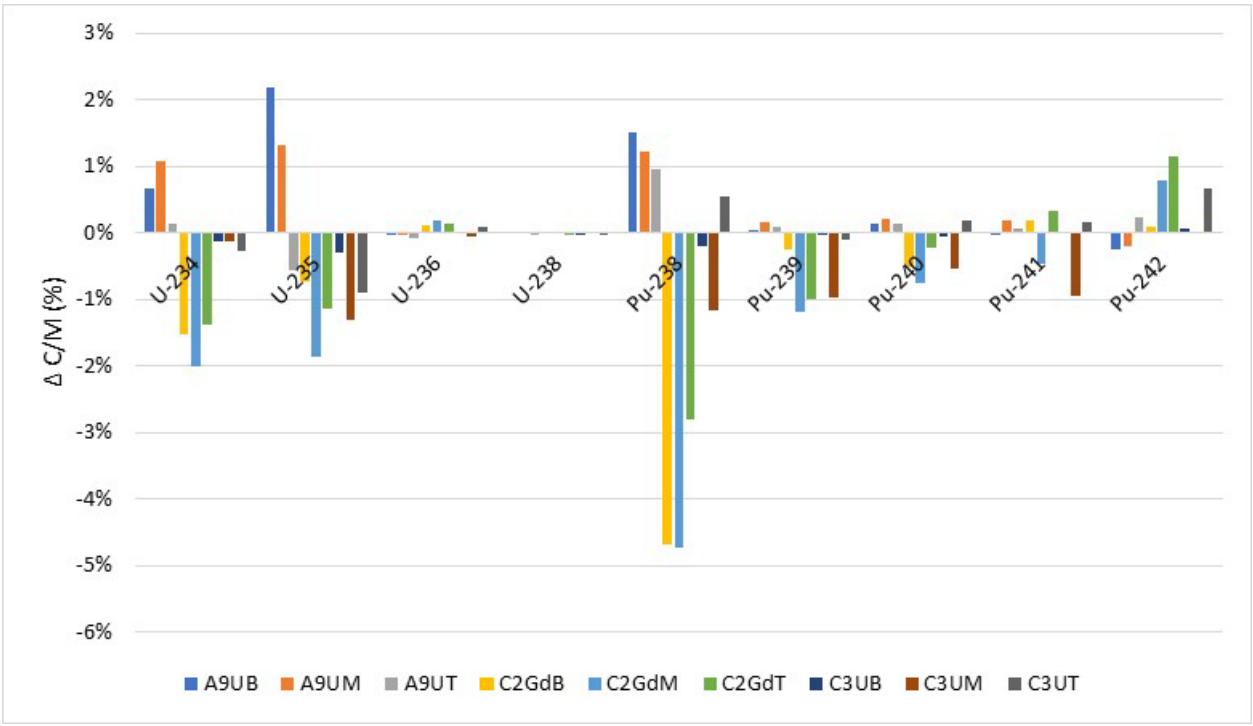

Source: ORNL, 2024.

Table 40. Change in C/M with sample power history for the 2F1ZN3 assembly samples

Isotope	$\Delta_{C/M}$ (%)								
	A9/UB	A9/UM	A9/UT	C2/GdB	C2/GdM	C2/GdT	C3/UB	C3/UM	C3/UT
U^{234}	0.67	1.08	0.14	-1.53	-2.01	-1.38	-0.12	-0.12	-0.27
U^{235}	2.19	1.32	-0.56	-0.74	-1.85	-1.14	-0.30	-1.29	-0.90
U^{236}	-0.01	-0.04	-0.07	0.12	0.18	0.14	0.01	-0.06	0.08
U^{238}	0.01	0.00	-0.01	0.01	0.01	0.00	0.00	0.02	-0.02
Pu^{238}	1.52	1.23	0.97	-4.67	-4.72	-2.79	-0.20	-1.17	0.55
Pu^{239}	0.03	0.17	0.08	-0.24	-1.18	-1.00	-0.04	-0.96	-0.10
Pu^{240}	0.15	0.20	0.13	-0.50	-0.75	-0.22	-0.04	-0.53	0.18
Pu^{241}	-0.02	0.18	0.08	0.18	-0.47	0.33	0.02	-0.93	0.16
Pu^{242}	-0.25	-0.20	0.25	0.09	0.80	1.14	0.07	0.01	0.66
Nd^{148}	-0.09	-0.07	0.20	0.04	0.19	0.38	0.02	-0.12	0.30
Nd^{143}	0.25	0.32	0.10	-0.32	-0.61	-0.06	-0.06	-0.59	0.06
Nd^{145}	-0.07	-0.03	0.14	-0.10	0.06	0.26	0.01	-0.05	0.21
Nd^{146}	-0.17	-0.09	0.23	-0.17	-0.01	0.24	0.03	-0.14	0.34
Cs^{137}	-	-0.29	-	-	0.93	-	-	-0.07	-
Mo^{95}	-	-0.04	-	-	0.11	-	-	-0.05	-
Tc^{99}	-	-0.04	-	-	0.16	-	-	-0.01	-
Ru^{101}	-	-0.07	-	-	0.09	-	-	-0.08	-
Ag^{109}	-	-0.06	-	-	0.08	-	-	-0.42	-
Cs^{133}	-	-0.04	-	-	0.07	-	-	-0.07	-
Sm^{147}	-	0.41	-	-	-1.40	-	-	0.04	-
Sm^{149}	-	-2.22	-	-	11.66	-	-	-0.16	-
Sm^{150}	-	-0.18	-	-	1.12	-	-	-0.24	-
Sm^{151}	-	-0.05	-	-	0.11	-	-	-0.93	-
Sm^{152}	-	-0.18	-	-	0.92	-	-	0.28	-
Eu^{151}	-	0.01	-	-	-0.19	-	-	-0.63	-
Eu^{153}	-	0.03	-	-	-0.01	-	-	-0.18	-
Gd^{155}	-	-0.07	-	-	0.29	-	-	-0.38	-
Rh^{103}	-	-0.07	-	-	0.40	-	-	-0.18	-
Eu^{155}	-	-0.09	-	-	0.73	-	-	-0.31	-

4.4.2. Density history

Three factors can change the fuel density:

- chamfering and dishing;
- packing/compression ratio;
- expansion of the fuel pin due to burn-up or thermal expansion.

On the other hand, coolant density is mainly a function of void fraction in BWRs. As discussed in the paper by Gauld and Mertyurek [25], nodal average void fractions can have uncertainties of ~ 5%, while the coolant for fuel rods around the periphery and in the

vicinity of water rods can have up to 25% less void fraction than the node's average void fraction.

4.4.2.1. Fuel

Chamfering and dishing information are not provided. The benchmark model assumes 1% dishing. This 1% reduction in fuel volume can be considered as 1% uncertainty in fuel density. Figure 14 and Figure 15 display the change in C/M due to 1% change in fuel density. The largest changes in U^{235} (2%) are observed at samples from Gd rods (C2) and corner rods (A9). The changes in other major actinide nuclides are ~ 1%. The data used in Figure 1 are provided in Table 41.

Since the expansion of the fuel pin is also a change in geometry, it is further discussed in Section 4.4.4.

Figure 14. Change in C/M with 1% increase in fuel density for the 2F1ZN2 assembly samples

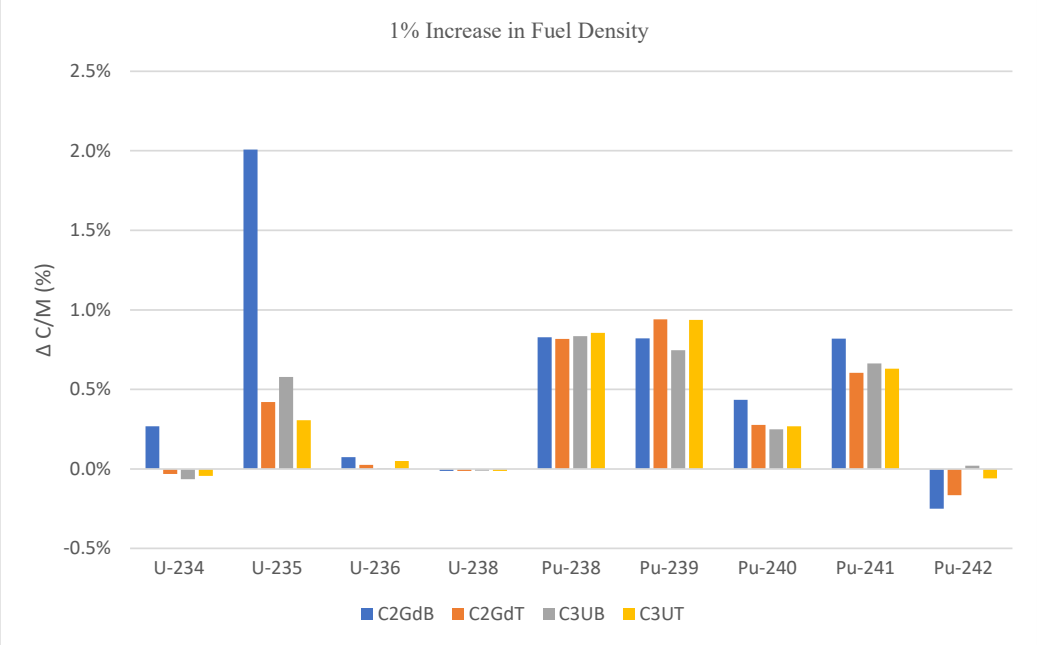

Source: ORNL, 2024.

Figure 15. Change in C/M with 1% increase in fuel density for the 2F1ZN3 assembly samples

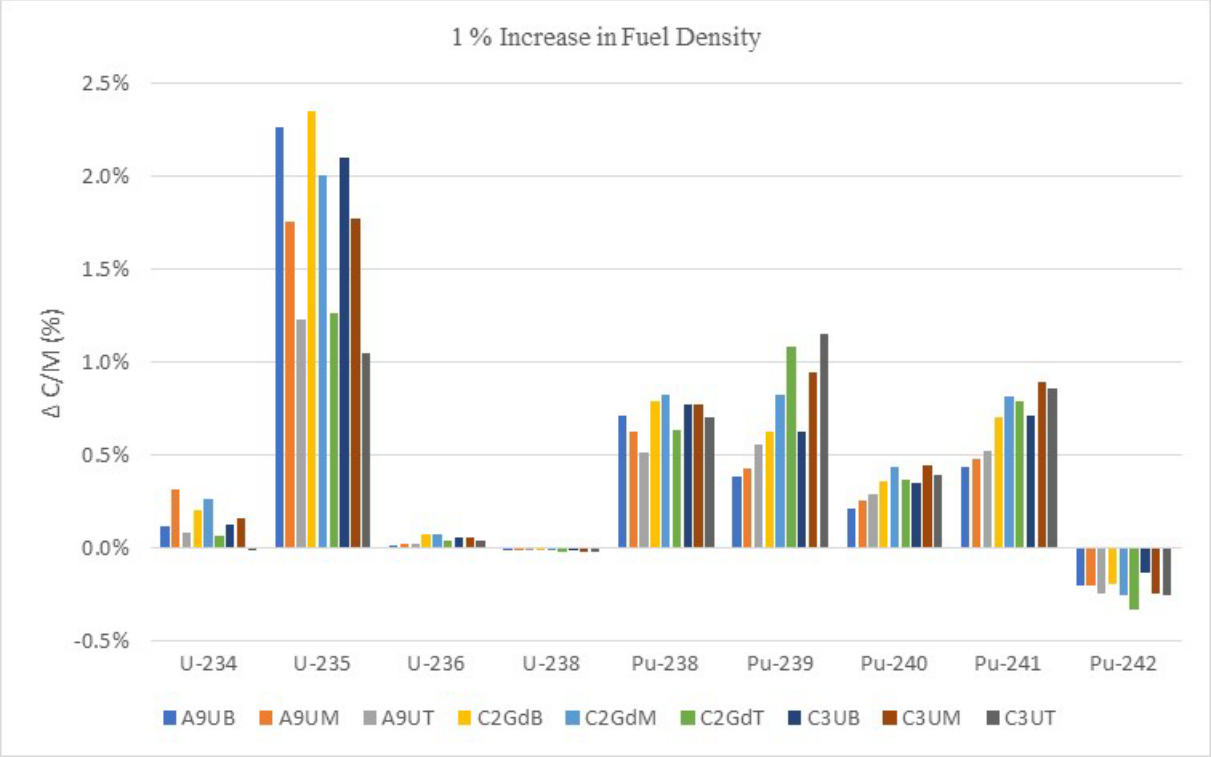

Source: ORNL, 2024.

Table 41. Change in C/M with 1% increase in fuel density for the 2F1ZN3 assembly samples

Isotope	$\Delta_{C/M}$ (%)								
	A9/UB	A9/UM	A9/UT	C2/GdB	C2/GdM	C2/GdT	C3/UB	C3/UM	C3/UT
U^{234}	0.12	0.32	0.09	0.21	0.27	0.07	0.12	0.16	-0.01
U^{235}	2.26	1.75	1.23	2.35	2.01	1.27	2.10	1.77	1.05
U^{236}	0.01	0.03	0.03	0.08	0.07	0.04	0.06	0.06	0.04
U^{238}	0.00	0.00	-0.01	-0.01	-0.01	-0.01	-0.01	-0.01	-0.02
Pu^{238}	0.71	0.63	0.52	0.79	0.83	0.64	0.78	0.77	0.71
Pu^{239}	0.39	0.43	0.56	0.63	0.82	1.08	0.63	0.94	1.15
Pu^{240}	0.21	0.26	0.29	0.36	0.43	0.37	0.35	0.44	0.39
Pu^{241}	0.44	0.48	0.53	0.71	0.82	0.79	0.71	0.89	0.86
Pu^{242}	-0.20	-0.20	-0.24	-0.19	-0.25	-0.33	-0.13	-0.25	-0.25
Nd^{148}	0.00	0.00	0.00	0.00	-0.01	-0.01	0.00	-0.01	-0.01
Nd^{143}	0.48	0.50	0.38	0.64	0.59	0.35	0.63	0.60	0.32
Nd^{145}	0.01	0.01	-0.01	0.01	-0.01	-0.05	-0.01	-0.02	-0.07
Nd^{146}	-0.01	-0.01	0.00	-0.03	-0.03	-0.01	-0.03	-0.02	0.01
Cs^{137}	-	0.00	-	-	-0.01	-	-	-0.01	-
Mo^{95}	-	0.00	-	-	-0.03	-	-	-0.04	-
Tc^{99}	-	-0.02	-	-	-0.02	-	-	-0.03	-
Ru^{101}	-	-0.03	-	-	-0.03	-	-	-0.03	-
Ag^{109}	-	-0.01	-	-	0.10	-	-	0.16	-
Cs^{133}	-	-0.01	-	-	0.00	-	-	-0.02	-
Sm^{147}	-	-0.03	-	-	-0.01	-	-	-0.06	-
Sm^{149}	-	0.29	-	-	0.71	-	-	0.73	-
Sm^{150}	-	0.14	-	-	0.12	-	-	0.14	-
Sm^{151}	-	0.45	-	-	0.92	-	-	0.89	-
Sm^{152}	-	-0.25	-	-	-0.30	-	-	-0.34	-
Eu^{151}	-	0.31	-	-	0.53	-	-	0.59	-
Eu^{153}	-	0.04	-	-	0.11	-	-	0.06	-
Gd^{155}	-	0.12	-	-	0.35	-	-	0.26	-
Rh^{103}	-	0.08	-	-	0.14	-	-	0.14	-
Eu^{155}	-	0.10	-	-	0.20	-	-	0.21	-

4.4.2.2. Coolant

Figure 16 and Figure 17 show the change in C/M due to a 5% relative increase and 5% relative reduction in sample void fraction. Increase in void fraction leads to increases in predicted actinide concentrations, except for Pu^{242}. The opposite behaviour is observed if the void fraction is decreased by 5%. The largest change is observed in samples from the corner rod (A9). As U^{235} is largely overpredicted in samples from the corner rod, the results indicate that the void fraction history for this rod is likely lower than the node's average void fraction. The same type of observation applies to samples from the Gd rods (C2).

The void fraction perturbation results point at increasing change in U^{235} concentrations with increasing axial elevation. However, the greater change at higher elevations is not due to increased void fraction sensitivity, but it is due to a larger absolute void fraction perturbation, as void fraction increases with elevation (see Figure 18). The data used in Figure 16 are provided in Table 42.

Figure 16. Change in C/M with 5% increase in void fractions for the 2F1ZN3 assembly samples

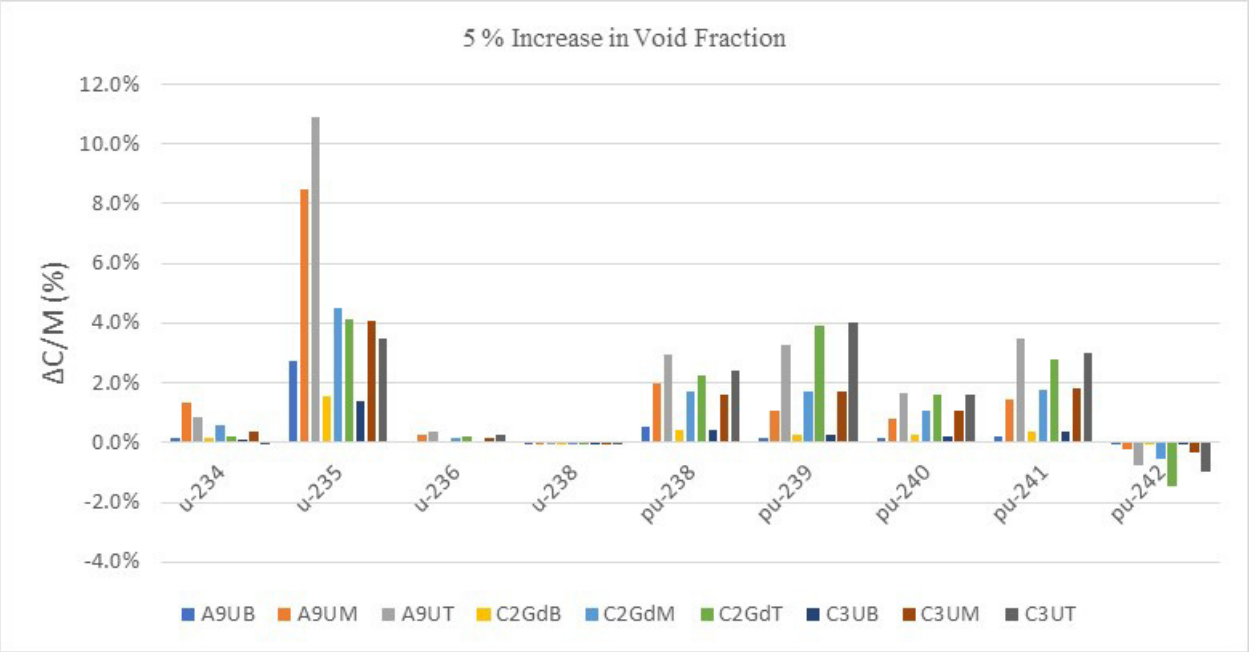

Source: ORNL, 2024.

Figure 17. Change in C/M with 5% reduction in void fractions for the 2F1ZN3 assembly samples

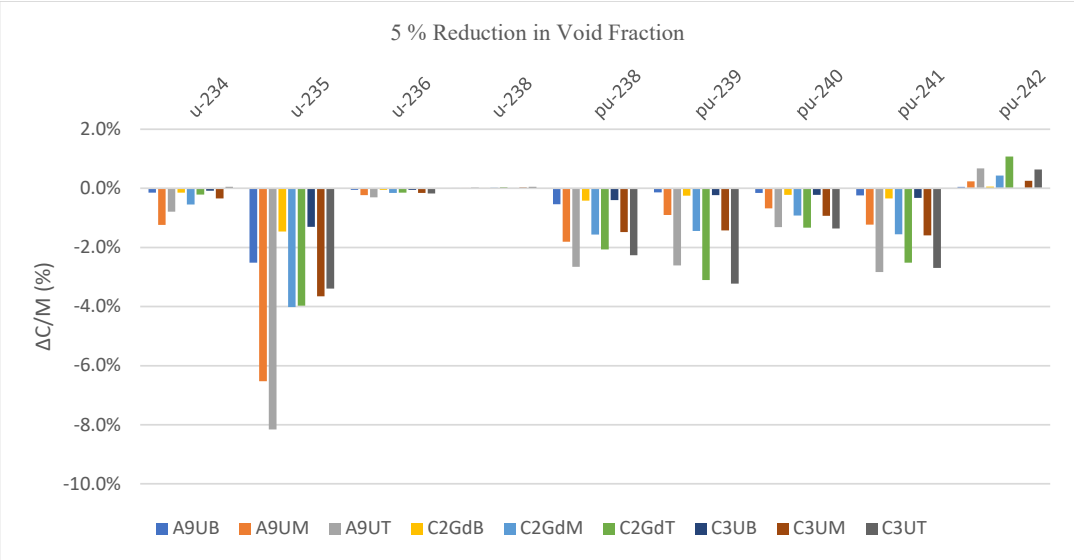

Source: ORNL, 2024.

Figure 18. Void fraction history of 2F1ZN3 assembly for top middle and bottom nodes

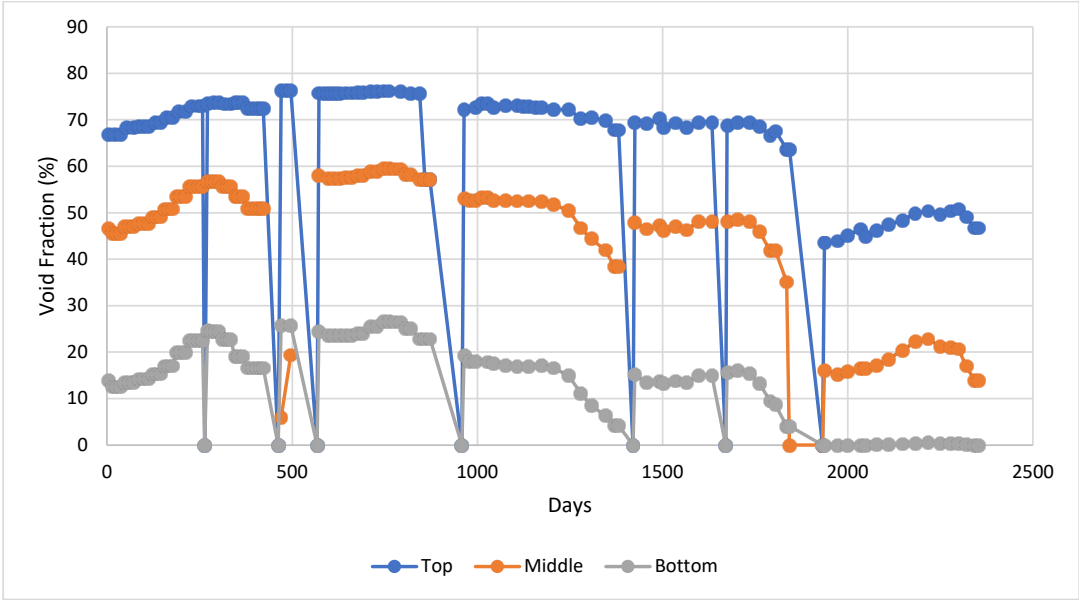

Source: ORNL, 2024.

Table 42. Change in C/M with 5% change in void fraction for the 2F1ZN3 assembly samples

Isotope	$\Delta_{C/M}$ (%)								
	A9/UB	A9/UM	A9/UT	C2/GdB	C2/GdM	C2/GdT	C3/UB	C3/UM	C3/UT
U^{234}	0.16	1.29	0.82	0.15	0.56	0.21	0.08	0.35	0.05
U^{235}	2.62	7.50	9.53	1.50	4.25	4.05	1.33	3.86	3.44
U^{236}	0.06	0.25	0.34	0.05	0.16	0.19	0.05	0.17	0.22
U^{238}	0.00	0.01	0.03	0.00	0.02	0.05	0.01	0.03	0.06
Pu^{238}	0.54	1.90	2.79	0.42	1.63	2.15	0.41	1.55	2.35
Pu^{239}	0.14	0.97	2.95	0.25	1.58	3.50	0.24	1.56	3.62
Pu^{240}	0.16	0.74	1.50	0.23	0.99	1.45	0.22	1.01	1.48
Pu^{241}	0.24	1.33	3.17	0.35	1.67	2.66	0.33	1.72	2.85
Pu^{242}	0.05	0.24	0.72	0.06	0.48	1.26	0.00	0.29	0.82
Nd^{148}	0.01	0.03	0.04	0.00	0.02	0.03	0.00	0.02	0.03
Nd^{143}	0.45	1.83	2.62	0.39	1.25	1.16	0.38	1.26	1.05
Nd^{145}	0.04	0.15	0.13	0.01	0.01	0.19	0.01	0.04	0.25
Nd^{146}	0.04	0.14	0.17	0.03	0.07	0.02	0.03	0.06	0.04
Cs^{137}	-	0.01	-	-	0.02	-	-	0.01	-
Mo^{95}	-	0.04	-	-	0.07	-	-	0.08	-
Tc^{99}	-	0.08	-	-	0.03	-	-	0.05	-
Ru^{101}	-	0.04	-	-	0.05	-	-	0.06	-
Ag^{109}	-	0.20	-	-	0.32	-	-	0.47	-
Cs^{133}	-	0.10	-	-	0.01	-	-	0.01	-
Sm^{147}	-	0.32	-	-	0.05	-	-	0.02	-
Sm^{149}	-	0.56	-	-	1.07	-	-	1.06	-
Sm^{150}	-	0.47	-	-	0.24	-	-	0.27	-
Sm^{151}	-	0.93	-	-	1.37	-	-	1.38	-
Sm^{152}	-	0.24	-	-	0.39	-	-	0.41	-
Eu^{151}	-	0.64	-	-	0.79	-	-	0.92	-
Eu^{153}	-	0.23	-	-	0.15	-	-	0.08	-
Gd^{155}	-	0.41	-	-	0.54	-	-	0.42	-
Rh^{103}	-	0.57	-	-	0.37	-	-	0.38	-
Eu^{155}	-	0.35	-	-	0.40	-	-	0.35	-

4.4.3. Temperature history

Fuel temperature history is not provided for the samples. Constant fuel temperature based on similar fuel designs is used in the benchmark. However, fuel temperature can vary by 100 K with burn-up. Figure 19 and Figure 20 show the effect of 100 K perturbation to fuel temperatures. As in the void fraction effect, increased fuel temperatures lead to increased actinide nuclide concentrations, except for U^{236}. Reduction in fuel temperature has the opposite effect. The largest variations in nuclide concentrations due to fuel temperature changes are observed for the samples from the corner rod (A9) and the Gd rod (C2). It should also be noted that power, void fraction, and fuel temperatures are correlated so that

low power samples would have lower void fractions and lower fuel temperatures than the node average values. Table 42 provides the data used in Figure 19.

Figure 19. Change in C/M with 100 K increase in fuel temperature for the 2F1ZN3 assembly samples

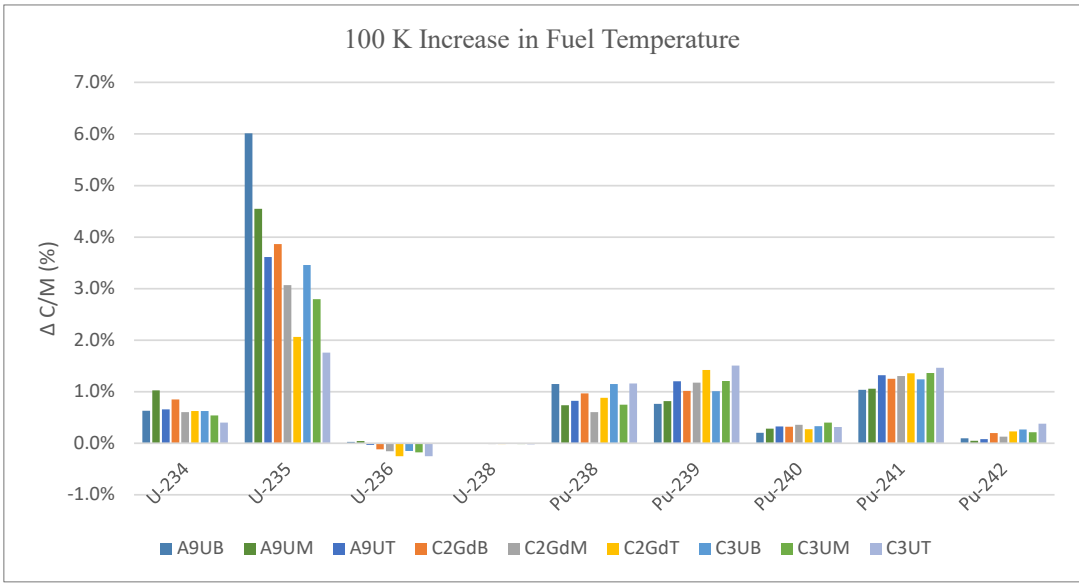

Source: ORNL, 2024.

Figure 20. Change in C/M with 100 K reduction in fuel temperature for the 2F1ZN3 assembly samples

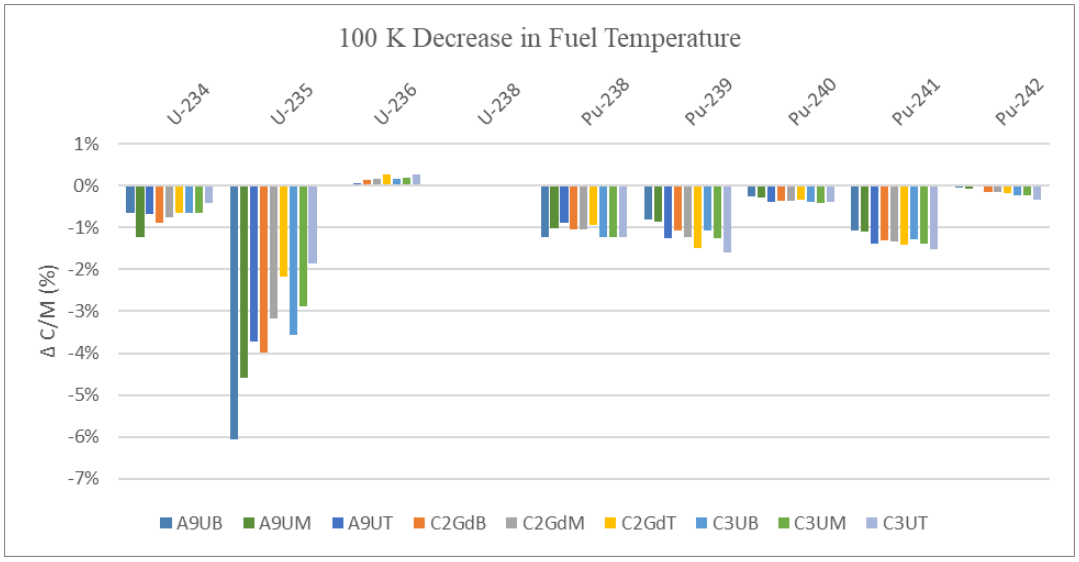

Source: ORNL, 2024.

Table 43. Change in C/M with 100 K change in fuel temperature for the 2F1ZN3 assembly samples

Isotope	$\Delta_{C/M}$ (%)								
	A9/UB	A9/UM	A9/UT	C2/GdB	C2/GdM	C2/GdT	C3/UB	C3/UM	C3/UT
U^{234}	-0.65	-1.22	-0.68	-0.89	-0.76	-0.65	-0.66	-0.64	-0.43
U^{235}	-6.06	-4.58	-3.72	-3.98	-3.16	-2.17	-3.58	-2.88	-1.85
U^{236}	-0.01	-0.03	0.05	0.13	0.17	0.27	0.17	0.19	0.27
U^{238}	0.01	0.01	0.01	0.01	0.02	0.02	0.02	0.02	0.03
Pu^{238}	-1.24	-1.03	-0.90	-1.04	-1.05	-0.94	-1.23	-1.22	-1.23
Pu^{239}	-0.80	-0.85	-1.27	-1.07	-1.22	-1.50	-1.06	-1.25	-1.59
Pu^{240}	-0.25	-0.28	-0.39	-0.37	-0.37	-0.34	-0.38	-0.42	-0.38
Pu^{241}	-1.08	-1.09	-1.38	-1.30	-1.34	-1.41	-1.28	-1.40	-1.52
Pu^{242}	-0.04	-0.07	-0.02	-0.15	-0.15	-0.18	-0.23	-0.24	-0.34
Nd^{148}	0.02	0.02	0.02	0.02	0.02	0.02	0.01	0.02	0.02
Nd^{143}	-1.22	-1.20	-1.04	-1.10	-0.92	-0.58	-1.08	-0.93	-0.52
Nd^{145}	-0.22	-0.22	-0.18	-0.14	-0.11	-0.04	-0.12	-0.10	-0.02
Nd^{146}	0.19	0.19	0.19	0.18	0.17	0.15	0.17	0.16	0.12
Cs^{137}	-	0.00	-	-	0.00	-	-	0.00	-
Mo^{95}	-	-0.06	-	-	0.01	-	-	0.03	-
Tc^{99}	-	-0.28	-	-	-0.16	-	-	-0.16	-
Ru^{101}	-	-0.06	-	-	-0.04	-	-	-0.05	-
Ag^{109}	-	-0.03	-	-	-0.10	-	-	-0.22	-
Cs^{133}	-	-0.22	-	-	-0.13	-	-	-0.13	-
Sm^{147}	-	-0.72	-	-	-0.50	-	-	-0.48	-
Sm^{149}	-	-0.56	-	-	-1.03	-	-	-1.04	-
Sm^{150}	-	-0.25	-	-	-0.09	-	-	-0.11	-
Sm^{151}	-	-0.91	-	-	-1.30	-	-	-1.32	-
Sm^{152}	-	-0.03	-	-	0.00	-	-	0.07	-
Eu^{151}	-	-0.62	-	-	-0.75	-	-	-0.88	-
Eu^{153}	-	-0.44	-	-	-0.44	-	-	-0.40	-
Gd^{155}	-	1.32	-	-	0.98	-	-	1.61	-
Rh^{103}	-	-1.15	-	-	-1.04	-	-	-1.08	-
Eu^{155}	-	1.17	-	-	1.53	-	-	1.44	-

4.4.4. Geometry

4.4.4.1. Gap closure

Fuel experience volumetric changes with burn-up due to fission gas detention that occurs during heating and swelling. Ignoring the changes in cladding caused by thermal expansion (discussed in Section 4.4.4.2), and axial expansion, the effect of gap closure on predicted nuclide concentrations are shown in Figure 21. In this calculation, the clad's inner diameter is assumed to be the same as the fuel pin diameter, with no gap present, and the fuel density is adjusted to ensure that the total mass of fuel is conserved (Equation 9).

$$\rho_{fuel}^{gap_closure} = \rho_{fuel}^{original} \frac{{r_{pin}}^2}{{r_{gap}}^2} \quad (9)$$

where r is radius and ρ is density.

Figure 21. Change in C/M with gap closure for the 2F1ZN3 assembly samples

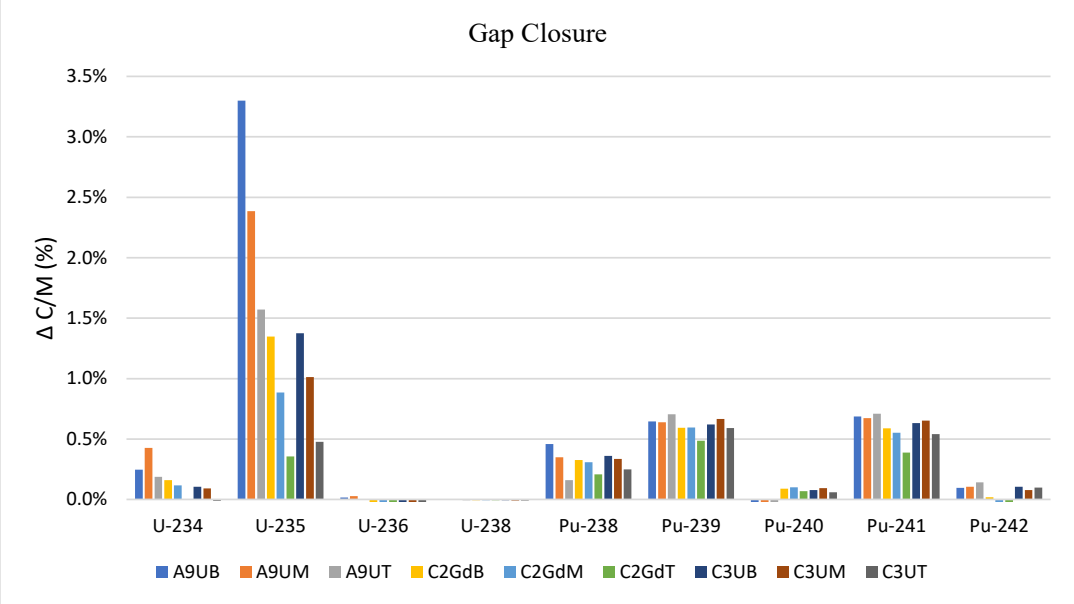

Source: ORNL, 2024.

Uranium and plutonium concentrations slightly increase with gap closure. The largest increase is observed in samples from the corner rod (A9).

4.4.4.2. Thermal expansion

Geometry data for fuel rods and structural material are provided at cold conditions. However, reactors operate at high temperatures, and due to thermal expansion, the assembly geometry, including pin pitch, changes during normal operation. The effect of thermal expansion on k_{eff} is discussed in detail in the literature [29] for pressurised water reactor (PWR) assemblies. Assuming that similar expansion ratios are applicable herein, fuel rod dimensions were modified using those ratios. The effect of the fuel rod's thermal expansion (see Table 44) on calculated nuclide content is shown in Figure 22 and Table 44. The dimensional changes in pin pitch and channel wall are not modelled.

Table 44. Change in fuel modelling parameters with thermal expansion

Parameter	Cold	Hot
Pellet radius (cm)	0.478	0.4809
Clad inner radius (cm)	0.488	0.489
Clad outer radius (cm)	0.559	0.560
UO_2 Density (g/cm^3)	10.520	10.325
UO_2-Gd_2O_3 Density(g/cm^3)	10.393	10.274

As in previous perturbations, the largest change in U^{235} is seen for the corner rod 2F1ZN3/A9/UB sample. However, the maximum increase in relative differences for U^{235} content is below 2%.

Figure 22. Change in C/M with thermal expansion of fuel for the 2F1ZN3 assembly samples

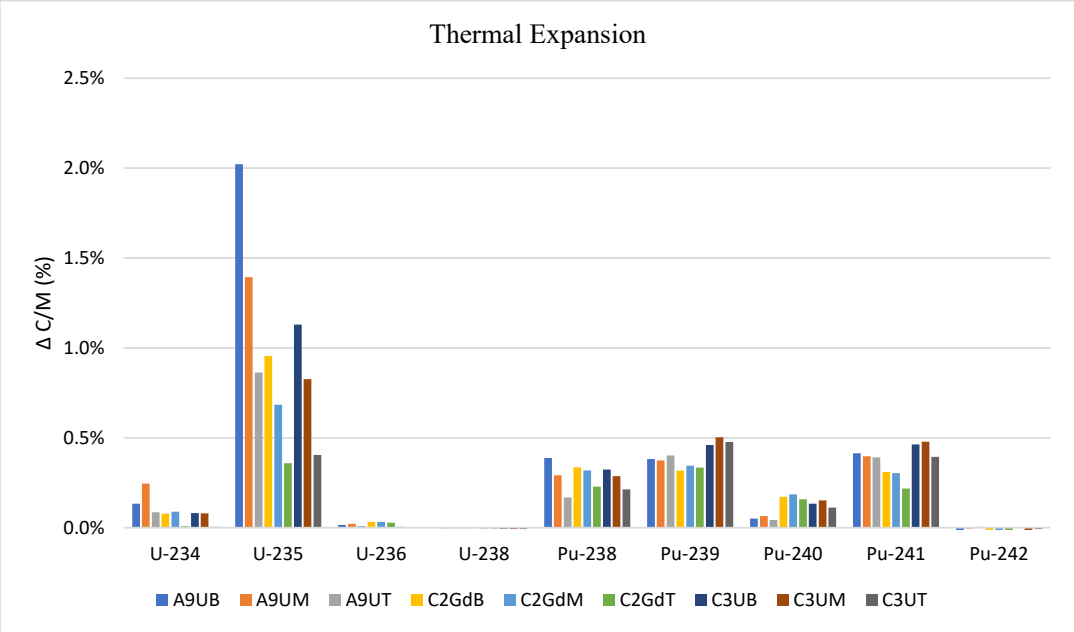

Source: ORNL, 2024.

4.4.4.3. Channel bow/bulge

The fuel channel is susceptive to dimensional changes and corrosion during its lifetime, especially at high burn-ups. The dimensional changes are driven by differential irradiation growth and/or differential hydrogen content across opposing channel faces. As a result of dimensional changes, the channel can bow, bulge or twist. Lattice physics analysis of different channel distortion types can be a complex task. However, the channel bow (see Figure 23) can be modelled using existing lattice physics capability by modifying bypass (channel gap) widths.

Figure 23. Channel bow [30]

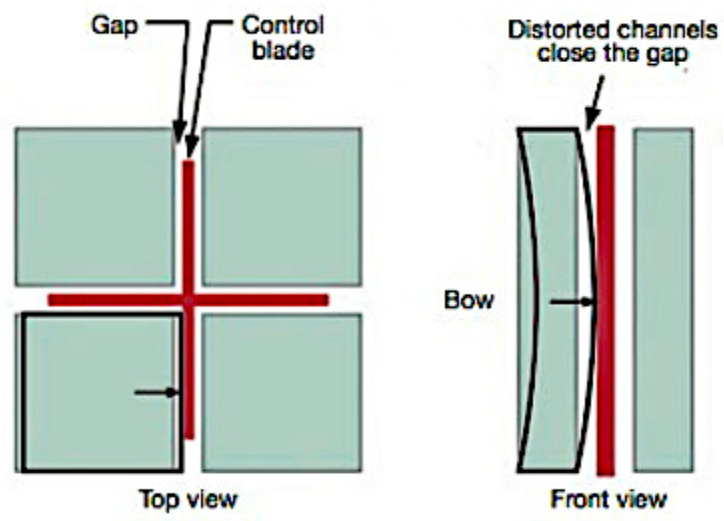

Source: ORNL, 2024.

A 25% change in channel gap would cause the control blade to get stuck, which is the main concern with the channel bow. Therefore, a 20% shift in channel gap in the northeast direction (wide-wide corner) is modelled as shown in Figure 24. The channel distortion rate is expected to increase after two cycles [31]. However, the shift in channel gap is modelled starting with the first cycle in this analysis for convenience. The change in the predicted nuclides with channel bow is shown in Figure 25. While no significant changes are observed in the nuclide contents of the samples from corner rod A9, samples from rods C2 and C3 exhibit large increases in ^{235}U and plutonium contents (except for ^{242}Pu). As depicted in Figure 24, the average moderator thickness for the A9 rod does not change. However, C2 and C3 rods are exposed to the reduced moderator from the west and the north surfaces.

Figure 24. Modelled channel bow

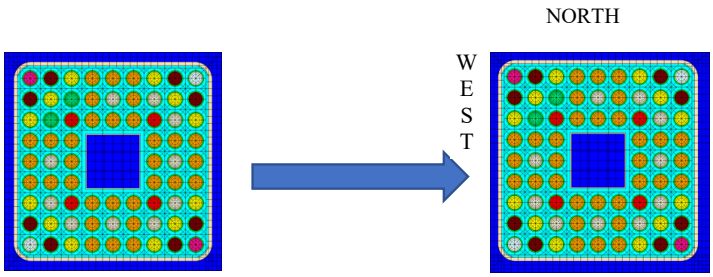

Source: ORNL, 2024.

Table 45. Change in C/M with thermal expansion of fuel for the 2F1ZN3 assembly samples

Nuclide	$\Delta_{C/M}$ (%)								
	A9/UB	A9/UM	A9/UT	C2/GdB	C2/GdM	C2/GdT	C3/UB	C3/UM	C3/UT
U^{234}	0.13	0.24	0.09	0.08	0.09	0.01	0.08	0.08	0.00
U^{235}	2.02	1.39	0.86	0.95	0.68	0.36	1.13	0.83	0.40
U^{236}	0.01	0.02	0.01	0.03	0.03	0.03	0.00	0.00	0.00
U^{238}	0.00	0.00	0.00	0.00	0.00	0.00	-0.01	-0.01	-0.01
Pu^{238}	0.39	0.29	0.17	0.34	0.32	0.23	0.32	0.29	0.21
Pu^{239}	0.38	0.37	0.40	0.32	0.35	0.33	0.46	0.50	0.48
Pu^{240}	0.05	0.06	0.04	0.17	0.19	0.16	0.13	0.15	0.11
Pu^{241}	0.41	0.40	0.39	0.31	0.30	0.22	0.46	0.48	0.39
Pu^{242}	-0.01	-0.01	0.01	-0.12	-0.14	-0.16	0.00	-0.02	-0.01
Nd^{148}	-0.01	-0.01	-0.01	0.00	0.00	0.00	-0.01	-0.01	-0.01
Nd^{143}	0.41	0.37	0.25	0.26	0.21	0.10	0.34	0.27	0.12
Nd^{145}	0.05	0.04	0.02	0.00	-0.01	-0.02	0.01	0.00	-0.02
Nd^{146}	-0.05	-0.04	-0.03	-0.01	0.00	0.01	-0.03	-0.03	-0.01
Cs^{137}	-	0.00	-	-	0.00	-	-	0.00	-
Mo^{95}	-	0.01	-	-	-0.01	-	-	-0.01	-
Tc^{99}	-	0.03	-	-	-0.01	-	-	-0.01	-
Ru^{101}	-	0.00	-	-	-0.01	-	-	-0.01	-
Ag^{109}	-	0.06	-	-	0.02	-	-	0.11	-
Cs^{133}	-	0.03	-	-	-0.01	-	-	0.00	-
Sm^{147}	-	0.09	-	-	-0.02	-	-	0.00	-
Sm^{149}	-	0.19	-	-	0.28	-	-	0.35	-
Sm^{150}	-	0.09	-	-	0.04	-	-	0.05	-
Sm^{151}	-	0.26	-	-	0.34	-	-	0.40	-
Sm^{152}	-	-0.06	-	-	-0.15	-	-	-0.12	-
Eu^{151}	-	0.18	-	-	0.19	-	-	0.26	-
Eu^{153}	-	0.10	-	-	0.03	-	-	0.07	-
Gd^{155}	-	0.12	-	-	0.14	-	-	0.13	-
Rh^{103}	-	0.15	-	-	0.04	-	-	0.10	-
Eu^{155}	-	0.11	-	-	0.09	-	-	0.10	-

Figure 25. Change in C/M with channel bow for the 2F1ZN3 assembly samples

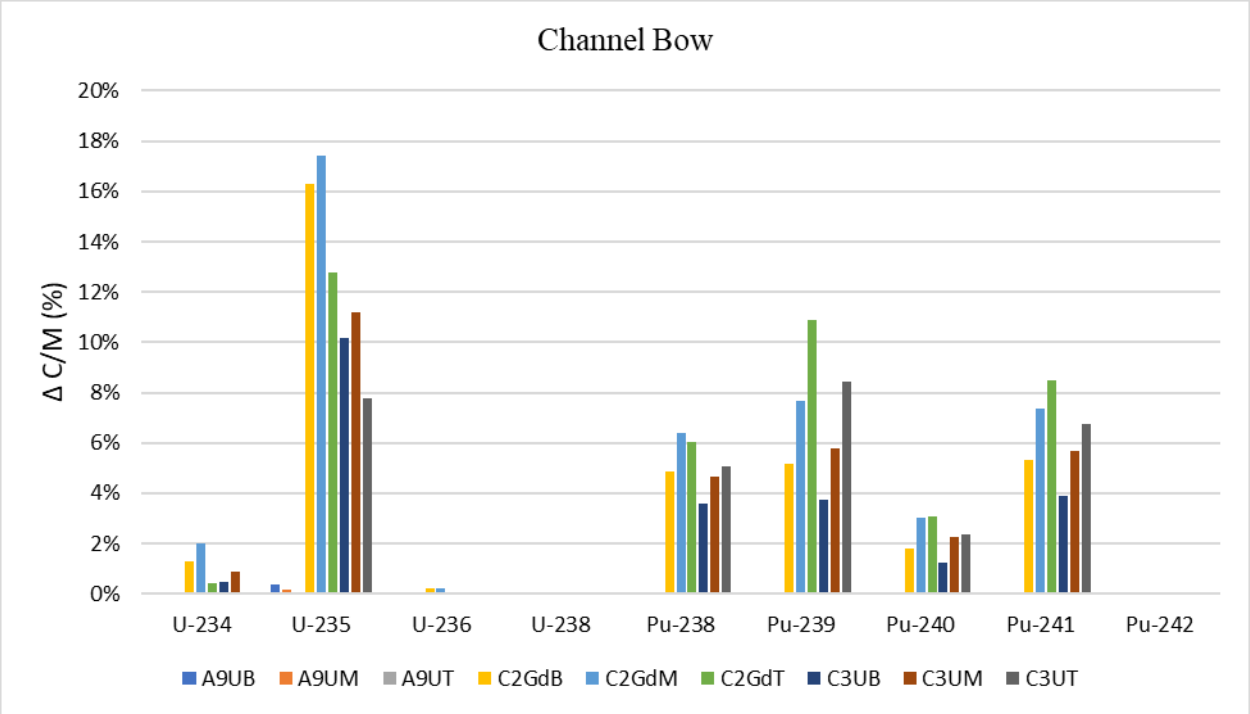

Source: ORNL, 2024.

4.4.4.4. Channel corner radius

The channel corner radius of the modelled lattice is not available in publicly available sources. Since the channel radius changes the coolant amount for corner fuel rods, it can affect isotopic distribution in these rods. The effect of the corner radius on isotopic distribution is expected to increase with increasing void fraction and to be limited to corner fuel rods.

The channel radius of an 8×8 assembly (r = 0.9653 cm) was used in modelling. However, the newer designs are expected to have smaller channel radii. Starting with corner radius close to zero (square channel), the effect of increasing the channel radius on predicted concentrations of isotopes of U and P was tested. Differences in C/M values are shown in Figure 26 for lattice models with channel radii of 0.1 cm and 0.7 cm. As the results indicate, an increase of up to 7% in U^{235} C/M can be seen if the channels are modelled as a square. The figure also shows that an increase in predicted U^{235} concentrations should be expected when the correct channel radius is used in modelling as compared with the square channel assumption.

Figure 26. Change in C/M with different channel radii 2F1ZN3 assembly samples

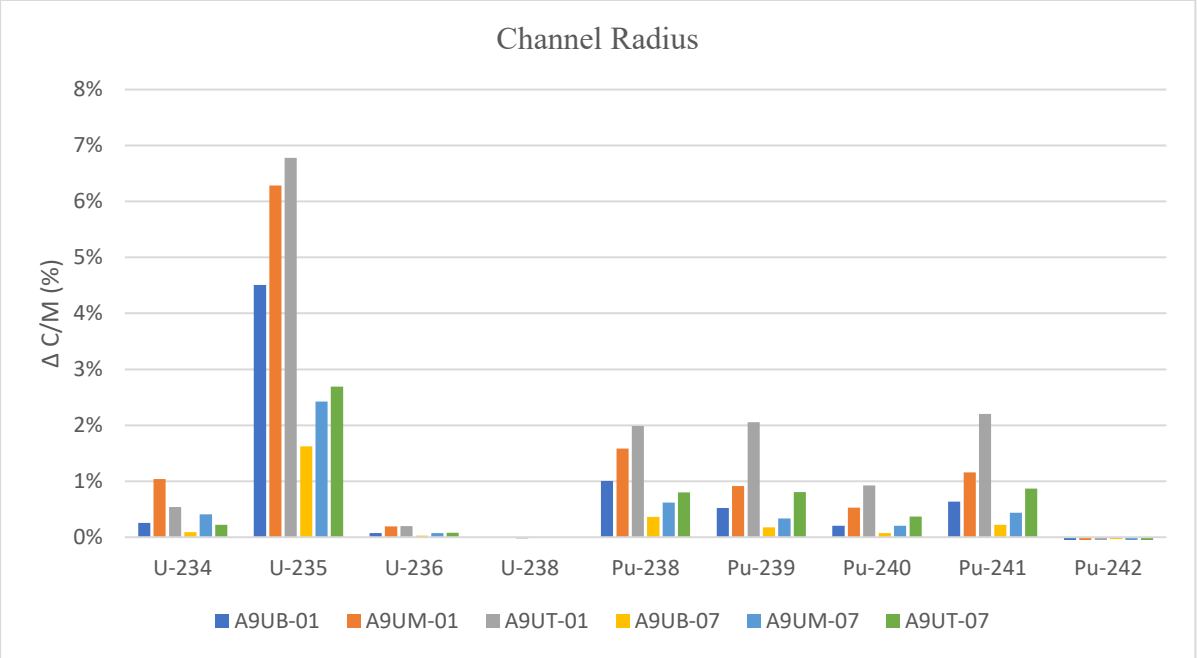

Source: ORNL, 2024.

4.4.4.5. Model geometry uncertainties

Reported fuel geometry parameters such as fuel rod radius have inherent manufacturing uncertainties. These uncertainties are either proprietary or unavailable. The SFCOMPO evaluation guide [32] suggests using the tolerances shown in Table 46.

Table 46. Assembly geometry manufacturing tolerances

Geometry parameter	Uncertainty
Pin radius	±10 μm
Clad radius	±25 μm

Since the manufacturing tolerances are standard deviations of a random distribution, it is best to employ stochastic sampling to calculate their effect on the calculated isotope contents. However, considering that the change in fuel pin radius due to thermal expansion is twice the suggested manufacturing tolerance, the effect is expected to be less than 1%. Therefore, this calculation-intensive analysis is not performed in the evaluation.

4.4.5. Burn-up

As discussed in Section 2.6, sample burn-up is calculated based on measurements of burn-up indicators, or it is provided by core simulators by numerical calculations. Burn-up estimates can vary, even for the same measurements based on data used in calculations. Burn-up estimates from different codes and measurements are compared in Section 2.6. More than an 8% relative difference or more than a 5 GWd/MTU absolute difference can be observed in the reported data. To demonstrate the effect of burn-up uncertainty on the C/M ratios, the burn-ups calculated with Polaris (to match measured Nd^{148} concentrations, as shown in Table 17) are perturbed by 1%. The effect on the C/M results is shown in Figure 27 and Figure 28. Bottom nodes show the largest impact. More than 9% reduction

in U^{235} concentration due to 1% burn-up increase is observed for corner sample 2F1ZN3/A9/UB. Table 46 provides the data used in Figure 27.

Figure 27. Change in C/M with 1% reduction in burn-up for the 2F1ZN3 assembly samples

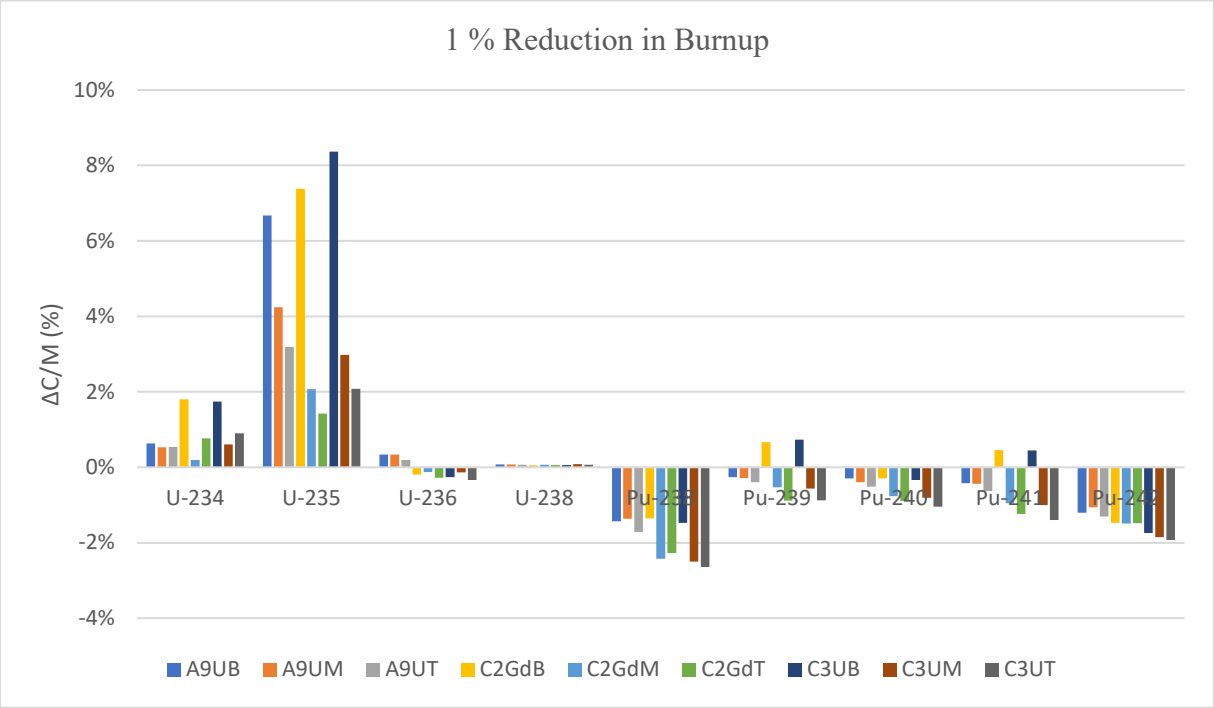

Source: ORNL, 2024.

Figure 28. Change in C/M with 1% increase in burn-up for the 2F1ZN3 assembly samples

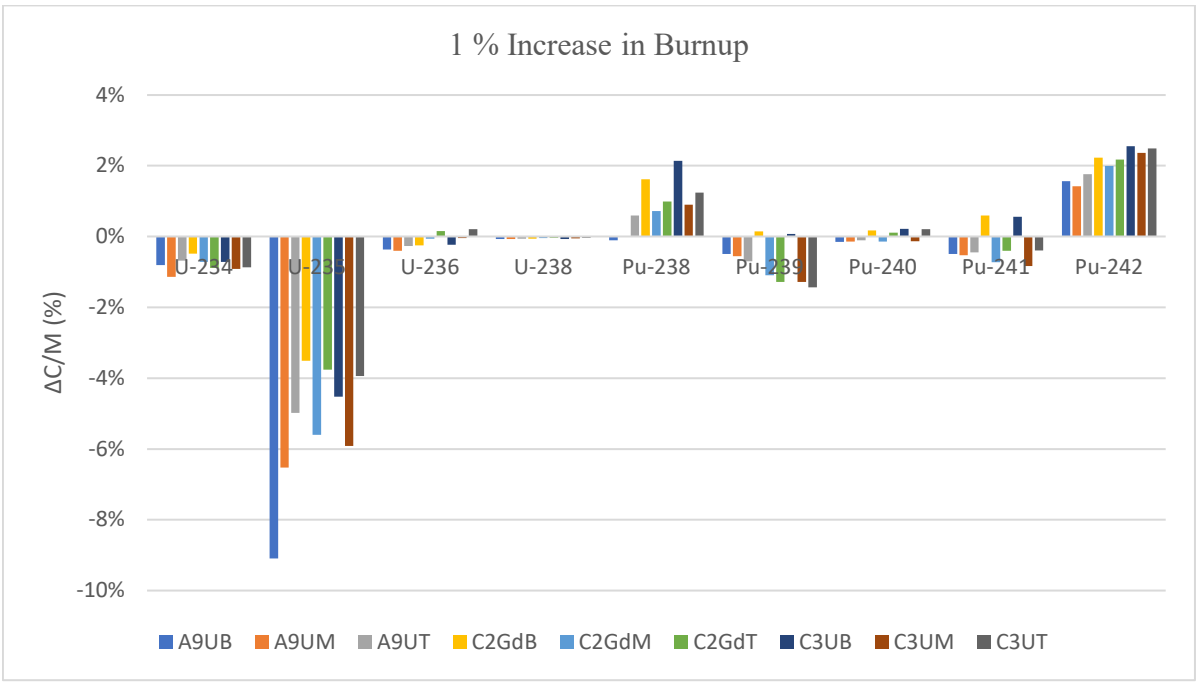

Source: ORNL, 2024.

Table 47. Change in C/M for 1% change in burn-up in the 2F1ZN3 assembly samples

Nuclide	$\Delta_{C/M}$ (%)								
	A9/UB	A9/UM	A9/UT	C2/GdB	C2/GdM	C2/GdT	C3/UB	C3/UM	C3/UT
U^{234}	0.72	0.83	0.61	1.14	0.46	0.83	1.23	0.76	0.89
U^{235}	7.88	5.38	4.08	5.45	3.84	2.59	6.44	4.45	3.01
U^{236}	0.35	0.37	0.23	0.22	0.10	0.21	0.24	0.09	0.27
U^{238}	0.07	0.07	0.06	0.06	0.05	0.04	0.07	0.07	0.05
Pu^{238}	0.77	0.68	1.16	1.49	1.57	1.63	1.81	1.70	1.94
Pu^{239}	0.38	0.42	0.55	0.41	0.81	1.08	0.40	0.92	1.16
Pu^{240}	0.22	0.27	0.31	0.23	0.46	0.50	0.28	0.47	0.62
Pu^{241}	0.46	0.48	0.54	0.52	0.84	0.82	0.50	0.92	0.90
Pu^{242}	1.39	1.24	1.53	1.85	1.74	1.83	2.15	2.11	2.21
Nd^{148}	1.02	1.01	1.01	1.00	0.99	0.99	1.00	1.00	1.00
Nd^{143}	0.47	0.50	0.39	0.37	0.61	0.37	0.68	0.63	0.35
Nd^{145}	0.63	0.64	0.69	0.65	0.69	0.75	0.58	0.61	0.72
Nd^{146}	1.16	1.15	1.14	1.15	1.12	1.10	1.21	1.18	1.14
Cs^{137}	-	0.91	-	-	0.86	-	-	0.88	-
Mo^{95}	-	0.72	-	-	0.72	-	-	0.69	-
Tc^{99}	-	1.11	-	-	1.08	-	-	1.02	-
Ru^{101}	-	0.89	-	-	0.91	-	-	0.89	-
Ag^{109}	-	1.05	-	-	1.78	-	-	1.95	-
Cs^{133}	-	0.66	-	-	0.71	-	-	0.67	-
Sm^{147}	-	0.02	-	-	0.07	-	-	0.19	-
Sm^{149}	-	0.49	-	-	0.70	-	-	0.71	-
Sm^{150}	-	0.82	-	-	0.96	-	-	0.98	-
Sm^{151}	-	0.45	-	-	0.91	-	-	0.88	-
Sm^{152}	-	0.67	-	-	0.68	-	-	0.68	-
Eu^{151}	-	0.31	-	-	0.52	-	-	0.58	-
Eu^{153}	-	0.66	-	-	0.78	-	-	0.85	-
Gd^{155}	-	0.74	-	-	0.56	-	-	1.08	-
Rh^{103}	-	0.33	-	-	0.51	-	-	0.39	-
Eu^{155}	-	0.66	-	-	0.89	-	-	0.96	-

4.5. Measurement uncertainties

The effect of relative measurement uncertainties (σ_M/M) reported in Table 11 and Table 12 on the calculated C/M values can be evaluated using Equation (10) assuming normal distributions:

$$\left(\frac{\sigma_{C/M}^{M}}{C/M}\right)^2 = \left(\frac{\sigma_M}{M}\right)^2 \tag{10}$$

where $\sigma_{C/M}^{M}$ is the uncertainty (change) in calculated C/M due to measurement uncertainty.

The calculated uncertainties are listed in Table 48 for the samples from 2F1ZN3 assembly. For consistency in notation with previously calculated uncertainties, $\Delta_{C/M}$ is used to represent $\sigma_{C/M}^{M}$.

Table 48. Change in C/M due to measurement uncertainties in 2F1ZN3 assembly samples

Nuclide	$\Delta_{C/M}$ (%)								
	A9/UB	A9/UM	A9/UT	C2/GdB	C2/GdM	C2/GdT	C3/UB	C3/UM	C3/UT
U^{234}	0.63	1.66	0.77	1.27	1.55	1.45	1.08	1.45	1.23
U^{235}	0.13	3.88	0.10	0.12	0.32	0.11	0.12	0.32	0.11
U^{236}	2.07	0.21	2.03	2.07	0.21	2.05	2.06	0.21	2.06
U^{238}	0.10	0.20	0.10	0.10	0.20	0.10	0.10	0.20	0.10
Pu^{238}	0.63	0.55	0.57	0.58	0.59	0.51	0.55	0.53	0.51
Pu^{239}	0.32	0.18	0.31	0.31	0.19	0.29	0.30	0.19	0.31
Pu^{240}	0.34	0.20	0.32	0.31	0.20	0.28	0.30	0.20	0.29
Pu^{241}	0.31	0.18	0.31	0.31	0.19	0.29	0.30	0.19	0.30
Pu^{242}	0.34	0.21	0.33	0.31	0.20	0.30	0.30	0.21	0.31
Nd^{148}	0.10	0.30	0.10	0.10	0.30	0.10	0.10	0.30	0.10
Nd^{143}	0.11	0.31	0.10	0.11	0.32	0.10	0.11	0.32	0.10
Nd^{145}	0.10	0.30	0.10	0.10	0.31	0.10	0.10	0.31	0.10
Nd^{146}	0.10	0.29	0.10	0.10	0.29	0.10	0.10	0.29	0.10
Cs^{137}	-	3.64	-	-	3.46	-	-	3.54	-
Mo^{95}	-	2.23	-	-	2.09	-	-	4.29	-
Tc^{99}	-	3.59	-	-	3.49	-	-	4.97	-
Ru^{101}	-	2.13	-	-	1.97	-	-	3.68	-
Ag^{109}	-	1.80	-	-	2.32	-	-	2.17	-
Cs^{133}	-	3.57	-	-	3.07	-	-	4.90	-
Sm^{147}	-	1.22	-	-	1.80	-	-	1.21	-
Sm^{149}	-	1.79	-	-	3.20	-	-	1.53	-
Sm^{150}	-	1.33	-	-	1.80	-	-	1.25	-
Sm^{151}	-	1.91	-	-	2.26	-	-	1.46	-
Sm^{152}	-	1.20	-	-	1.76	-	-	1.23	-
Eu^{151}	-	0.86	-	-	1.32	-	-	0.82	-
Eu^{153}	-	0.70	-	-	2.18	-	-	0.52	-
Gd^{155}	-	1.36	-	-	8.25	-	-	1.21	-
Rh^{103}	-	1.92	-	-	2.10	-	-	3.79	-
Eu^{155}	-	5.52	-	-	5.85	-	-	5.81	-

4.6. Total uncertainty results

Total uncertainties are calculated assuming that there are no correlations between individual parameter uncertainties or uncertainties between concentrations of different nuclides. Therefore, the total uncertainty is calculated using Equation (11).

$$\sigma^{total} = \sqrt{\sum_{i} (\sigma^{i})^{2}} \tag{11}$$

where σ^{i} is the uncertainty in C/M due to uncertainty in parameter i.

It is also assumed that 1-sigma burn-up uncertainties are equal to or less than 1%, and void fraction 1-sigma uncertainties are equal to or less than 5%. For uncertainties calculated by direct perturbations, the largest value is used for a conservative calculation.

None of these assumptions is strictly true. Power history, fuel, and coolant temperatures are correlated. Similarly, concentrations of different fission products and actinide nuclides are also correlated. Relative difference in burn-ups calculated by different codes can be as large as 8% and the relative standard deviation (standard deviation/mean) can reach 4% at corner rods (see Table 17). Void fraction uncertainty can be as large as 25% at corner rods and as large as 10% at gadolinia-loaded rods. While correlations decrease the total uncertainty, more realistic uncertainties in burn-up and void fraction increase the total uncertainty.

However, considering the large sensitivities to burn-up and void fractions, the total uncertainty is expected to be slightly larger than what is calculated. Channel bow and channel corner radius uncertainties are not included in the total uncertainties. Since the real values for these parameters are not known, the uncertainties were only calculated to show the importance of these parameters.

The calculated C/M ratios, associated uncertainties, and the total uncertainty for each sample in the 2F1ZN3 assembly are listed in Chapter 5.

5. Results of sample calculations

Computational models are developed using the benchmark specifications provided in Chapter 3. Calculated results are compared to measurements in this section for each measured nuclide.

5.1. Codes and nuclear data libraries

Nuclide inventories of the measured samples were predicted using Polaris within SCALE 6.2.3, with the 56-group ENDF/B-VII.1 neutron cross-section library. Gadolinium-loaded fuel pins were modelled with seven equal volume rings. Details of Polaris models are available in the sample input file provided in Appendix (see Section 7.1). Figure 8 illustrates the special meshing used in the calculations.

5.2. Comparison of sample calculations and measurements

Ratios of Polaris-calculated isotope concentrations and measured isotope concentrations (C/M) for samples from assemblies 2F1ZN2 and 2F1ZN3 are listed as percentages in Tables 49 and 50, respectively. The largest C/M ratios for U^{235} are observed for samples from bottom nodes. In general, less than 5% relative difference is observed between the calculated and the measured isotope content for U^{235} and Pu^{239}. Large differences in U^{235} are observed in samples from the corner rod (A9) of 33.81% and in samples from gadolinia rods (C2) at 15.53%. Among major actinides, U^{234} shows the largest deviations from measurement values overall. Except for U^{235} enrichment, data were not provided in the literature [1,2] for the initial uranium initial isotopic compositions. While U^{234} measured concentrations are known to be sensitive to their initial concentrations, measurement and prediction for the 2F1ZN3/A9/UB sample show a larger-than-expected difference of ~36%. The large differences observed in isotopic comparisons for the samples from the A9 rod are consistent with predictions by SWAT/4 and MVP-BURN codes [1,2]. Figure 29 and Figure 30 show the C/M-1 (%) values for actinide and Nd nuclides in the measured samples from fuel assemblies 2F1ZN2 and 2F1ZN3, respectively; Figure 31 shows the C/M-1 (%) values for the fission products measured in five samples from these fuel assemblies. The C/M-1 values and various uncertainties evaluated for the nine fuel samples from the 2F1ZN3 fuel assembly are provided in Table 51 through Table 59.

Table 49. C/M-1 for the 2F1ZN2 assembly samples

Nuclide	C/M-1 (%)			
	C2/GdB	C2/GdT	C3/UB	C3/UT
U^{234}	-17.94	8.72	-5.75	-3.75
U^{235}	6.26	3.20	2.41	4.44
U^{236}	1.22	2.07	2.07	2.35
U^{238}	-0.07	-0.16	-0.09	-0.20
Pu^{238}	7.37	8.10	6.18	2.64
Pu^{239}	3.88	6.11	2.94	4.02
Pu^{240}	-0.06	0.26	-1.00	-3.45
Pu^{241}	2.09	3.51	1.39	0.69
Pu^{242}	0.48	3.04	0.95	-1.85
Nd^{148}	-0.26	-0.30	0.30	-0.15
Nd^{143}	2.84	2.01	2.36	2.39
Nd^{145}	0.43	0.49	0.78	0.72
Nd^{146}	-1.64	-1.38	-0.80	-1.27
Cs^{137}	-	-6.18	-	-8.25
Mo^{95}	-	-7.59	-	-4.39
Tc^{99}	-	37.37	-	39.86
Ru^{101}	-	-3.13	-	-2.12
Ag^{109}	-	46.11	-	50.37
Cs^{133}	-	-	-	1.38
Sm^{147}	-	-0.89	-	-1.27
Sm^{149}	-	5.19	-	14.31
Sm^{150}	-	1.43	-	3.97
Sm^{151}	-	2.10	-	3.91
Sm^{152}	-	5.96	-	7.00
Eu^{151}	-	-30.96	-	-7.46
Eu^{153}	-	11.21	-	5.25
Gd^{155}	-	-6.74	-	14.69
Rh^{103}	-	0.34	-	0.88
Eu^{155}	-	15.61	-	6.73

Table 50. C/M-1 for the 2F1ZN3 assembly samples

Nuclide	C/M-1 (%)								
	A9/UB	A9/UM	A9/UT	C2/GdB	C2/GdM	C2/GdT	C3/UB	C3/UM	C3/UT
U^{234}	-36.62	18.60	-22.65	26.71	11.03	44.96	8.47	3.42	23.35
U^{235}	33.81	-3.08	-2.65	15.53	6.35	8.59	16.59	7.58	10.21
U^{236}	3.49	3.46	1.27	3.51	2.80	2.68	3.21	3.33	2.94
U^{238}	-0.17	-0.08	-0.17	-0.16	-0.17	-0.17	-0.15	-0.20	-0.24
Pu^{238}	26.93	10.69	13.94	15.33	17.99	2.62	10.75	6.47	2.20
Pu^{239}	5.30	-9.00	2.36	3.38	-5.08	-1.90	0.52	-3.73	2.61
Pu^{240}	12.70	0.43	6.24	4.43	-2.06	-5.15	-0.13	-2.27	-2.43
Pu^{241}	4.80	-9.40	1.68	2.14	-5.27	-2.63	-1.09	-3.93	1.62
Pu^{242}	12.10	3.62	11.06	4.78	1.86	-0.23	-0.65	3.19	1.71
Nd^{148}	0.00	-0.49	-0.42	-0.40	0.21	0.38	-0.43	0.07	-0.47
Nd^{143}	6.10	2.56	2.20	6.93	5.36	4.78	7.33	5.13	4.66
Nd^{145}	2.21	1.48	0.90	1.80	2.32	1.68	1.77	2.06	1.23
Nd^{146}	-2.31	-2.72	-2.51	-2.23	-2.11	-1.53	-2.38	-1.87	-2.09
Cs^{137}	-	-8.94	-	-	-13.38	-	-	-11.48	-
Mo^{95}	-	-3.18	-	-	-4.92	-	-	-4.56	-
Tc^{99}	-	49.43	-	-	45.28	-	-	42.12	-
Ru^{101}	-	-3.32	-	-	-1.39	-	-	-3.20	-
Ag^{109}	-	20.25	-	-	54.78	-	-	44.93	-
Cs^{133}	-	1.90	-	-	-1.09	-	-	2.04	-
Sm^{147}	-	1.45	-	-	0.05	-	-	0.61	-
Sm^{149}	-	-14.65	-	-	-5.84	-	-	2.24	-
Sm^{150}	-	2.39	-	-	0.27	-	-	4.04	-
Sm^{151}	-	-9.12	-	-	-5.96	-	-	-2.66	-
Sm^{152}	-	9.26	-	-	9.73	-	-	11.48	-
Eu^{151}	-	-38.66	-	-	-47.29	-	-	-36.63	-
Eu^{153}	-	0.17	-	-	3.69	-	-	4.56	-
Gd^{155}	-	4.54	-	-	-2.98	-	-	10.27	-
Rh^{103}	-	1.08	-	-	5.23	-	-	2.39	-
Eu^{155}	-	-8.00	-	-	-2.43	-	-	-3.11	-

Figure 29. C/M-1 for actinide and Nd nuclides for the 2F1ZN2 assembly samples

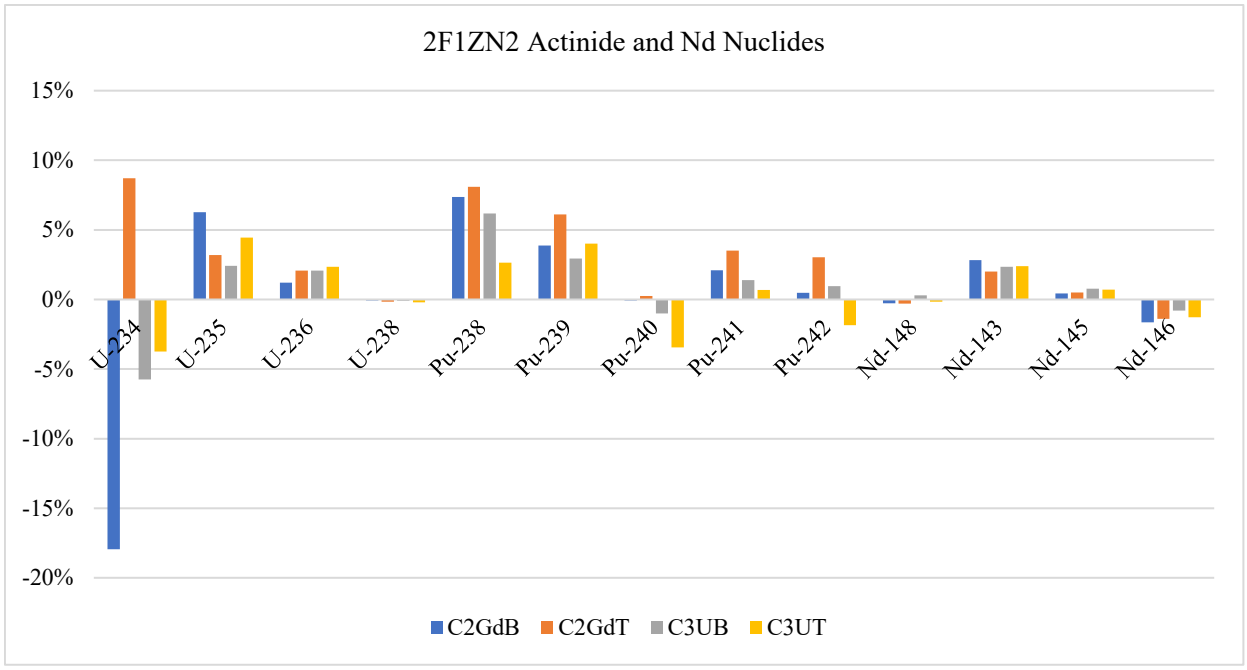

Source: ORNL, 2024.

Figure 30. C/M-1 for actinide and Nd nuclides for the 2F1ZN3 assembly samples

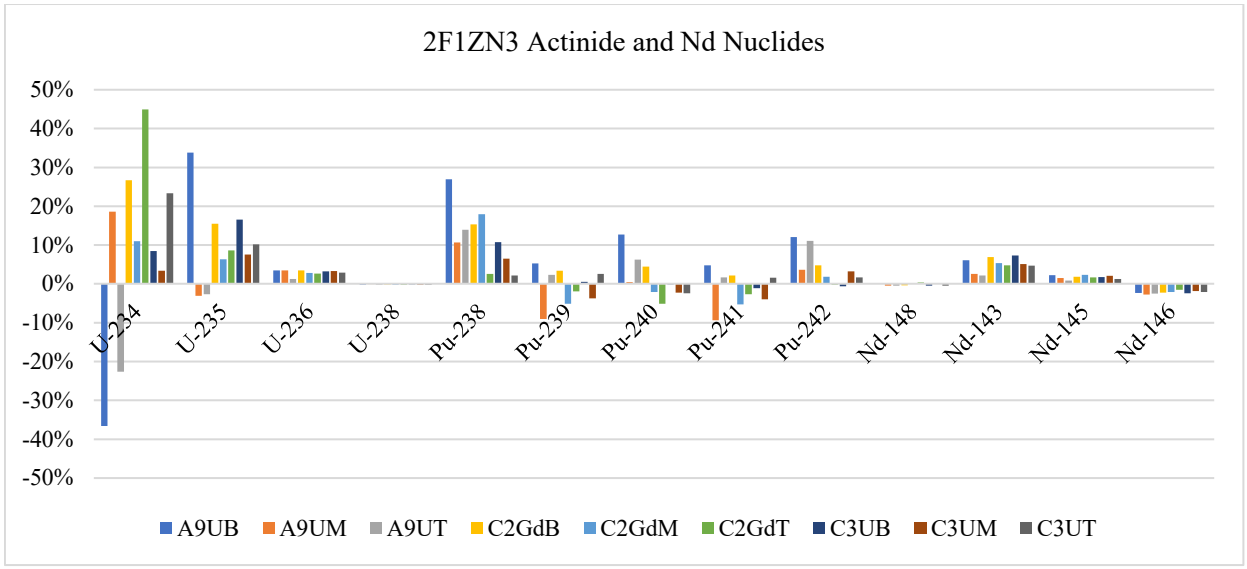

Source: ORNL, 2024.

Figure 31. C/M-1 for fission products for the 2F1ZN2 (C2GdT and C3UT) and 2F1ZN3 (A9UM, C2GdM, and C3UM) samples

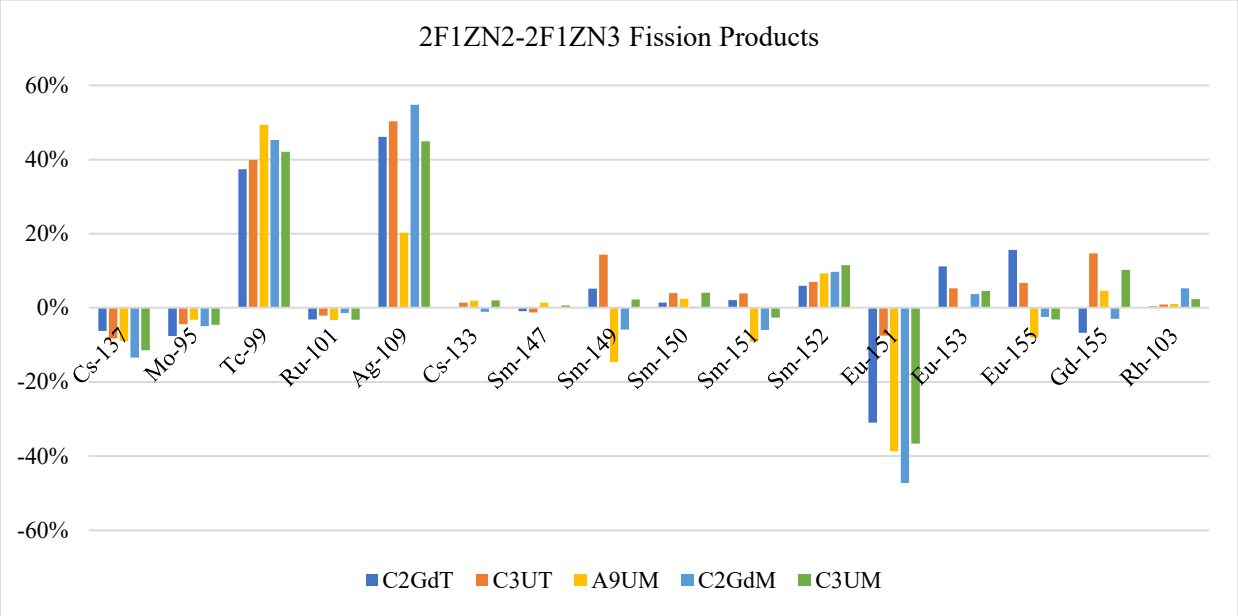

Source: ORNL, 2024.

Table 51. C/M-1 and uncertainties for the 2F1ZN3 assembly A9/UB sample

Nuclide	C/M-1 (%)	Uncertainties in (C/M-1) (%)							
	A9/UB	Burn-up	Void F.	Fuel temp.	Thermal expansion	Power history	Fuel density	Measurement	Total
U^{234}	-36.62	0.72	0.16	0.65	0.13	0.67	0.12	0.63	1.36
U^{235}	33.81	7.88	2.62	6.06	2.02	2.19	2.26	0.13	10.94
U^{236}	3.49	0.35	0.06	0.01	0.01	0.01	0.01	2.07	2.10
U^{238}	-0.17	0.07	0.00	0.01	0.00	0.01	0.00	0.10	0.12
Pu^{238}	26.93	0.77	0.54	1.24	0.39	1.52	0.71	0.63	2.41
Pu^{239}	5.30	0.38	0.14	0.80	0.38	0.03	0.39	0.32	1.10
Pu^{240}	12.70	0.22	0.16	0.25	0.05	0.15	0.21	0.34	0.57
Pu^{241}	4.80	0.46	0.24	1.08	0.41	0.02	0.44	0.31	1.37
Pu^{242}	12.10	1.39	0.05	0.04	0.01	0.25	0.20	0.34	1.46
Nd^{148}	0.00	1.02	0.01	0.02	0.01	0.09	0.00	0.10	1.02
Nd^{143}	6.10	0.47	0.45	1.22	0.41	0.25	0.48	0.11	1.54
Nd^{145}	2.21	0.63	0.04	0.22	0.05	0.07	0.01	0.10	0.68
Nd^{146}	-2.31	1.16	0.04	0.19	0.05	0.17	0.01	0.10	1.20

Table 52. C/M-1 and uncertainties for the 2F1ZN3 assembly A9/UM sample

Nuclide	C/M-1 (%)	Uncertainties in (C/M-1) (%)							
	A9/UM	Burn-up	Void F.	Fuel temp.	Thermal expansion	Power history	Fuel density	Measurement	Total
U^{234}	18.6	0.83	1.29	1.22	0.24	1.08	0.32	1.66	2.82
U^{235}	-3.08	5.38	7.50	4.58	1.39	1.32	1.75	3.88	11.31
U^{236}	3.46	0.37	0.25	0.03	0.02	0.04	0.03	0.21	0.50
U^{238}	-0.08	0.07	0.01	0.01	0.00	0.00	0.00	0.20	0.21
Pu^{238}	10.69	0.68	1.90	1.03	0.29	1.23	0.63	0.55	2.72
Pu^{239}	-9.00	0.42	0.97	0.85	0.37	0.17	0.43	0.18	1.50
Pu^{240}	0.43	0.27	0.74	0.28	0.06	0.20	0.26	0.20	0.93
Pu^{241}	-9.40	0.48	1.33	1.09	0.40	0.18	0.48	0.18	1.91
Pu^{242}	3.62	1.24	0.24	0.07	0.01	0.20	0.20	0.21	1.32
Nd^{148}	-0.49	1.01	0.03	0.02	0.01	0.07	0.00	0.30	1.05
Nd^{143}	2.56	0.50	1.83	1.20	0.37	0.32	0.50	0.31	2.37
Nd^{145}	1.48	0.64	0.15	0.22	0.04	0.03	0.01	0.30	0.76
Nd^{146}	-2.72	1.15	0.14	0.19	0.04	0.09	0.01	0.29	1.21
Cs^{137}	-8.94	0.91	0.01	0.00	0.00	0.29	0.00	3.64	3.77
Mo^{95}	-3.18	0.72	0.04	0.06	0.01	0.04	0.00	2.23	2.34
Tc^{99}	49.43	1.11	0.08	0.28	0.03	0.04	0.02	3.59	3.76
Ru^{101}	-3.32	0.89	0.04	0.06	0.00	0.07	0.03	2.13	2.31
Ag^{109}	20.25	1.05	0.20	0.03	0.06	0.06	0.01	1.80	2.10
Cs^{133}	1.90	0.66	0.10	0.22	0.03	0.04	0.01	3.57	3.64
Sm^{147}	1.45	0.02	0.32	0.72	0.09	0.41	0.03	1.22	1.51
Sm^{149}	-14.65	0.49	0.56	0.56	0.19	2.22	0.29	1.79	3.03
Sm^{150}	2.39	0.82	0.47	0.25	0.09	0.18	0.14	1.33	1.67
Sm^{151}	-9.12	0.45	0.93	0.91	0.26	0.05	0.45	1.91	2.41
Sm^{152}	9.26	0.67	0.24	0.03	0.06	0.18	0.25	1.20	1.43
Eu^{151}	-38.66	0.31	0.64	0.62	0.18	0.01	0.31	0.86	1.33
Eu^{153}	0.17	0.66	0.23	0.44	0.10	0.03	0.04	0.70	1.09
Gd^{155}	4.54	0.74	0.41	1.32	0.12	0.07	0.12	1.36	2.08
Rh^{103}	1.08	0.33	0.57	1.15	0.15	0.07	0.08	1.92	2.34
Eu^{155}	-8.00	0.66	0.35	1.17	0.11	0.09	0.10	5.52	5.70

Table 53. C/M-1 and uncertainties for the 2F1ZN3 assembly A9/UT sample

Nuclide	C/M-1 (%)	Uncertainties in (C/M-1) (%)							
	A9/UT	Burn-up	Void F.	Fuel temp.	Thermal expansion	Power history	Fuel density	Measurement	Total
U^{234}	-22.65	0.61	0.82	0.68	0.09	0.14	0.09	0.77	1.46
U^{235}	-2.65	4.08	9.53	3.72	0.86	0.56	1.23	0.10	11.13
U^{236}	1.27	0.23	0.34	0.05	0.01	0.07	0.03	2.03	2.07
U^{238}	-0.17	0.06	0.03	0.01	0.00	0.01	0.01	0.10	0.12
Pu^{238}	13.94	1.16	2.79	0.90	0.17	0.97	0.52	0.57	3.39
Pu^{239}	2.36	0.55	2.95	1.27	0.40	0.08	0.56	0.31	3.35
Pu^{240}	6.24	0.31	1.50	0.39	0.04	0.13	0.29	0.32	1.64
Pu^{241}	1.68	0.54	3.17	1.38	0.39	0.08	0.53	0.31	3.57
Pu^{242}	11.06	1.53	0.72	0.02	0.01	0.25	0.24	0.33	1.76
Nd^{148}	-0.42	1.01	0.04	0.02	0.01	0.20	0.00	0.10	1.04
Nd^{143}	2.2	0.39	2.62	1.04	0.25	0.10	0.38	0.10	2.88
Nd^{145}	0.9	0.69	0.13	0.18	0.02	0.14	0.01	0.10	0.75
Nd^{146}	-2.51	1.14	0.17	0.19	0.03	0.23	0.00	0.10	1.19

Table 54. C/M-1 and uncertainties for the 2F1ZN3 assembly C2/GdB sample

Nuclide	C/M-1 (%)	Uncertainties in (C/M-1) (%)							
	C2/GdB	Burn-up	Void F.	Fuel temp.	Thermal expansion	Power history	Fuel density	Measurement	Total
U^{234}	26.71	1.14	0.15	0.89	0.08	1.53	0.21	1.27	2.47
U^{235}	15.53	5.45	1.50	3.98	0.95	0.74	2.35	0.12	7.40
U^{236}	3.51	0.22	0.05	0.13	0.03	0.12	0.08	2.07	2.09
U^{238}	-0.16	0.06	0.00	0.01	0.00	0.01	0.01	0.10	0.12
Pu^{238}	15.33	1.49	0.42	1.04	0.34	4.67	0.79	0.58	5.13
Pu^{239}	3.38	0.41	0.25	1.07	0.32	0.24	0.63	0.31	1.42
Pu^{240}	4.43	0.23	0.23	0.37	0.17	0.50	0.36	0.31	0.87
Pu^{241}	2.14	0.52	0.35	1.30	0.31	0.18	0.71	0.31	1.67
Pu^{242}	4.78	1.85	0.06	0.15	0.12	0.09	0.19	0.31	1.90
Nd^{148}	-0.4	1.00	0.00	0.02	0.00	0.04	0.00	0.10	1.00
Nd^{143}	6.93	0.37	0.39	1.10	0.26	0.32	0.64	0.11	1.44
Nd^{145}	1.8	0.65	0.01	0.14	0.00	0.10	0.01	0.10	0.68
Nd^{146}	-2.23	1.15	0.03	0.18	0.01	0.17	0.03	0.10	1.18

Table 55. C/M-1 and uncertainties for the 2F1ZN3 assembly C2/GdM sample

Nuclide	C/M-1 (%)	Uncertainties in (C/M-1) (%)							
	C2/GdM	Burn-up	Void F.	Fuel temp.	Thermal expansion	Power history	Fuel density	Measurement	Total
U^{234}	11.03	0.46	0.56	0.76	0.09	2.01	0.27	1.55	2.76
U^{235}	6.35	3.84	4.25	3.16	0.68	1.85	2.01	0.32	7.13
U^{236}	2.8	0.10	0.16	0.17	0.03	0.18	0.07	0.21	0.38
U^{238}	-0.17	0.05	0.02	0.02	0.00	0.01	0.01	0.20	0.21
Pu^{238}	17.99	1.57	1.63	1.05	0.32	4.72	0.83	0.59	5.45
Pu^{239}	-5.08	0.81	1.58	1.22	0.35	1.18	0.82	0.19	2.62
Pu^{240}	-2.06	0.46	0.99	0.37	0.19	0.75	0.43	0.20	1.47
Pu^{241}	-5.27	0.84	1.67	1.34	0.30	0.47	0.82	0.19	2.51
Pu^{242}	1.86	1.74	0.48	0.15	0.14	0.80	0.25	0.20	2.01
Nd^{148}	0.21	0.99	0.02	0.02	0.00	0.19	0.01	0.30	1.05
Nd^{143}	5.36	0.61	1.25	0.92	0.21	0.61	0.59	0.32	1.90
Nd^{145}	2.32	0.69	0.01	0.11	0.01	0.06	0.01	0.31	0.76
Nd^{146}	-2.11	1.12	0.07	0.17	0.00	0.01	0.03	0.29	1.18
Cs^{137}	-13.38	0.86	0.02	0.00	0.00	0.93	0.01	3.46	3.69
Mo^{95}	-4.92	0.72	0.07	0.01	0.01	0.11	0.03	2.09	2.22
Tc^{99}	45.28	1.08	0.03	0.16	0.01	0.16	0.02	3.49	3.66
Ru^{101}	-1.39	0.91	0.05	0.04	0.01	0.09	0.03	1.97	2.18
Ag^{109}	54.78	1.78	0.32	0.10	0.02	0.08	0.10	2.32	2.95
Cs^{133}	-1.09	0.71	0.01	0.13	0.01	0.07	0.00	3.07	3.15
Sm^{147}	0.05	0.07	0.05	0.50	0.02	1.40	0.01	1.80	2.33
Sm^{149}	-5.84	0.70	1.07	1.03	0.28	11.66	0.71	3.20	12.23
Sm^{150}	0.27	0.96	0.24	0.09	0.04	1.12	0.12	1.80	2.35
Sm^{151}	-5.96	0.91	1.37	1.30	0.34	0.11	0.92	2.26	3.23
Sm^{152}	9.73	0.68	0.39	0.00	0.15	0.92	0.30	1.76	2.16
Eu^{151}	-47.29	0.52	0.79	0.75	0.19	0.19	0.53	1.32	1.88
Eu^{153}	3.69	0.78	0.15	0.44	0.03	0.01	0.11	2.18	2.36
Gd^{155}	-2.98	0.56	0.54	0.98	0.14	0.29	0.35	8.25	8.35
Rh^{103}	5.23	0.51	0.37	1.04	0.04	0.40	0.14	2.10	2.47
Eu^{155}	-2.43	0.89	0.40	1.53	0.09	0.73	0.20	5.85	6.18

Table 56. C/M-1 and uncertainties for the 2F1ZN3 assembly C2/GdT sample

Nuclide	C/M-1 (%)	Uncertainties in (C/M-1) (%)							
	C2/GdT	Burn-up	Void F.	Fuel temp.	Thermal expansion	Power history	Fuel density	Measurement	Total
U^{234}	44.96	0.83	0.21	0.65	0.01	1.38	0.07	1.45	2.27
U^{235}	8.59	2.59	4.05	2.17	0.36	1.14	1.27	0.11	5.55
U^{236}	2.68	0.21	0.19	0.27	0.03	0.14	0.04	2.05	2.10
U^{238}	-0.17	0.04	0.05	0.02	0.00	0.00	0.01	0.10	0.12
Pu^{238}	2.62	1.63	2.15	0.94	0.23	2.79	0.64	0.51	4.08
Pu^{239}	-1.9	1.08	3.50	1.50	0.33	1.00	1.08	0.29	4.25
Pu^{240}	-5.15	0.50	1.45	0.34	0.16	0.22	0.37	0.28	1.66
Pu^{241}	-2.63	0.82	2.66	1.41	0.22	0.33	0.79	0.29	3.26
Pu^{242}	-0.23	1.83	1.26	0.18	0.16	1.14	0.33	0.30	2.55
Nd^{148}	0.38	0.99	0.03	0.02	0.00	0.38	0.01	0.10	1.07
Nd^{143}	4.78	0.37	1.16	0.58	0.10	0.06	0.35	0.10	1.41
Nd^{145}	1.68	0.75	0.19	0.04	0.02	0.26	0.05	0.10	0.83
Nd^{146}	-1.53	1.10	0.02	0.15	0.01	0.24	0.01	0.10	1.14

Table 57. C/M-1 and uncertainties for the 2F1ZN3 assembly C3/UB sample

Nuclide	C/M-1 (%)	Uncertainties in (C/M-1) (%)							
	C3/UB	Burn-up	Void F.	Fuel temp.	Thermal expansion	Power history	Fuel density	Measurement	Total
U^{234}	8.47	1.23	0.08	0.66	0.08	0.12	0.12	1.08	1.78
U^{235}	16.59	6.44	1.33	3.58	1.13	0.30	2.10	0.12	7.87
U^{236}	3.21	0.24	0.05	0.17	0.00	0.01	0.06	2.06	2.09
U^{238}	-0.15	0.07	0.01	0.02	0.01	0.00	0.01	0.10	0.12
Pu^{238}	10.75	1.81	0.41	1.23	0.32	0.20	0.78	0.55	2.45
Pu^{239}	0.52	0.40	0.24	1.06	0.46	0.04	0.63	0.30	1.43
Pu^{240}	-0.13	0.28	0.22	0.38	0.13	0.04	0.35	0.30	0.71
Pu^{241}	-1.09	0.50	0.33	1.28	0.46	0.02	0.71	0.30	1.68
Pu^{242}	-0.65	2.15	0.00	0.23	0.00	0.07	0.13	0.30	2.19
Nd^{148}	-0.43	1.00	0.00	0.01	0.01	0.02	0.00	0.10	1.01
Nd^{143}	7.33	0.68	0.38	1.08	0.34	0.06	0.63	0.11	1.52
Nd^{145}	1.77	0.58	0.01	0.12	0.01	0.01	0.01	0.10	0.60
Nd^{146}	-2.38	1.21	0.03	0.17	0.03	0.03	0.03	0.10	1.22

Table 58. C/M-1 and uncertainties for the 2F1ZN3 assembly C3/UM sample

Nuclide	C/M-1 (%)	Uncertainties in (C/M-1) (%)							
	C3/UM	Burn-up	Void F.	Fuel temp.	Thermal expansion	Power history	Fuel density	Measurement	Total
U^{234}	3.42	0.76	0.35	0.64	0.08	0.12	0.16	1.45	1.80
U^{235}	7.58	4.45	3.86	2.88	0.83	1.29	1.77	0.32	6.97
U^{236}	3.33	0.09	0.17	0.19	0.00	0.06	0.06	0.21	0.35
U^{238}	-0.2	0.07	0.03	0.02	0.01	0.02	0.01	0.20	0.22
Pu^{238}	6.47	1.70	1.55	1.22	0.29	1.17	0.77	0.53	3.01
Pu^{239}	-3.73	0.92	1.56	1.25	0.50	0.96	0.94	0.19	2.64
Pu^{240}	-2.27	0.47	1.01	0.42	0.15	0.53	0.44	0.20	1.40
Pu^{241}	-3.93	0.92	1.72	1.40	0.48	0.93	0.89	0.19	2.77
Pu^{242}	3.19	2.11	0.29	0.24	0.02	0.01	0.25	0.21	2.16
Nd^{148}	0.07	1.00	0.02	0.02	0.01	0.12	0.01	0.30	1.05
Nd^{143}	5.13	0.63	1.26	0.93	0.27	0.59	0.60	0.32	1.93
Nd^{145}	2.06	0.61	0.04	0.10	0.00	0.05	0.02	0.31	0.69
Nd^{146}	-1.87	1.18	0.06	0.16	0.03	0.14	0.02	0.29	1.24
Cs^{137}	-11.48	0.88	0.01	0.00	0.00	0.07	0.01	3.54	3.65
Mo^{95}	-4.56	0.69	0.08	0.03	0.01	0.05	0.04	4.29	4.35
Tc^{99}	42.12	1.02	0.05	0.16	0.01	0.01	0.03	4.97	5.08
Ru^{101}	-3.2	0.89	0.06	0.05	0.01	0.08	0.03	3.68	3.79
Ag^{109}	44.93	1.95	0.47	0.22	0.11	0.42	0.16	2.17	3.00

Table 58. C/M-1 and uncertainties for the 2F1ZN3 assembly C3/UM sample (continued)

Nuclide	C/M-1 (%)	Uncertainties in (C/M-1) (%)							
	C3/UM	Burn-up	Void F.	Fuel temp.	Thermal expansion	Power history	Fuel density	Measurement	Total
Cs^{133}	2.04	0.67	0.01	0.13	0.00	0.07	0.02	4.90	4.95
Sm^{147}	0.61	0.19	0.02	0.48	0.00	0.04	0.06	1.21	1.32
Sm^{149}	2.24	0.71	1.06	1.04	0.35	0.16	0.73	1.53	2.39
Sm^{150}	4.04	0.98	0.27	0.11	0.05	0.24	0.14	1.25	1.64
Sm^{151}	-2.66	0.88	1.38	1.32	0.40	0.93	0.89	1.46	2.89
Sm^{152}	11.48	0.68	0.41	0.07	0.12	0.28	0.34	1.23	1.53
Eu^{151}	-36.63	0.58	0.92	0.88	0.26	0.63	0.59	0.82	1.86
Eu^{153}	4.56	0.85	0.08	0.40	0.07	0.18	0.06	0.52	1.10
Gd^{155}	10.27	1.08	0.42	1.61	0.13	0.38	0.26	1.21	2.37
Rh^{103}	2.39	0.39	0.38	1.08	0.10	0.18	0.14	3.79	3.99
Eu^{155}	-3.11	0.96	0.35	1.44	0.10	0.31	0.21	5.81	6.09

Table 59. C/M-1 and uncertainties for the 2F1ZN3 assembly C3/UT sample

Nuclide	C/M-1 (%)	Uncertainties in (C/M-1) (%)							
	C3/UT	Burn-up	Void F.	Fuel temp.	Thermal expansion	Power history	Fuel density	Measurement	Total
U^{234}	23.35	0.89	0.05	0.43	0.00	0.27	0.01	1.23	1.60
U^{235}	10.21	3.01	3.44	1.85	0.40	0.90	1.05	0.11	5.14
U^{236}	2.94	0.27	0.22	0.27	0.00	0.08	0.04	2.06	2.11
U^{238}	-0.24	0.05	0.06	0.03	0.01	0.02	0.02	0.10	0.13
Pu^{238}	2.2	1.94	2.35	1.23	0.21	0.55	0.71	0.51	3.45
Pu^{239}	2.61	1.16	3.62	1.59	0.48	0.10	1.15	0.31	4.32
Pu^{240}	-2.43	0.62	1.48	0.38	0.11	0.18	0.39	0.29	1.73
Pu^{241}	1.62	0.90	2.85	1.52	0.39	0.16	0.86	0.30	3.50
Pu^{242}	1.71	2.21	0.82	0.34	0.01	0.66	0.25	0.31	2.50
Nd^{148}	-0.47	1.00	0.03	0.02	0.01	0.30	0.01	0.10	1.05
Nd^{143}	4.66	0.35	1.05	0.52	0.12	0.06	0.32	0.10	1.27
Nd^{145}	1.23	0.72	0.25	0.02	0.02	0.21	0.07	0.10	0.80
Nd^{146}	-2.09	1.14	0.04	0.12	0.01	0.34	0.01	0.10	1.20

6. References

[1] Okumura, K., K. Kaneko and K. Tsuchihashi (1996), SRAC95, *General Purpose Neutronics Code System*, JAERI-Data/Code 96-015, JAERI.

[2] Okumura, K., T. Mori, M. Nakagawa et al. (2000), "Validation of a continuous-energy Monte Carlo Burn-Up Code MVP-BURN and its application to analysis of post irradiation experiment", *J. Nucl. Sci. Technol.* 37[2], 128.

[3] Yamamoto, T. and Y. Kanayama (2008), "Lattice physics analysis of burnups and isotope inventories of U, Pu, and Nd of irradiated BWR 9× 9-9 UO_2 fuel assemblies", *J. Nucl. Sci. and Tech.* 45, pp. 547–566.

[4] Suzuki, M., et al. (2013), "Lattice physics analysis of measured isotopic compositions of irradiated BWR 9×9 UO_2 fuel", *J. Nucl. Sci. and Tech.* 50, pp. 1161–1176.

[5] NEA (n.d.), SFCOMPO *Database of Measured Isotopic Concentrations of Spent Nuclear Fuel, with Operational Histories and Design Data*, www.oecd-nea.org/sfcompo, accessed 4 September 2019.

[6] TEPCO (2019), *Overview of facility of Fukushima Daini Nuclear Power Station*, www.tepco.co.jp/en/nu/fukushima-np/outline_f2/index-e.html, accessed 4 September 2019.

[7] Yamamoto, T. (2014), *Irradiation Report of Fuel Samples of BWR 9×9-9 Fuel*, report prepared for the OECD NEA Data Bank contribution to SFCOMPO, February 2014.

[8] Word Nuclear Association (2019), Fukushima Daini 2, www.world-nuclear.org/reactor/default.aspx/FUKUSHIMA-DAINI-2, accessed 4 September 2019.

[9] Moore, R.S. (1989), *Physical Characteristics of GE BWR Fuel Assemblies*, ORNL/TM-10902, United States.

[10] Nuclear Engineering International (2007), "*World Nuclear Industry Handbook"*, London, United Kingdom, 2007.

[11] NEA (2003), *Physics of Plutonium Recycling: Volume VII: Fuels BWR MOX Benchmark Specification and Results,* 92-64-19905-5, OECD Publishing, Paris, www.oecd-nea.org/jcms/pl_13476.

[12] NRC (2019), *TN-68 Dry Storage Cask, Updated Final Safety Analysis Report*, Revision 4, Appendix 6A https://www.nrc.gov/docs/ML0815/ML081510909.pdf, accessed 4 September 2019.

[13] Yamamoto, T. (2009), *Compilation of Measurement and Analysis Results of Isotopic Inventories of Spent BWR Fuels*, JNES, 2009, available online at https://www.oecd-nea.org/science/wpncs/ADSNF/reports/JNES/JNESreport2009.pdf, accessed 4 September 2019.

[14] NEA (2012), "Burnup Credit Criticality Benchmark Phase IIIC: Nuclide Composition and Neutron Multiplication Factor of BWR Spent Fuel Assembly for Burnup Credit and Criticality Control of Damaged Nuclear Fuel", OECD Publishing, Paris, www.oecd-nea.org/nea-nsc-r-2015-6.

[15] Kelly, D.J. (1995), "Depletion of a BWR lattice using the RACER continuous energy Monte Carlo Code", *Proc. Int. Natl. Conf. on Mathematics and Computations, Reactor Physics, and Environmental Analyses*, Portland, Vol. II, 1011.

[16] eFunda (n.d.), "The Ultimate Online Reference for Engineers, Steam Tables", accessed 4 September 2019, www.efunda.com/materials/water/steamtable_sat.cfm.

[17] O'Donnell, G.M., et al. (2001), *A New Comparative Analysis of LWR Fuel Designs*, NUREG-1754, US NRC, United States.

[18] Radulescu, H.R. (2003), *Limerick Unit 1 Radiochemical Assay Comparisons to SAS2H Calculations*, CAL-DSU-NU-000002 Rev 00A, Office of Civilian Radioactive Waste Management.

[19] de Kruijf, W.J.M. and A.J. Janssen (2017), "The effective fuel temperature to be used for calculating resonance absorption in a $^{238}UO_2$ lump with a nonuniform temperature profile", *Nuclear Science and Engineering* 123:1, 121–135, https://doi.org/10.13182/NSE94-108.

[20 IAEA (1996), *Characteristics and Use of Urania Gadolinia Fuels, 3. Fuel Manufacturing*, TECDOC-844, 50-58, Vienna.

[21] IAEA (1991), *Guidebook on QC of MOX and Gd Bearing Fuels*, IAEA-TECDOC-584, Vienna.

[22] Fink, J.K. (999), International Nuclear Safety Center Material Properties Data Base, http://www.insc.anl.gov/matprop.

[23] Rearden, B.T. and M.A. Jessee (2016), Eds. 2016 *SCALE Code System,* Version 6.2.3, Technical Report ORNL/TM-2005/39. Oak Ridge, TN: Oak Ridge National Laboratory, United States.

[24] Parks, C.V., M.D. DeHart, and J.C. Wagner (2018), *Margins for Uncertainty in the Predicted Spent Fuel Isotopic Inventories for BWR Burnup Credit*, NUREG/CR-7251, US Nuclear Regulatory Commission, February 2018.

[25] Gauld I. and U. Mertyurek (1995), "Void fraction distribution in BWR fuel assembly and evaluation of subchannel code", *Journal of Nuclear Science and Technology* 32(7), pp. 629–640 (July 1995).

[26] Morooka, S., T. Ishizuka, M. Iizuka and K. Yoshimura (1989), "Experimental study on void fraction in a simulated BWR fuel assembly (Evaluation of Cross-Sectional Averaged Void Fraction)", *Nuclear Engineering and Design* 114, pp. 91–98.

[27] Palanki, B. (2016), "Fabrication of UO_2-Gd_2O_3 fuel pellets", *Journal of Materials Science and Chemical Engineering* 4, pp. 8-21.

[28] Standard Test Method for Atom Percent Fission in Uranium and Plutonium Fuel (Neodymium-148 Method), ASTM E321-96, (Reapproved 2005), Pennsylvania, PA: ASTM- International (2007).

[29] Palmtag, S. (2016), *Investigation of Thermal Expansion Effects in MPACT*, CASL-U-2016-1015-000.

[30] NS Energy (2013), "Avoiding BWR Channel Distortion", *Nuclear Engineering International*, October 2013, available at http://www.neimagazine.com/features/featureavoiding-bwr-channel-distortion/.

[31] Garzarolli, F. et al. (2011), *BWR Fuel Channel Distortion,* ZIRAT16 Special Topical Report, ANT International, Molnlycke, Sweden.

[32] NEA (2016), *Evaluation Guide for the Evaluated Spent Nuclear Fuel Assay Database (SFCOMPO)* NEA/NSC/R (2015), OECD Publishing, Paris, www.oecd-nea.org/jcms/pl_19678.

[33] Bowman, S.M. and T. Suto (1996), *Analysis of Pressurized Water Reactor Critical Configurations: Volume 5 – North Anna Unit 1 Cycle 5*, ORNL/TM-12294/V5.

Appendix A

A.1. Polaris model for 2F1ZN3/C3/UB

```
=polaris
title "Atrium-9 model 2F1ZN3/C3/UB "

lib "xn56v7.1"
sys BWR

geom FuelNode : ASSM 9 1.45
channel COOL
hgap 0.67 : MOD.1
%box icdist=0.175 rad=1.143 thick=0.25 xlen=0.0 xrad=0.0
box 0.25 0.9652 6.7
shield ALL=N FUEL=P GAD=P
deplete FUEL=YES GAD=YES
opt CRITSPEC Method="P1"

mat FUEL.1 : uo2_f100 temp=900 dens=10.52
comp uo2_f100 : UOX 4.9

mat FUEL.2 : uo2_f102 temp=900 dens=10.52
comp uo2_f102 :UOX 4.2

mat FUEL.21 : uo2_f102 temp=900 dens=10.52
mat FUEL.22 : uo2_f102 temp=900 dens=10.52

mat FUEL.3 : uo2_f103 temp=900 dens=10.52
comp uo2_f103 : UOX 3.6

mat FUEL.31 : uo2_f103 temp=900 dens=10.52

mat FUEL.4 : uo2_f104 temp=900 dens=10.52
comp uo2_f104 : UOX 3.0

mat FUEL.41 : uo2_f104 temp=900 dens=10.52

mat FUEL.5 :uo2_f105 temp=900 dens=10.52
comp uo2_f105 : UOX 2.1

mat GAD.1 : uo2gd_f50 temp=900 dens=10.32
comp uox34 : UOX 3.0
comp uo2gd_f50 : WT GD2O3=5.0 uox34=-100

mat COOL.1 : H2O temp=559 :void=14
mat MOD.1 : H2O temp=559 :void=0
mat FUEL.100 : uo2_f100 temp=900 dens=10.52
mat GAD.100 : uo2gd_f50 temp=900 dens=10.32
mat FUEL.500 :uo2_f105 temp=900 dens=10.52

pin C2 : 0.47800 0.48790 0.55900
: GAD.100 gap.1 clad.1
pin C3 : 0.47800 0.48790 0.55900
: FUEL.100 gap.1 clad.1
pin A9 : 0.47800 0.48790 0.55900
: FUEL.500 gap.1 clad.1
pin 1 : 0.47800 0.48790 0.55900
: FUEL.1 gap.1 clad.1
pin 2 : 0.47800 0.48790 0.55900
: FUEL.2 gap.1 clad.1
pin 3 : 0.47800 0.48790 0.55900
: FUEL.3 gap.1 clad.1
pin 4 : 0.47800 0.48790 0.55900
: FUEL.4 gap.1 clad.1
pin 5 : 0.47800 0.48790 0.55900
: FUEL.5 gap.1 clad.1
pin 9 : 0.47800 0.48790 0.55900
```

```
: GAD.1 gap.1 clad.1
pin 21 : 0.47800 0.48790 0.55900
: FUEL.21 gap.1 clad.1
pin 22 : 0.47800 0.48790 0.55900
: FUEL.22 gap.1 clad.1
pin 41 : 0.47800 0.48790 0.55900
: FUEL.41 gap.1 clad.1
pin 31 : 0.47800 0.48790 0.55900
: FUEL.31 gap.1 clad.1
pin W 3.0 : 1.85 1.925 : MOD.1 CAN.1 : SQR SQR

pinmap 5
       4 3
       3 C2 C3
       2 2 2 W
       2 9 2 W W
       2 2 2 W W W
       3 9 1 2 2 2 1
       4 3 9 2 9 2 9 3
      A9 4 3 2 2 2 3 4 5

mesh MOD : nf=3 nd=4 nx=6 ny=6 ns=8 nr=4
mesh FUEL : nr=3 ns=8
mesh GAD : nr=5 ns=8
mesh TUBE : ns=8

state ALL : temp=559
FUEL : temp=800
GAD : temp=800
MOD : void=0
COOL : void=14
%-------------------------------------------------------------------------------%
% Irradiation Report of Fuel Samples of BWR 9x9-9 Fuel
% Japan Nuclear Energy Safety Organization Toru YAMAMOTO (JNES 2014)
%-------------------------------------------------------------------------------%
basis ALL=no FUEL.100=yes

read history
%power is reduced by 0.98 void is reduced by 1.0
%cycle 12 ZN3C3UB
STATE COOL : void = 13.9 12.5 12.5 12.5 13.4 13.4 13.4 14.2 14.2 14.2 14.2 15.3 15.3 15.3 17.0
17.0 17.0 19.9 19.9 19.9 22.5 22.5 22.5 22.5 22.5
power 34.8 36.172 36.172 36.172 35.799 35.799 35.799 35.966 35.966 35.966 35.966 37.583 37.583
37.583 38.367 38.367 38.367 39.964 39.964 39.964 42.473 42.473 42.473 42.473 42.473
dt 4.0 10.67 10.67 10.67 11.67 11.67 11.67 10.5 10.5 10.5 10.5 10.67 10.67 10.67 10.33 10.33 10.33
11.67 11.67 11.67 11.67 11.67 11.67 6.0 6.0
power 0.0
dt 6.0
STATE COOL : void = 24.6 24.5 24.5 24.5 22.7 22.7 22.7 19.1 19.1 19.1 16.6 16.6 16.6
power 38.063 43.845 43.845 43.845 43.404 43.404 43.404 41.493 41.493 41.493 36.172 36.172 36.172
dt 7.0 10.33 10.33 10.33 10.67 10.67 10.67 11.0 11.0 11.0 18.5 18.5 18.0
power 0.0
dt 40.0

%cycle 13 ----------------------------------
STATE COOL : void = 25.7 25.7
power 32.066 32.064
dt 8.0 26.0
power 0.0
dt 71.0
STATE COOL : void = 24.5 23.6 23.6 23.6 23.6 23.6 23.6 24.0 24.0 25.5 25.5 26.7 26.7 26.5 26.5
25.0 25.0 22.8 22.8
power 104.909 44.531 44.531 44.227 44.227 43.953 43.953 43.982 43.982 44.766 44.766 46.138 46.138
46.53 46.53 45.57 45.57 43.571 43.571
dt 5.0 12.0 12.0 16.0 16.0 15.5 15.5 16.0 16.0 19.0 19.0 16.0 16.0 15.5 15.5 14.0 14.0 24.0 28.0
power 0.0
dt 86.0

%cycle 14 ----------------------------------
STATE COOL : void = 19.3 18.0 17.9 17.5 17.1 16.9 16.9 17.2 16.6 14.9 11.1 8.5 6.4 4.2 4.2
power 14.984 40.209 38.779 38.494 38.877 38.475 38.465 38.935 38.651 37.24 33.986 31.321 27.754
26.048 26.048
```

```
dt 6.0 31.0 32.0 17.0 32.0 31.0 32.0 35.0 31.0 42.0 32.0 28.0 38.0 25.0 11.0
power 0.0
dt 39.0

%cycle 15 ----------------------------------
STATE COOL : void = 15.2 13.5 13.6 13.3 13.8 13.5 15.0 15.0
power 23.814 33.467 32.663 32.556 33.055 33.193 34.153 34.153
dt 5.0 32.0 35.0 10.0 33.0 29.0 33.0 36.0
power 0.0
dt 37.0
STATE COOL : void = 15.6 16.1 15.4 13.2 9.5 8.7 4.1 4.1
power 25.637 35.466 34.937 32.85 30.89 29.047 26.519 26.519
dt 4.0 28.0 32.0 28.0 28.0 14.0 31.0 7.0
power 0.0
dt 90.0

%cycle 16 ----------------------------------
STATE COOL : void = 0.0 0.0 0.0 0.0 0.0 0.1 0.1 0.2 0.4 0.6 0.4 0.3 0.3 0.1 0.0 0.0
power 9.565 18.444 18.091 18.042 18.218 18.787 19.032 19.698 20.825 21.58 21.648 20.864 19.884
19.335 17.591 17.591
dt 5.0 35.0 28.0 35.0 13.0 29.0 33.0 37.0 35.0 35.0 32.0 27.0 22.0 22.0 22.0 12.0
power 0.0
dt 962.0
power 0.0
dt 39.0


end history
end
```